RICE UNIVERSITY

The Impact of D-amino acids on Formation and Integrity of Biofilm – Effect of Growth Condition and Bacteria Type

by

Xuening Li

A THESIS SUBMITTED
IN PARTIAL FULFILLMENT OF THE
REQUIREMENTS FOR THE DEGREE

Master of Science

APPROVED, THESIS COMMITTEE

Qilin Li, Chair
Associate Professor, Civil &
Environmental Engineering

Pedro J. Alvarez
George R. Brown Professor,
Department Chair, Civil &
Environmental Engineering

Mason B. Tomson
Professor, Civil & Environmental
Engineering

HOUSTON, TEXAS

May 2013

ABSTRACT

The Impact of D-amino acids on Formation and Integrity of Biofilm – Effect of Growth Condition and Bacteria Type

by

Xuening Li

Biofouling is a major issue in applying NF/RO technologies for wastewater treatment. Biofilm formed on the surface of membranes will cause flux decline and energy waste. In this study, a novel anti-biofouling method that applies D-amino acids to inhibit biofilm formation was investigated. The D-amino acids previously reported to inhibit biofilm formation and disrupt existing biofilm – D-tyrosine and the mixture of D-tyrosine, D-tryptophan, D-leucine and D-methionine were tested. *Pseudomonas aeruginosa* and *Bacillus subtilis* were used as model Gram-negative and Gram-positive bacteria, respectively. D-amino acids had better effect on inhibition of biofilm formation and disruption of exiting biofilm to *B. subtilis* than to *P. aeruginosa*. Microtiter plate assay for quantitative biofilm measurement was systematically evaluated and optimized for screening biofilm control agents. This study also showed that D-tyrosine could effectively inhibit organic fouling and *P. aeruginosa* biofouling on NF90 membrane surface in bench scale dead end filtration experiment.

ACKNOWLEDGEMENT

First of all, I would like to express my greatest appreciate to my advisor Dr. Qilin Li. Thank you to her for giving me detailed guidance throughout my two years of master's study at Rice University, which is an excellent experience that I will cherish for the rest of my life. As my academic advisor, she taught me professional knowledge in environmental engineering, and opened the door of biological anti-biofouling strategy for NF/RO membrane for me. I was deeply inspired by her serious altitude and enthusiasm to science.

Great thanks to all my lab members: Michael Liga, Xiaolei Qu, Jinjian Wu, Cong Yu, Tianxiao Wang, Patty Coogan, and Amy Heldenbrand. It was a great time working with you. Special thanks to Xiaolei Qu, Jinjian Wu and Cong Yu for their enormous help on my research and experiments and for encouraging me to overcome all the difficulties.

Thank you to my beloved parents, who gave me courage and support my living and study in the US.

Thank you to all my friends, thanks for the great memories I shared with you during my stay in the US.

TABLE OF CONTENTS

ABSTRACT II
ACKNOWLEDGEMENT III
TABLE OF CONTENTS IV
LIST OF FIGURES VI
LIST OF TABLES XIII
LIST OF EQUATIONS XIV
1. Introduction 1
2. Literature review 5
2.1 Clean water issue and membrane filtration technology 5
2.2 Membrane biofouling 7
2.2.1 Membrane fouling cause and consequences 7
2.2.2 Biofilm formation 8
2.2.3 Effects of biofouling on NF/RO membrane performance 9
2.3 Biofouling control strategies in NF/RO systems 10
2.3.1 Feed Water Pretreatment 11
2.3.2 Biocide addition 11
2.3.3 Membrane surface modification 12
2.3.4 Membrane cleaning 13
2.3.5 Biological methods for biofouling inhibition 14
2.4 D-amino acids in biofouling prevention 16
3. Experimental methods 19
3.1 Materials 19
3.1.1 Chemicals 19
3.1.2 Growth Media 20
3.1.3 Biofilm culture plates 21
3.1.4 Membrane 22
3.1.5 Model bacteria 23
3.2 Methods 24
3.2.1 Evaluating the effect of D-amino acids on bacterial biofilm formation

.... 24

3.2.2 Evaluating the effect of D-amino acids on existing bacterial biofilm 27

3.2.3 Bench scale dead-end filtration experiment..... 28

4. Results and discussion..... 32

4.1 Determination of growth conditions for robust biofilm..... 32

4.1.1 Effect of incubation temperature on bacteria growth..... 33

4.1.2 Effect of incubation time on biofilm growth 34

4.1.3 Effect of nutrient medium on biofilm growth..... 37

4.1.4 Effect of microtiter plate size 40

4.1.5 Washing protocol..... 43

4.1.6 Fixation 43

4.1.7 Staining 44

4.1.8 Measurement of the biofilm..... 45

4.1.9 Interpretation of the results..... 47

4.2 Effect of D-amino acids on bacterial biofilm 48

4.2.1 Effect of D-amino acids on *B. subtilis* biofilm formation..... 49

4.2.2 Effect of D-amino acids on existing *B. subtilis* biofilm 51

4.2.3 Effect of D-amino acids on *P. aeruginosa* biofilm formation..... 55

4.2.4 Effect of D-amino acids on existing *P. aeruginosa* biofilm..... 63

4.3 Bench scale dead end filtration experiment 69

4.3.1 Effect of D-tyrosine in preventing organic fouling and biofouling in bench scale dead end NF90 filtration experiment 70

5. Conclusions and future research 74

REFERENCES 76

APPENDIX..... 82

LIST OF FIGURES

Figure 1. 96-well-plate 21
Figure 2. 24-well-plate 22
Figure 3. 12-well-plate 22
Figure 4. 35x10mm style tissue culture dish 22
Figure 5. Bench scale dead end filtration system [57] 29
Figure 6. Composition of stainless steel stirred cell 30
Figure 7. Effect of incubation temperature on *P. aeruginosa* growth. (A) Absorbance of CV at 600nm of *P. aeruginosa* after 12h incubation in 96-well-plate in LB medium at different incubation temperature. (B) Absorbance of CV at 600nm of *P. aeruginosa* after 12h incubation in 24-well-plate in R2A medium at different incubation temperature. (C) Absorbance of CV at 600nm of *P. aeruginosa* after 24h incubation in 24-well-plate in M63 medium at different incubation temperature..... 33
Figure 8. Effect of incubation time on *P. aeruginosa* growth. (A) Absorbance of CV at 600nm of *P. aeruginosa* incubated in 24-well-plate in M63 medium at 30°C after different incubation time. (B) Absorbance of CV at 600nm of *P. aeruginosa* incubated in 24-well-plate in R2A medium at 37°C after different incubation time. (C) Absorbance of CV at 600nm of *P. aeruginosa* incubated in 12-well-plate in M63 medium at 37°C after different incubation time. 34
Figure 9. *P. aerugisnosa* incubated 8 hours at 37°C in M63 medium, shaking at rpm 95. The biofilm was not visually observable by naked eyes..... 36
Figure 10. *P. aerugisnosa* incubated 12 hours at 37°C in M63 medium, shaking at rpm 95. The biofilm was not visually observable by naked eyes. 36
Figure 11. *P. aerugisnosa* incubated 18 hours at 37°C in M63 medium, shaking at rpm 95. Robust and well-attached biofilm formed. 36

Figure 12. *P. aerugisnosa* incubated 24 hours at 37°C in M63 medium, shaking at rpm 95. After washing the biofilm started to peel off. 36
Figure 13. *B. subtilis* incubated 15 hours at 37°C in M63 medium, shaking at rpm 95. No obvious biofilm formed. 37
Figure 14. *B. subtilis* incubated 24 hours at 37°C in M63 medium, shaking at rpm 95. No robust biofilm was formed. 37
Figure 15. *B. subtilis* incubated 24 hours at 37°C in M63 medium, no shaking. Robust and well-attached biofilm formed. 37
Figure 16. Effect of nutrient medium on *P. aeruginosa* growth. (A) Absorbance of CV at 600nm of *P. aeruginosa* after 24h incubation at 37°C in 12-well-plate, shaking at 95 rpm in different nutrient medium. (B) Absorbance of CV at 600nm of *P. aeruginosa* after 24h incubation at 37°C in 24-well-plate in different nutrient medium. (C) Absorbance of CV at 600nm of *P. aeruginosa* after 12h incubation at 37°C in 24-well-plate in different nutrient medium. (D) Absorbance of CV at 600nm of *P. aeruginosa* after 18h incubation at 37°C in 12-well-plate, shaking at 95 rpm in different nutrient medium. 38
Figure 17. Effect of nutrient medium on *B. subtilis* growth. Absorbance of CV at 600nm of *B. subtilis* after 24h incubation at 37°C in 12-well-plate in different nutrient medium. 39
Figure 18. Effect of microtiter plate size. (A) Absorbance of CV at 600nm of *P. aeruginosa* after 12h incubation at 37°C in LB medium in different microtiter plate. (B) Absorbance of CV at 600nm of *P. aeruginosa* after 24h incubation at 37°C in M63 medium in different microtiter plate. (C) Absorbance of CV at 600nm of *P. aeruginosa* after 18h incubation at 37°C in M63 medium shaking at rpm 95 and stained with 0.2% CV, in different microtiter plate. 41
Figure 19. Effect of microtiter plate size. Absorbance of CV at 600nm of *B.subtilis* after 24h incubation at 37°C in M63 with 2% glucose medium in different microtiter plate. 42
Figure 20. 1% crystal violet stained *P. aeruginosa,* after 18h incubation in M63 with 2% glucose, shaking at 95 rpm. Before extracted by 95% ethanol (left figure); after extracted by 95% ethanol (right figure), the crystal violet had

not been fully extracted. 45
Figure 21. 1% crystal violet stained *P. aeruginosa,* after 18h incubation in M63 with 2% glucose, shaking at 95 rpm. Before extracted by 95% ethanol (left figure); after extracted by 95% ethanol (right figure), the crystal violet had been fully extracted 45
Figure 22. The calibration curve between absorbance of CV at 600nm and the concentration of CV 47
Figure 23. Effect of D-AA on biofilm reduction of *B. subtilis,* incubated in M63 with 2% glucose for 24h at 37°C without shaking, with addition of DAA initially (12-well-plate) 49
Figure 24. Effect of D-AA on biofilm reduction of *B. subtilis,* incubated in 2% glucose M63 for 24h at 37°C without shaking, with addition of DAA initially (tissue culture dish) 50
Figure 25. Effect of D-AA on biofilm removal of *B. subtilis,* incubated in 2% glucose M63 for 24h at 37°C without shaking, then clean with PBS diluted D-AA for 30min at room temperature (12-well-plate) 52
Figure 26. Effect of D-AA on biofilm removal of *B. subtilis,* incubated in 2% glucose M63 for 24h at 37°C without shaking, then clean with PBS diluted D-AA for 30min at room temperature (tissue culture dish) 54
Figure 27. The absorbance of CV at 600nm of *B.sutilis* control group and PBS cleaned *B.sutilis* control group in tissue culture dish 54
Figure 28. Effect of D-AA on biofilm formation by *P. aeruginosa,* after incubated in R2A for 14h at 30°C with addition of D-AA initially (24 well plate) 56
Figure 29. Effect of D-AA on biofilm formation by *P. aeruginosa,* after incubated in M63 at 37°C for 24h with addition of D-AA initially (24-well-plate) 56
Figure 30. Confocal Laser Scanning Microscope images of single layer of biofilm formed by *P. aeruginosa,* after 24h incubation in glass slide in glass petri dish in M63 with 2% glucose, with shaking at 95 rpm. Figures in the top showed the biofilm formed with addition of 100μM D-tyrosine initially, while figures in the bottom showed control group without D-tyrosine addition. The first figure in the left represented the amount of combination

of DNA, protein and polysaccharides. Blue color represented the amount of DNA, green color represented the amount of protein, and red color represented the amount of polysaccharides, which showed that after addition of D-tyrosine, biofilm still formed lots of polysaccharides. Source: Cong Yu. Unpublished results 58

Figure 31. Effect of D-tyrosine on biofilm formation by *P. aeruginosa,* after incubated in R2A at 37°C for 12h/24h with addition of D-tyrosine initially (24-well-plate) 59

Figure 32. Effect of D-AA on biofilm formation by *P. aeruginosa*, after incubated in M63 at 30°C for different time with addition of D-AA initially (24-well-plate) 60

Figure 33. Effect of D-tyrosine on biofilm formation by *P. aeruginosa,* one condition is incubated in R2A at 37°C for 12h with addition of D-tyrosine initially, and the other condition is after incubated in R2A at 37°C for 14h then add D-tyrosine for 4h at 37°C (24 well plate) 61

Figure 34. Effect of D-AA on biofilm formation by *P. aeruginosa,* after incubated in M63 at 37°C for 18h, shaking at rpm 95, with addition of D-AA initially (tissue culture dish) 62

Figure 35. Effect of mixture D-AA on biofilm formation by *P. aeruginosa,* after incubated in R2A for 14h at 37°C with addition of mixture D-AA initially (24-well-plate) 62

Figure 36. Effect of D-tyrosine on biofilm removal of *P. aeruginosa,* after incubated in R2A for 14h at 37°C, then clean with R2A diluted D-tyrosine for different time and temperature (24-well-plate) 64

Figure 37. Effect of mixture D-AA on biofilm removal of *P. aeruginosa,* after incubated in R2A for 14h at 37°C, then clean with R2A diluted mixture D-AA for 4h at room temperature (24-well-plate) 64

Figure 38. Effect of D-tyrosine on biofilm removal of *P. aeruginosa,* incubated in M63 for 24h at 30°C, then clean with M63 diluted D-tyrosine for different time at room temperature (24-well-plate) 65

Figure 39. Effect of D-AA on biofilm removal of *P. aeruginosa,* after incubated in M63 with 2% glucose for 18h at 37°C, shaking at rpm 95, then clean with M63 with 2% glucose diluted D-AA for 1h at room temperature

(12-well-plate) 66
Figure 40. Effect of D-AA on biofilm removal of *P. aeruginosa,* incubated in M63 with 2% glucose for 18h at 37°C, shaking at rpm 95, then clean with PBS diluted D-AA for 0.5h at room temperature (12-well-plate)..... 66
Figure 41. Effect of D-AA on biofilm removal of *P. aeruginosa,* after incubated in M63 for 18h at 37°C, shaking at rpm 95, then clean with PBS diluted D-AA for 0.5h at room temperature (tissue culture dish) 67
Figure 42. The absorbance of CV at 600nm of *P.aeruginosa* control group and PBS cleaned *P.aeruginosa* control group in tissue culture dish 68
Figure 43. Bench scale dead end NF90 membrane filtration experiment without D-tyrosine addition 70
Figure 44. The effect of D-tyrosine on inhibiting flux decline caused by organic fouling (LB) in conditioning stage (normalized flux) 71
Figure 45. The effect of D-tyrosine on inhibiting flux decline caused by organic fouling (LB) and *P. aeruginosa* biofouling in fouling stage (normalized flux) 72
Figure 46. Effect of 4-mixture D-AA on *P. aeruginosa* biofilm formation, after 14h incubation at 37°C in R2A medium, with addition of 4-mixture D-AA initially. 82
Figure 47. Effect of D-tyrosine on *P. aeruginosa* biofilm formation, after 24h incubation at 37°C in R2A medium, with addition of D-tyrosine initially. 83
Figure 48. Effect of D-tyrosine on *P. aeruginosa* biofilm formation, after 12h incubation at 37°C in R2A medium, with addition of D-tyrosine initially. 83
Figure 49. Effect of D-AA on *P. aeruginosa* biofilm formation, after 14h incubation at 30°C in R2A medium, with addition of D-AA initially..... 84
Figure 50. Effect of D-AA on *P. aeruginosa* biofilm formation, after 48h incubation at 30°C in M63 medium, with addition of D-AA initially..... 84
Figure 51. Effect of D-AA on *P. aeruginosa* biofilm formation, after 24h incubation at 30°C in M63 medium, with addition of D-AA initially..... 85
Figure 52. Effect of D-AA on *P. aeruginosa* biofilm formation, after 18h

incubation at 30°C in M63 medium, with addition of D-AA initially..... 85
Figure 53. Effect of D-AA on *P. aeruginosa* biofilm formation, after 24h incubation at 37°C in M63 medium, with addition of D-AA initially..... 86
Figure 54. Effect of D-tyrosine on existing *P. aeruginosa* biofilm, after 14h incubation at 37°C in R2A medium, then clean with R2A diluted D-tyrosine for 4h at 37°C. 86
Figure 55. Effect of D-tyrosine on existing *P. aeruginosa* biofilm, after 24h incubation at 30°C in M63 medium, then clean with M63 diluted D-tyrosine for 15min at room temperature. 87
Figure 56. Effect of D-tyrosine on existing *P. aeruginosa* biofilm, after 24h incubation at 30°C in M63 medium, then clean with M63 diluted D-tyrosine for 30min at room temperature. 87
Figure 57. Effect of D-tyrosine on existing *P. aeruginosa* biofilm, after 24h incubation at 30°C in M63 medium, then clean with M63 diluted D-tyrosine for 1h at room temperature. 88
Figure 58. Effect of D-AA on existing *P. aeruginosa* biofilm, after 18h incubation at 37°C in M63 with 2% glucose with shaking at 95 rpm, then clean with M63 with 2% glucose diluted D-AA for 1h at room temperature. 88
Figure 59. Effect of D-AA on existing *P. aeruginosa* biofilm, after 18h incubation at 37°C in M63 with 2% glucose with shaking at 95 rpm, then clean with PBS diluted D-AA for 0.5h at room temperature..... 89
Figure 60. Effect of D-tyrosine on *B. subtilis* biofilm formation, after 24h incubation at 37°C in M63 with 2% glucose, with addition of D-tyrosine initially. 90
Figure 61. Effect of 4-mixture D-AA on *B. subtilis* biofilm formation, after 24h incubation at 37°C in M63 with 2% glucose, with addition of 4-mixture D-AA initially. 90
Figure 62. Effect of D-tyrosine on existing *B. subtilis* biofilm, after 24h incubation at 37°C in M63 with 2% glucose, then clean with PBS diluted D-tyrosine for 0.5h at room temperature. 91
Figure 63. Effect 4-mixture D-AA on existing *B. subtilis* biofilm, after 24h incubation at 37°C in M63 with 2% glucose, then clean with PBS diluted

4-mixture D-AA for 0.5h at room temperature. 92

LIST OF TABLES

Table 1. D-amino acids tested 20
Table 2. Growth media 20
Table 3. Ingredient of each screening test solution 25
Table 4. Solution ingredient of each stage in filtration experiment 32
Table 5. Operation time for each stage 32

LIST OF EQUATIONS

Equation 1. 31
Equation 2. Beer-Lambert Law..... 46
Equation 3. 55

1. Introduction

Nowadays, conventional fresh water supplies are polluted due to industrialization and cannot meet the clean water demand in many parts of the world. The treatment of alternative water supplies (brackish water, seawater and wastewater) is an urgent demand around the world, and thus people have paid more attention to membrane filtration processes. Nano-filtration (NF) and Reverse Osmosis (RO) technologies play an important role in wastewater reclamation as well as seawater desalination. However, the most important barrier these treatment technologies face is membrane fouling. In particular, membrane biofouling is considered the bottleneck that limits the application of NF and RO in water and wastewater treatment.

Membrane biofouling refers to the undesirable bacteria attachment and proliferation on the wet membrane surface. Membrane biofouling will cause energy waste due to the increased operation pressure. Membrane biofouling will deteriorate permeate water quality, require frequent chemical cleaning, and even shorten the membrane lifetime. Existing strategies for mitigating NF/RO biofouling include: addition of sanitization agents, such as copper sulfate; use of microfiltration, ultrafiltration, or ultraviolet irradiation as pretreatment methods; application of fouling resistant membranes; and membrane cleaning. Chlorine is a commonly used biocide, but there are major limitations in this pretreatment method. Free chlorine is a strong oxidant, which could damage the active layer of polyamide based thin film composite membranes. Also, chlorination generates carcinogenic disinfection byproducts, leading to human health risk, especially in drinking water treatment [1]. In addition, no pretreatment method can remove bacteria completely from NF/RO

feed water. Even just a few bacteria can grow to a large number if there are enough nutrients. Therefore, even 99.99% removal of bacteria in feed water may not inhibit biofilm formation on the membrane [2]. Excessively frequent chemical cleaning of the membrane will cause chemical corrosion of the membrane.

Recent studies discovered that biological methods have great potential in preventing biofilm formation. Instead of chemically inactivating bacteria, these methods inhibit biofilm formation by quorum quenching, interference of DNA, proteins, and EPS by specific enzyme, inducing biofilm dispersion using biochemical signal compounds such as NO, and disrupting biofilm using D-amino acids [3].

D-amino acid is a component in bacteria cell wall, and is excreted by a wide spectrum of bacteria [4]. Kolodkin-Gal et al. showed that *Bacillus subtilis* excretes four D-amino acids (D-leucine, D-methionine, D-tyrosine, and D-tryptophan) in the late mature stage of biofilm growth. These four D-amino acids serve as signals to trigger disassembly of *Bacillus subtilis* biofilm [5]. When applied to other bacterial species, D-tyrosine was found to effectively inhibit biofilm formation of *Staphylococcus aureus* and *Pseudomonas aeruginosa* on polystyrene surface[5].

D-amino acids do not inhibit bacterial growth at low concentrations and are friendly to membrane material, which is a beneficial aspect in MBR system. Also, D-amino acids are highly effective in inhibiting biofilm formation at low concentration. The application of D-amino acids to inhibit biofilm formation in industry is promising, but there is still some questions need to be resolved before applying D-amino acids to NF/RO system.

Kolodkin-Gal *at el.* [5] discovered that in Gram-positive bacteria, D-tyrosine substituted the terminal D-alanine in the peptide side chains of peptidoglycan in the cell wall. This led to the detachment of a fibrous surface protein, TasA that anchored

on D-alanine in the cell wall, and hence triggered the disassembly of the biofilm. However, whether this mechanism is applied to Gram-negative bacteria or not is still unknown. The bacterial cell wall structure is different between Gram-positive and Gram-negative bacteria. In Gram-positive bacteria, the cell wall is consists of a very thick peptidoglycan layer, which contains N-Acetyl Glucosamine (NAG) and N-Acetyl Muramic acid (NAM). While in Gram-negative bacteria, there are two membranes contained in the cell wall. The inner membrane is a thin peptidoglycan layer linked to the cytoplasmic membrane, and the outer membrane is consists of phospholipids and lipopolysaccharides. Since in Gram-negative bacteria the peptidoglycan layer is not exposed to the environment, so D-tyrosine in solution cannot substitute the terminal D-alanine in the peptide side chains of peptidoglycan. Thus, the mechanism of how D-amino acids inhibits biofilm formation to Gram-negative bacteria still needs to be investigated.

The paper published by Kolodkin-Gal *at el.* [5] revealed that D-tyrosine was effective in inhibiting biofilm formed by *Bacillus subtilis* in air-liquid interface. However, biofilm is formed on the membrane surface in seawater desalination process, which is liquid-solid interface. So whether D-amino acids are effective on inhibition of biofilm formed on liquid-solid interface needs to be addressed before further apply this method in industry. Also, the impact of bacteria growth conditions to the inhibition of biofilm formation effect of D-amino acids is unknown. In the paper published by Kolodkin-Gal *at el.* [5], D-amino acids were effective on inhibition of biofilm formation to *Bacillus subtilis* after incubating in MSgg at 22°C for 3 days. However, different growth conditions (nutrient level, incubation time and temperature, substrate material) will influence the effect of D-amino acids on inhibition of biofilm formation. This aspect needs to be tested in order to determine

the applicability of D-amino acids in NF and RO system.

Based on the questions addressed, the objective of this study is to investigate the effect of D-amino acids on inhibition of biofilm formation, as well as disruption of the existing biofilm to Gram-positive and Gram-negative bacteria on polystyrene surface under different growth conditions. D-tyrosine and the mixture of D-amino acids (D-leucine, D-methionine, D-tyrosine, and D-tryptophan) were tested. *Pseudomonas aeruginosa* and *Bacillus subtilis* were the model bacteria of Gram-negative bacteria and Gram-positive bacteria used in all experiments.

A reproducible and high throughput assay for such purpose was developed by screening tests. D-amino acids have little effect and some effect on inhibition of biofilm formation and disruption of exiting biofilm to *Pseudomonas aeruginosa*, but have good effect to *Bacillus subtilis,* which is mainly because of their different bacterial type.

Also, the conditions for growing robust and well-attached biofilm were studied. The effect of D-tyrosine on inhibition of organic fouling and *P. aeruginosa* biofouling on NF90 membrane surface in bench scale dead end filtration experiment was examined, which showed that D-tyrosine could effectively inhibit organic fouling and *P. aeruginosa* biofouling on NF90 membrane surface.

The conclusion in this study reveals that D-amino acids are promising in applying to industrial NF/RO system for biofilm inhibition. But other researches should be done prior to this, for example, the inhibition effect of biofilm formation of D-amino acids on mix-culture bacteria, and the cleaning effect of D-amino acids on exiting biofilm to different membrane modules.

2. Literature review

2.1 Clean water issue and membrane filtration technology

Water scarcity is a serious issue that people are facing nowadays. World population grows rapidly in the 21st century, as well as the development of technology and industrialization. People have excessively exploited the water resource around the world; conventional fresh water supplies can no longer meet people's clean water demand. People start to focus on the treatment of alternative water supplies (brackish water, seawater, wastewater) in order to solve the clean water scarcity. Developing effective treatment technologies for alternative water supplies is an urgent demand. Nanofiltration (NF) and Reverse Osmosis (RO) technologies are potential solution to the global water crisis.

One of the commonly used wastewater treatment methods is filtration. Filtration is the physical process that separates the unwanted substances from fluids by inserting a filter in the fluids phase so that unwanted substances would be excluded from the filter. Filtration methods include sand filtration, diatomaceous earth filtration and membrane filtration. Membrane filtration technology has been widely used in wastewater treatment plant and has improved permeate effluent quality.

A membrane is a thin layer of semi-permeable material that separates substances based on their size or chemical property differences, and membrane separation process works as a pressure driving the fluid through the membrane from the feed water side to the effluent water side. Membranes used for drinking water treatment are made of polymeric material and ceramic material [3]. Membrane filtration can

remove organic matter, bacteria and microorganisms based on different types of membrane material.

Four types of membrane are used in water and wastewater treatment: microfiltration (MF), ultrafiltration (UF), nanofiltration (NF), and reverse osmosis (RO). Based on the operating pressure, MF and loose UF are categorized as low-pressure membranes; while tight UF, NF, and RO are considered high-pressure membranes [6]. MF membranes have pore sizes between 0.03 and 10 microns and require an operating pressure of 15 to 60 psi. MF membranes can remove clays, sand and most bacteria. They are commonly used as a pretreatment process for RO and NF systems to remove particulate matter in order to decrease possible fouling. UF membranes have pore size of 0.02 to 0.1 microns and require operating pressure of 30 to 100 psi. Both MF and UF are used for disinfection purpose as it can remove microorganisms and some viruses. NF membranes have pore sizes of ~ 0.001 microns and operate at 90 to 150 psi. NF can remove all bacteria and viruses and can be used for softening due to its high rejection of divalent ions. RO membranes are considered non-porous and remove contaminants through size exclusion and Donnan exclusion. RO can remove some inorganic contaminants from water, as well as bacteria and viruses. Membrane filtration technology has becoming more and more popular and widespread nowadays as membrane filtration can achieve high removal of contaminants [7].

NF and RO membrane treatment is the key component in treating alternative water supplies for potable and non-potable applications. Pressure is the driving force in NF/RO membrane filtration. NF is broadly used in brackish water and wastewater treatment, while RO is widely applied in seawater desalination and wastewater reuse.

The advantage of NF/RO technology is its high productivity and high effluent quality. However, the limitation of NF/RO technology is the membrane fouling issue.

2.2 Membrane biofouling

2.2.1 Membrane fouling cause and consequences

Membrane fouling is defined as the unwanted material accumulated on the membrane surface. Different types of membrane fouling are inorganic fouling, organic fouling, colloidal fouling and biofouling. The common foulants in water and wastewater are natural organic matter (NOM), particulate matter, suspended solid, inorganic colloids, ions and microorganism. Among them, NOM, inorganic matter and microorganism are the most important foulants [8]. Membrane fouling has two categories: reversible fouling and irreversible fouling. Reversible fouling is due to cake layer or concentration polarization mechanism, and can be restored by physical washing procedures. While chemical sorption and pore plugging mechanism cause irreversible fouling, which cannot be recovered by physical washing [6]. Biomass and feed water characteristic, as well as operation conditions affect membrane fouling [9]. The consequence of membrane fouling is the increase of membrane flow resistance caused by pore blocking, cake formation and concentration polarization [10]. Membrane fouling will reduce effluent water quality and productivity, require extensive pretreatment and frequent chemical cleaning, and premature replacement of membrane modules, which all lead to higher maintenance cost.

2.2.2 Biofilm formation

Among membrane fouling, biofouling is the most difficult to control and is a severe challenge in membrane treatment technology [11]. Biofouling is triggered by deposition, attachment and proliferation of the bacteria on wet membrane surface [12].

In the life cycle of a biofilm, the bacteria experience five phases: planktonic cell, attached cell, microcolony, biofilm and detached cell [13]. In the first stage, the planktonic bacteria deposit and attach loosely on the membrane surface. This process occurs in seconds and the attachment is reversible. This reversible attachment of bacteria on the membrane surface is influenced by many factors: motility, bacteria characterization, hydrophobic interaction, and membrane surface characteristics [14]. The electrostatic and hydrophobic interactions between bacteria and membrane surface are crucial for the initial bacteria attachment. The attachment is more easily to happen on non-polar hydrophobic surfaces [15]. In the second stage the bacteria secrete extracellular polysaccharide substances (EPS), which bind to the membrane surface and lead to irreversible attachment of bacteria. The EPS matrix consists of polysaccharides, glycoproteins, lipoproteins, proteins, DNA, humic acids and lipids. [16]. It helps to enhance microbial attachment and protects bacteria from antibiotic agents and hydraulic shear force [17]. In the third stage, biofilm grows and mature. The attached bacteria grow and multiply over several days and form biofilm, in which bacteria communicate through quorum sensing. The porous structure of the biofilm allows water and nutrient passage. In the final stage due to the lack of nutrients, the bacteria cells will disperse from the center of microcolonies and cells may leave the biofilm [17].

Membrane biofouling is a very complex process and is influenced by many factors, like operation conditions, membrane material, bacteria characteristics and aqueous solution condition [18]. Biofouling occurs in NF/RO system when microorganism deposit, attach and proliferate on NF/RO membrane surface. The operation conditions, bacteria characteristics, and feed water composition will affect the biofouling on NF/RO system.

2.2.3 Effects of biofouling on NF/RO membrane performance

Membrane biofouling has severe negative impact on membrane filtration systems. Biofouling causes damage on membrane materials by biodegradation, decrease in salt rejection, flux decline, and higher energy and maintenance cost [19]. The main consequences of biofilm formation on NF/RO membranes are permeate flux reduction and salt rejection decline [20]. The permeate flux decline is caused by the hydraulic resistance generated by biofilm, as well as the "biofilm-enhanced osmotic pressure" caused by bacteria in EPS [21]. The flux decline due to biofouling usually exhibits a two-phase behavior: a rapid decline phase followed by a slow decline phase. The initial rapid flux decline is due to the attachment and subsequent multiplication of bacteria on the membrane surface, while the gradual decline is related to the low rate of bacterial transport to the membrane surface due to the lower permeate flux, as well as the increased hydraulic shear due to the reduced cross-sectional area of the flow channel [1]. The formation of the biofilm will cause the increasing of the pressure demand in order to maintain the constant permeate flux, which results in a huge increase in energy consumption in large membrane treatment plants.

Herzberg and Elimelech [22] elucidated the different roles of bacteria cell and EPS in RO permeate flux decline. The deterioration of RO membrane performance is

due to the increased hydraulic resistance, which is caused by the EPS surrounding bacteria cells, and increased trans-membrane osmotic pressure, which is caused by accumulation of bacteria cell that improved the concentration polarization of salt on the membrane surface. Salt rejection decline is caused by concentration polarization, which is the result of formation of EPS matrix. Besides EPS, biofilm formed on the membrane surface will enhance the transportation of salt across the membrane [22, 23]. Biodegradation of the RO membrane material is another reason for salt rejection decrease [24].

2.3 Biofouling control strategies in NF/RO systems

Biofouling is the bottleneck in the application of NF/RO technology. The components of other fouling (inorganic fouling, organic fouling, and colloidal fouling) can be removed by pretreatment process [25]. However, biofouling cannot be totally controlled by pretreatment. Bacteria can self-multiply and even they are removed by 99.99%, the remaining bacteria will grow and multiply if there are enough nutrients [2]; and there is always nutrients in natural water and wastewater. Because RO and NF membranes retain almost all organic compounds, nutrients accumulate on the membrane surface on the feed water side, i.e., the concentrations of nutrients are higher near the membrane surface than in the bulk feed water. The high nutrient concentration at the membrane surface facilitates bacterial adhesion and biofilm formation [26].

Conventional methods for biofouling prevention and control in membrane systems include feed water pretreatment, biocide addition, membrane surface modification and membrane cleaning [1].

2.3.1 Feed Water Pretreatment

The purpose of pretreatment is to reduce the potential fouling substances in the feed water [1]. After pretreatment, organic and inorganic particles and microorganisms will be partially removed. Pretreatment is crucial in NF/RO processes as it can significant reduce the possibility for membrane fouling [27]. Both conventional and unconventional treatment processes have been used for NF/RO feed water pretreatment. Conventional pretreatment involves disinfection, coagulation/flocculation and sand filtration processes. While unconventional pretreatment includes microfiltration (MF) and ultrafiltration (UF) systems [28]. Nowadays people tend to apply unconventional pretreatment methods due to the high efficiency of membrane technology and the avoidance of feed water deterioration by conventional pretreatment [29]. UF/MF pretreatment results in lower fouling potential, lower energy consumption, and longer membrane module lifetime [30]. UF based RO pretreatment has been widely applied, as UF can remove particulate and microorganism, which can lower the fouling potential on RO membrane [29].

2.3.2 Biocide addition

Biocides are disinfecting chemical that can kill microorganisms and control biofouling on membrane surface. Conventional biofouling inhibition method is to continuously add biocides into the feed water in order to control microbial growth [31]. Chlorine, ozone and UV light are the commonly used chemicals or physical biocides for membrane biofouling control. Chlorine is an effective biocide for inhibiting biofilm formation. A residual of 0.04-0.05 mg/L free chlorine in feed water will inhibit biofilm formation [32]. Other than free chlorine, mono-chloramine and

chlorine dioxide are also considered as effective biocides [33]. Ozone has been broadly applied in drinking water treatment plant because of its strong oxidation ability, as well as less production of halogenated by-products while it works as a disinfectant [20]. Ultraviolet (UV) light irradiation at 254 nm can prevent bacteria growth by damaging the microorganism genetic code [34].

However, the disadvantage of applying chlorine and ozone as biocides is their strong oxidation ability that will damage the polyamide skin layer of thin film composite NF and RO membrane [35]. Therefore, residual chlorine and ozone should be removed before the feed water entering the RO membrane process. The normally used de-chlorination reagent is sodium bisulfite ($NaHSO_3$). The challenges of using ozone are its high cost and it should be removed from feed water prior to NF/RO treatment [36].

2.3.3 Membrane surface modification

Membrane surface modification is to change the membrane surface properties in order to achieve anti-bacteria and/or bacterial anti-adhesion functions. Because the initial bacterial adhesion on a surface is governed by physicochemical interactions including electrostatic interaction and hydrophobic interaction, the surface charge and hydrophobicity of the membrane material have been manipulated to minimize bacterial adhesion. Studies have shown that increasing the membrane surface hydrophilicity or negative charge can significantly inhibit membrane biofouling [37].

Another approach is to incorporate biocides into the membrane so as to kill the bacteria that attach on the membrane surface. Broadly used coating biocides include heavy metals, photocatalysts, antimicrobial polymers, and carbon nanomaterials [38].

The most broadly used semiconductor photocatalyst is titanium dioxide (TiO2). After activated by UV-A irradiation, the photocatalytic effect of TiO2 can degrade organic substances and kill bacteria and viruses [39]. TiO2 photocatalysis can produce reactive oxygen species (ROS) through both oxidative and reductive pathways under UV light, and the produced ROS can damage bacteria membrane and kill the bacteria [40]. The effective concentration of TiO2 to kill bacteria depends on the size of the bacteria and the wavelength of the UV light. Typical concentration used is between100 and 1000 ppm [38, 40].

Another widely used anti-biofouling agent is silver. UV light irradiation will enhance the germicidal activity of silver irons [41]. Silver ions can effectively control bacteria growth by combining with thiol groups in bacterial proteins, and thus inactivate the bacteria [42]. Silver ions can inhibit bacteria's DNA replication and damage the structure and permeability of the bacteria cell membrane [43]. Two mechanisms of anti-microbial for silver nanoparticles are as follows: silver nanoparticles will enter into bacterial cells and damage their DNA; silver nanoparticles can release antimicrobial silver irons [38, 44].

2.3.4 Membrane cleaning

In practice, RO/NF membrane cleaning is performed to recover the permeate flux after the permeate flux declines by 10% of the original permeate flux [45]. Frequently used chemical cleaning reagents include acids, alkalis, surfactants, chelating agents, and enzymes. The choice of chemical cleaning reagent is based on the feed water composition and fouling material on the membrane surface [46]. Alkalis solution is effective in cleaning organic scaling and acids solution is effective in cleaning

inorganic scaling [47]. Enzymes are especially used to clean biofouling. Surfactants and chelating agents are usually used to clean NF/RO membrane.

The mechanism of cleaning the biofilm is to use chemical reagents to weaken the bonds formed among bacteria cells, EPS and the membrane surface and therefore damage the biofilm, or to remove the biofilm from the membrane surface by hydraulic shear force [1, 20]. However, oxidants reagent will degrade the membrane material due to its high oxidation ability. Using enzymes to clean membrane biofouling is another option, but it takes a long time for the enzyme to degrade the biofilm [3]. A better solution for biofilm cleaning is needed.

2.3.5 Biological methods for biofouling inhibition

Biological control of biofilm formation is a novel strategy. Instead of killing the bacteria, biological strategies focus on impeding the biofilm formation process. Biological strategies have great potential in control biofilm formation in membrane bioreactors, as bacteria death is unwanted. Also biological strategies will not damage membrane material, as it does not have oxidation ability. Compared to using antibiotic reagents, biological methods will not trigger the resistance to antibiotics reagents of bacteria.

Several biological mechanisms have been shown to inhibit biofilm formation by disrupting biofilm formation process, including applying signal molecule NO to disrupt quorum sensing [3].

Bacteria can use quorum sensing to communicate among single and various species [48], and coordinate a number of biological behaviors, such as motility, sporulation, production of extracellular polysaccharides, as well as formation of biofilm [49]. Quorum sensing involves the production, release and detection of

quorum sensing signal compounds, which are called autoinducers (AIs) [3]. Scientists have identified three types of autoinducers: N-acylhomoserine lactones (AHL), autoinducer-2 (AI-2) synthesized by LuxS, and oligopeptides. Oligopeptides are used among Gram-positive bacteria, while AHL regulates Gram-negative bacteria. AI-2 is a universal signal that is used for interspecies communication including that between Gram-positive and Gram-negative bacteria [50].

It is commonly believed that as the concentration of the autoinducer increased to a threshold concentration caused by increased bacteria density, the autoinducer binds to the receptor protein, so that the regulator protein is triggered and it activates target DNA sequences, further enables transcription of quorum sensing controlled genes. All these processes will eventually activate bacteria social biological behaviors [51]. As quorum sensing plays an important role in bacteria communication and biofilm formation process, disturbing or inhibition of quorum sensing system among microorganisms will be a promising method in inhibiting membrane biofouling [52]. Moreover, experimental evidence has proved that inhibition of AI or quorum sensing regulator genes can control membrane biofouling [53].

There are four ways to control quorum sensing: blockage of the production of AIs; inactivation or degradation of autoinducers; using analogs of AIs to block AI receptor sites; and damage of AI receptors [54]. Among them, inactivation or degradation of AIs is the most effective method in controlling quorum-sensing system in lab studies; for example, N-acylhomoserine lactones (AHL)-degrading enzymes can degrade AHLs and prevent the quorum sensing process. Two groups of enzymes can degrade AHLs: AHL-lactonases and AHL-acylases [53, 55].

Disruption of quorum sensing did not inhibit bacteria growth and can trigger the biofilm dispersion, so this is a promising method for inhibition of biofilm formation strategies.

2.4 D-amino acids in biofouling prevention

Amino acids are the building blocks of proteins. Bacteria use L-amino acids as their food and structural components, but bacteria or other biological species do not commonly use D-amino acids. D-amino acids, such as D-alanine and D-glutamate, are found in all eubacteria cell wall [56]. Many bacteria generate different kinds of D-amino acids in stationary phase, For example, *B. subtilis* generates D-tyrosine and D-phenylalanine, and *V. cholerae* generates D-leucine and D-methionine [4].

Scientists recently find that D-amino acids are effective in controlling biofilm formation without inhibition of bacteria growth [5, 52]. Kolodkin-Gal *at el.* [5] discovered that after 6-8 days of incubation, the pellicles formed by *B. subtilis* at the surface of a liquid medium that encourages biofilm growth started to disassemble; the disassembly of the biofilm was attributed to the presence of four D-amino acids that the *B. subtilis* biofilm secretes: D-tyrosine, D-tryptophan, D-leucine and D-methonine. Their corresponding L-amino acids had no inhibited effect on *B. subtilis* biofilms. The minimum effective concentration of each D-amino acid was reported to be 3μM, 2mM, 5mM, and 8.5 mM for D-tyrosine, D-methionine, D-tryptophan, and D-leucine. Mixture of these four D-amino acids has synergetic effect and the minimum effective concentration of all these four D-amino acids is 10nM. When applied to other bacterial species, D-tyrosine was found to effectively inhibit biofilm formation of *Staphylococcus aureus* grown in TSB medium containing glucose (0.5%) and NaCl (3%), and *Pseudomonas aeruginosa* grown in M63 medium on polystyrene surface

[5].

In another study, Xu *at el.* proved that when the activated sludge microorganisms, which grew in synthetic substrate, were exposed to 6mg/L D-tyrosine, the bacterial attachment to nylon membrane surface reduced significantly without inhibition of bacteria growth. D-tyrosine could also inhibit the secretion of AI-2 and production of EPS without changing the cellular ATP content. D-tyrosine could remove the fixed biomass on nylon membrane surface, and higher D-tyrosine concentration had better removal effect. This study demonstrated that D-tyrosine was effective on inhibition of biofilm formation on membrane surface and cleaning of biofouled membrane [52]

Two different mechanisms were reported in these two studies. Kolodkin-Gal *at el.* [5] showed that in *B. subtilis*, D-tyrosine substituted the terminal D-alanine in the peptide side chains of peptidoglycan in the cell wall. This led to the detachment of a fibrous surface protein, TasA that anchored on D-alanine in the cell wall, and hence triggered the disassembly of the biofilm. This mechanism can be applied in the inhibition of biofilm formation of *Staphylococcus aureus,* as *Staphylococcus aureus* is also a Gram-positive bacterium. However, the mechanism cannot be applied in inhibition of biofilm formation in *Pseudomonas aeruginosa,* as *Pseudomonas aeruginosa* is a Gram-negative bacterium. The bacterial cell wall structure is different between Gram-positive and Gram-negative bacteria. In Gram-positive bacteria, the cell wall is consists of a very thick peptidoglycan layer, which contains N-Acetyl Glucosamine (NAG) and N-Acetyl Muramic acid (NAM). While in Gram-negative bacteria, there are two membranes contained in the cell wall. The inner membrane is a thin peptidoglycan layer linked to the cytoplasmic membrane, and the outer membrane is consists of phospholipids and lipopolysaccharides. Since in Gram-negative bacteria the peptidoglycan layer is not exposed to the environment, so

D-tyrosine in solution cannot substitute the terminal D-alanine in the peptide side chains of peptidoglycan. Xu *at el.* [52], however, suggested that D-tyrosine could inhibit the production of AI-2 and EPS.

The strong inhibitive effect of D-amino acids on biofilm formation of both Gram positive and Gram negative bacteria suggest that they may have potential in biofouling control applications. They are particularly attractive in water and wastewater treatment systems as D-amino acids are non-toxic. D-amino acids do not inhibit bacteria growth. D-tyrosine does not influence bacteria growth, substrate utilization and the synthesis of cellular ATP. [52, 57]

3. Experimental methods

Effects of D-amino acids on inhibition of biofilm formation and disruption of existing biofilm to *P. aeruginosa* and *B. subtilis* were tested by microtiter plate and tissue culture dish biofilm assay. Effect of D-tyrosine on inhibition of organic fouling and *P. aeruginosa* biofouling on NF90 membrane was tested by bench scale dead end filtration experiments.

3.1 Materials

3.1.1 Chemicals

Crystal violet indicator (Fisher Scientific, Pittsburg, PA) is for staining biofilm. The ethanol (Fisher Scientific, Pittsburg, PA) used to extract the crystal violet dye is 200 proof.

23 L-amino acids naturally exist as organic compounds in proteins; only 19 of them have D-isomers, which are called D-amino acids. D-tyrosine and D-amino acids mixture (D-tyrosine, D-tryptophan, D-leucine and D-methionine) were tested, which are the most effective ones in inhibition of biofilm formation.

Table 1. D-amino acids tested

Name	Molecular weight (g/mol)	Molecular structure	Molecular formula	Purity	Vendor
D-tyrosine	181.19	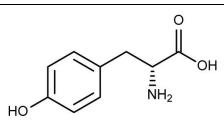	$C_9H_{11}NO_3$	99%	ALDRICH Chemistry
D-tryptophan	204.23	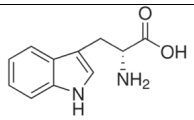	$C_{11}H_{12}N_2O_2$	99%	Alfa Aesar
D-leucine	131.17	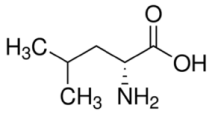	$C_6H_{13}NO_2$	99%	ALDRICH Chemistry
D-methionine	149.21	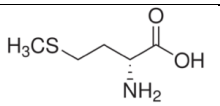	$C_5H_{11}NO_2S$	99%	MP Biomedicals

3.1.2 Growth Media

Table 2. Growth media

Growth Media	Ingredient	General purpose
BBL™ Trypticase™ Soy Broth (BD, Fisher Scientific, Pittsburg, PA)	17g pancreatic digest of casein, 3g papaic digest of soybean, 5g sodium chloride, 2.5g dipotassium phosphate, 2.5g dextrose	Prepare for TSA plates, TSB liquid culture
Bacto™ Agar (BD, Fisher Scientific, Pittsburg, PA)	Agar	Prepare for TSA plates
BBL™ Luria-Bertani (LB) broth (BD, Fisher Scientific, Pittsburg, PA)	10g tryptone, 5g yeastn extract, 5g sodium chloride per liter	Bench scale filtration experiment as the liquid nutrient media
R2A Broth Media (TEKnova, Hollister, CA)	0.05% proteose peptone, 0.05% casamino acids, 0.05% yeast extract, 0.05% glucose, 0.05% starch, 0.03% sodium pyruvate, 0.03% dipotassium phosphate, 0.005% magnesium sulfate.	Nutrient media for screening tests
M63 Media Broth (per liter of ultra pure water)	12g Potassium Phosphate Monobasic (Fisher Scientific, Pittsburg, PA), 28g Potassium Phosphate Dibasic Trihydrate (Sigma-Aldrich, St. Louis, MO), 8g Ammonium Sulfate (Fisher Scientific, Pittsburg, PA),	Nutrient media for screening tests

	supplemented with 1mmol/L of Magnesium Sulfate (Avantor, Center Valley, PA), 0.2% D-(+)-Glucose anhydrous (Sigma-Aldrich, St. Louis, MO) and 0.5% Casamino Acids (Fisher Scientific, Pittsburg, PA)	
2% glucose M63 Media Broth (per liter of ultra pure water)	12g Potassium Phosphate Monobasic (Fisher Scientific, Pittsburg, PA), 28g Potassium Phosphate Dibasic Trihydrate (Sigma-Aldrich, St. Louis, MO), 8g Ammonium Sulfate (Fisher Scientific, Pittsburg, PA), supplemented with 1mmol/L of Magnesium Sulfate (Avantor, Center Valley, PA), 2% D-(+)-Glucose anhydrous (Sigma-Aldrich, St. Louis, MO) and 0.5% Casamino Acids (Fisher Scientific, Pittsburg, PA)	Nutrient media for screening tests

3.1.3 Biofilm culture plates

Polystyrene 96-well-plate treated for tissue culture, flat bottom with lid (Costar, Coring, NY), Polystyrene 24-well-plate treated for tissue culture, flat bottom with lid (Costar, Coring, NY), Polystyrene 12-well-plate treated for tissue culture, flat bottom with lid (Costar, Coring, NY), 35x10mm style tissue culture dish treated for tissue culture (Falcon, Franklin Lakes, NJ) were used for the microtiter plate assay.

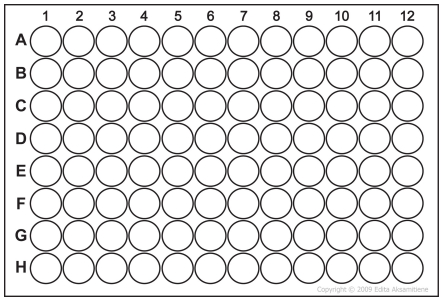

Figure 1. 96-well-plate

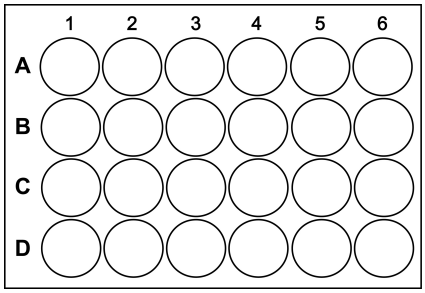

Figure 2. 24-well-plate

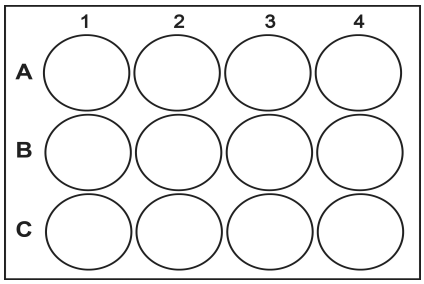

Figure 3. 12-well-plate

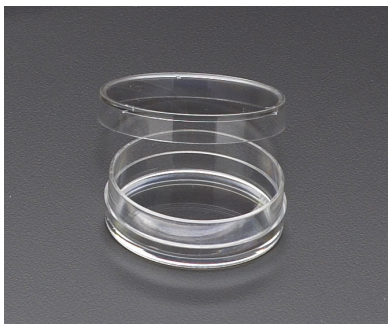

Figure 4. 35x10mm style tissue culture dish

3.1.4 Membrane

A commercial polyamide thin-film composite nanofiltration membrane, NF90 (DOW FilmTec, Minneapolis, MN) was used in the membrane biofouling experiments. The membrane was received in the form of dry flat sheets. It was cut into 35.3 cm^2 round coupons and stored in ultrapure water at 4°C for at least 24 hours before use.

3.1.5 Model bacteria

Pseudomonas aeruginosa (P. aeruginosa) ATCC #700829 and *Bacillus subtilis (B. subtilis)* ATCC #6051 were used as model bacteria to study the effect of D-amino acids on biofilm formation by Gram positive and Gram negative bacteria. *P. aeruginosa* is a Gram negative bacterium and *B. subtilis* is a Gram positive bacterium. They are both biofilm-forming bacteria commonly used as model bacteria in NF/RO membrane antifouling studies.

P. aeruginosa and *B. subtilis* purchased from ATCC were kept in glycerol at -80°C. To grow the bacteria cultures, the inoculum was retrieved, spread over a trypticase soy agar (TSA) plate, and incubated for 24 hours at 37°C. Then a colony of the bacteria cell will be retrieved again to another TSA plate and incubated for 24 hours at 37°C. The bacteria from this TSA plate were used as the seed for all following experiments; also the inoculums from this plate were used for the liquid cultures. This TSA plate was kept in dark at 4°C in a refrigerator prior to use, and was re-inoculated from the previous plate every week.

To prepare liquid cultures for the experiments, a loopful of bacterial cells were transferred to a 15 mL plastic tube (Fisher Scientific, Pittsburg, PA) that had 6mL of Trypticase Soy Broth (TSB), and the tube would be incubated at 37°C. *P. aeruginosa* was incubated for 24 hours and *B. subtilis* was incubated for 18 hours.

The cell concentration in the liquid cultures was determined by plate counting. After the incubation, the concentration of each kind of bacteria of was around 1×10^8 CFU/mL, which was measured by TSA plate counting. The cell suspension was serially diluted with sterilized phosphate biological saline (PBS) buffer (1X), and 100 μL of the diluted suspension was transferred and spread using a glass spreader onto a

TSA agar plate.

3.2 Methods

3.2.1 Evaluating the effect of D-amino acids on bacterial biofilm formation

Liquid cultures of *P. aerugisnosa* and *B. subtilis* were grown in TSB at 37°C for 24 and 18 hours, respectively. The viable bacteria cell concentration was determined by plate counting, which was around 1×10^8 CFU/mL. The liquid culture was washed twice by centrifugation using PBS buffer, and diluted with PBS buffer to $\sim1\times10^5$ CFU/mL, which was the concentration added into the plate. Each of the solution was prepared as following.

Table 3. Ingredient of each screening test solution

Column	Blank (Volume fraction)	Control (Volume fraction)	Treatment (Volume fraction)	D-amino acids clean (Volume fraction)
Sterilized DI water	20%	10%	--	--
Nutrient medium	80%	80%	80%	--
D-amino acids solution (1mM, 500μM, 50μM, 10μM, 5μM, 10nM, 5nM)	--	--	10%	--
Bacteria solution (10^5 CFU/mL)	--	10%	10%	--
D-amino acids diluted with PBS buffer (1mM, 500μM, 50μM, 10μM, 5μM, 10nM, 5nM)	--	--	--	100%

96-well-plate, 24-well-plate, 12-well-plate and tissue culture dish were used to incubate the biofilm. The volume of control and treatment solution, PBS solution, crystal violet solution, 95% ethanol solution, and the D-amino acids cleaning solution added into each well was different among 96-well-plate, 24-well-plate, 12-well-plate and tissue culture dish, which were in ratio with the bottom surface of each well. So that the ratio of the volume of solution with bacteria cells number was the same in different plate types.

On 96-well-plate, columns 1 to 3 were used as blank (media only), columns 4 to 6 as negative control (no D-amino acids) and columns 7 to 12 for treatment (with

D-amino acids addition). Each well contained a total volume of 100μL solution and the composition in each well is shown in Table 3.

On 24-well-plate, column 1 was used as blank (media only), column 2 as negative control (no D-amino acid) and columns 3 to 6 for treatment (with D-amino acid addition). Each well contained a total volume of 1mL solution and the composition in each well is shown in Table 3.

On each 12-well plate, column 1 was used as the blank (media only), column 2 as negative control (no D-amino acid) and columns 3 and 4 for treatment (with D-amino acid addition). Each well contained a total volume of 2 mL solution and the composition in each well is shown in Table 3.

On 35x10 mm style tissue culture dish, each dish was used as the blank (media only), negative control (no D-amino acids) and treatment (with D-amino acids addition). Each well contained a total volume of 2.5 mL solution and the composition in each well is shown in Table 3.

For *P. aerugisnosa*, the microtiter plate was incubated at 37°C, both shaking at rpm 95 or without shaking, the incubation time was tested for 8h, 12h, 18h, 24h or 48h; for *B. subtilis*, the microtiter plate was incubated at 37°C, both shaking at rpm 95 or without shaking, the incubation time was tested for 15h or 24h. After incubation, the liquid in each well was discarded; the way of discarding the liquid out was tested by pipetting the liquid out of each well and by inverting the plates upside down to dump the liquid. Then each well was washed with PBS buffer for two times. Each of the experiment was tested in parallel; the number of experiments was listed in Appendix part.

For the crystal violet assay, 25μL (for 96-well-plate), 250μL (for 24-well-plate), 380μL (for 12-well-plate) 1% Crystal Violet, 450μL (for tissue culture dish) 0.2%

Crystal Violet was added into each well, and waited for 25min in order to let the crystal violet stain the biofilm. The concentration of crystal violet solution was 1% when applying 96-well-plate, 24-well-plate and 12-well-plate, and was changed to 0.2% after applying tissue culture dish.

Then each well was washed with 200μL (for 96-well-plate), 2mL (for 24-well-plate), 2.5mL (for 12-well-plate), 3mL (for tissue culture dish) sterilized DI water for 2 times, and then 200μL (for 96-well-plate), 2mL (for 24-well-plate), 2.5mL (for 12-well-plate), 3mL (for tissue culture dish) 95% ethanol (200 proof, Fisher Scientific, Pittsburg, PA) was added into each well to extract the Crystal Violet. The plates were put in the incubator at 37°C for 2 hours, then 125μL of the extracted ethanol in each well was transfer to the 96-well-plate to measure the absorbance of crystal violet at 600nm in microtiter plate reader.

Fixation step was applied after earlier failure of biofilm lost. It was applied before the crystal violet staining step. The fixation step was tested by room temperature air drying, fixation by methanol addition, and heat fixation by leaving the plates in incubator (Isotemp Oven) at 60°C for 1 hour.

3.2.2 Evaluating the effect of D-amino acids on existing bacterial biofilm

To investigate the impact of D-amino acids on existing biofilm, biofilm was grown in 24-well-plate, 12-well-plate and tissue culture dish following a protocol similar to that described previously. For 24-well-plate and 12-well-plate, column 1 was blank wells (media only), and the rest wells were filled with media and bacteria (control wells in Table 3); for tissue culture dish, one dish was blank (media only), others were filled with media and bacteria (control wells in Table 3). For *P.*

aerugisnosa, the microtiter plates were incubated at 30°C or 37°C, both shaking at rpm 95 or without shaking for 14h, 18h or 24h, the media tested were R2A, M63 and M63 with 2% glucose; for *B. subtilis*, the microtiter plates were incubated at 37°C without shaking for 24h, the media tested was M63 with 2% glucose. After incubation, the liquid in each well was discarded by inverting the plates upside down to dump the liquid. To the blank wells (column 1) and control wells (column 2), 1mM PBS buffer was added in 24-well-plate, and 2mL PBS buffer was added in 12-well-plate, while 1mL of D-tyrosine solution or the mixture of the 4 D-amino acids solution of the designed concentrations was added to each of the remaining wells with grown biofilm (treatment wells, column 3 to the last column of each microtiter plate) in 24-well-plate, 2mL of D-tyrosine solution or the mixture of the 4 D-amino acids solution of the designed concentrations was added to each of the remaining wells with grown biofilm (treatment wells, column 3 to the last column of each microtiter plate) in 12-well-plate. The microtiter plate was then shaken on an orbital shaker table (VWR, Radnor, PA) at 37°C or room temperature for 15min, 30min, 1h or 4h, after which the liquid in all wells was discarded by inverting the plates upside down to dump the liquid, each well was gently rinsed with 1mL PBS buffer for 24-well-plate and 2 mL PBS buffer for 12-well-plate for two times, and the residual biomass quantified using the crystal violet assay previously described.

3.2.3 Bench scale dead-end filtration experiment

This filtration experiment was operated in a bench scale dead end filtration system. The experimental system (Figure 5) is composed of eight parts: a compressed nitrogen gas tank, three stainless steel feed solution reservoirs, a 400mL modified stainless steel stirred cell (Millipore, Bedford, MA), a four way valve, a digital

balance (DENVER instrument, Bohemia, NY), and a 4000mL plastic beaker.

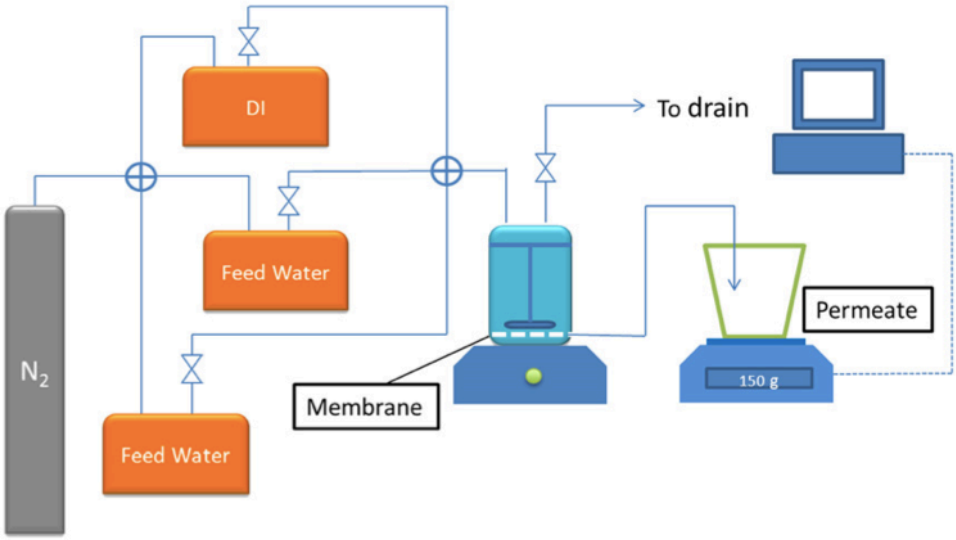

Figure 5. Bench scale dead end filtration system [57]

In the system, feed solution in each reservoir were pressurized by the compressed nitrogen gas to the stainless steel stirred cell, and the four way valve is used to control the direction of the nitrogen gas to flow to a specific reservoir. The stainless steel stirred cell (Figure 6) is composed of six parts: a stainless steel cover for water inlet, a stainless steel cylinder, a magnet stirrer, two rubber O-rings, and a bottom structure for water outlet. The membrane surface area is 35.3 cm^2. The membrane is placed on the bottom of the stirred cell, and a plastic mesh is placed under the membrane as a spacer. The magnet stirrer is suspended on top of the membrane in order to mix the liquid in the stirred cell and avoid concentration polarization.

Figure 6. Composition of stainless steel stirred cell

The filtration experiment consists of five stages: cleaning, compaction, conditioning, inoculation and fouling. Cleaning. The stirred cell and three reservoirs were washed with detergent, and then the system and the pipelines were rinsed with DI water for three times to wash off the detergent. The filtration system and the pipelines were washed with 1% SDS (Dodecylbenzenesulforic acid), then the pH was adjusted to 10 by adding sodium hydrate before use. After that, ethanol (200 proof) was used to sterilize the three reservoirs and pipelines. At last, the whole filtration system was cleaned with sterilized DI water to wash off the remaining ethanol. 2L sterilized DI water was added into the first reservoir; 2L electrolyte liquid (electrolyte liquid is consists of NaCl (7mM), $CaCl_2$ (1mM), LB (0.1%)) was added into the second reservoir, and 4L electrolyte liquid was added into the third reservoir. The NF90 membrane coupon was rinsed with ethanol (200 proof) for three times, then it was cleaned with sterilized DI water.

Compaction. After the system had been sterilized, the four-way valve was connected to the first reservoir, and the NF90 membrane coupon was compacted with sterilized DI water for 2 hours at 150 psi without stirring.

Conditioning. The NF90 membrane coupon is conditioned with electrolyte liquid from the second reservoir for 2 hours at 150 psi, with stirring at level five.

Inoculation. After stopping the conditioning step, 4mL of the liquid inside the stirred cell was sucked out, and 4mL *P. aerugisnosa* bacteria solution with the concentration of 1×10^8 CFU/mL was added into the stirred cell, in order to make the bacteria concentration in the stirred cell is 1×10^6 CFU/mL, which is similar to the seriously biofouled reverse osmosis membrane in seawater treatment plant. Then stirring was stopped and filtering was started for 30 minutes at 150 psi by the electrolyte liquid from the second reservoir, in order to let the bacteria deposit on the membrane surface. In the mean time, the amount of liquid collected was recorded.

Fouling. The nitrogen gas was stopped; all the liquid inside the stirred cell was sucked out by pipette from outlet A, which is on the cover. Then filtration was started with the valve connected to the third reservoir for 20 hours at 150 psi with stirring at level five.

The membrane permeate is collected in a 4000mL plastic beaker, and is measured by a digital balance that is connected to the computer, the weight of the accumulated permeate is measured every 60 seconds. The membrane flux is calculated by the following equation:

$$j = \frac{\Delta \mathrm{M}}{\rho \cdot \mathrm{A} \cdot \mathrm{t}} \tag{1}$$

Where j is the membrane permeate flux (m/s); $\Delta\mathrm{M}$ is the accumulated weight of membrane permeate during every 60 seconds (g); ρ is the density of water (1,000,000 g/cm^3); A is the membrane area (m^2, in this experiment it's 0.00353 m^2); t is the time interval (60 s).

Table 4 is the solution ingredient of each stage in filtration experiment:

Table 4. Solution ingredient of each stage in filtration experiment

Filtration stage	Compaction	Conditioning	Inoculation	Fouling
Without LB	Sterilized DI water	Electrolyte	--	--
NF90	Sterilized DI water	Electrolyte/LB	4mL 1×10^8 CFU/mL *P. aerugisnosa*	Electrolyte/LB
NF90 with 30μM D-tyrosine	Sterilized DI water	Electrolyte/LB/30μM D-tyrosine	4mL 1×10^8 CFU/mL *P. aerugisnosa*	Electrolyte/LB/ 30μM D-tyrosine
NF90	Sterilized DI water	Electrolyte/LB	4mL 1×10^8 CFU/mL *P. aerugisnosa*	Electrolyte/LB/ 30μM D-tyrosine
NF90	Sterilized DI water	Electrolyte/LB/30uM D-tyrosine until stable	4mL 1×10^8 CFU/mL *P. aerugisnosa*	Electrolyte/LB/ 30μM D-tyrosine

Table 5. Operation time for each stage

Filtration stage	Compaction	Conditioning	Inoculation	Fouling
Time (min)	120	120	30	1200
Conditioning until stable	120	180	30	1200

4. Results and discussion

4.1 Determination of growth conditions for robust biofilm.

The objective of this part of study is to determine the bacteria growth conditions to form well-attached, robust biofilm. Several key controlling factors in biofilm formation as well as the method for quantitative measurement of the biofilm formed by *P. aerugisnosa* and *B. subtilis* were discussed.

Each bar was the average of absorbance of CV at 600nm of wells that were tested under this condition, and the number of wells tested was shown as the number on top of each bar.

4.1.1 Effect of incubation temperature on bacteria growth

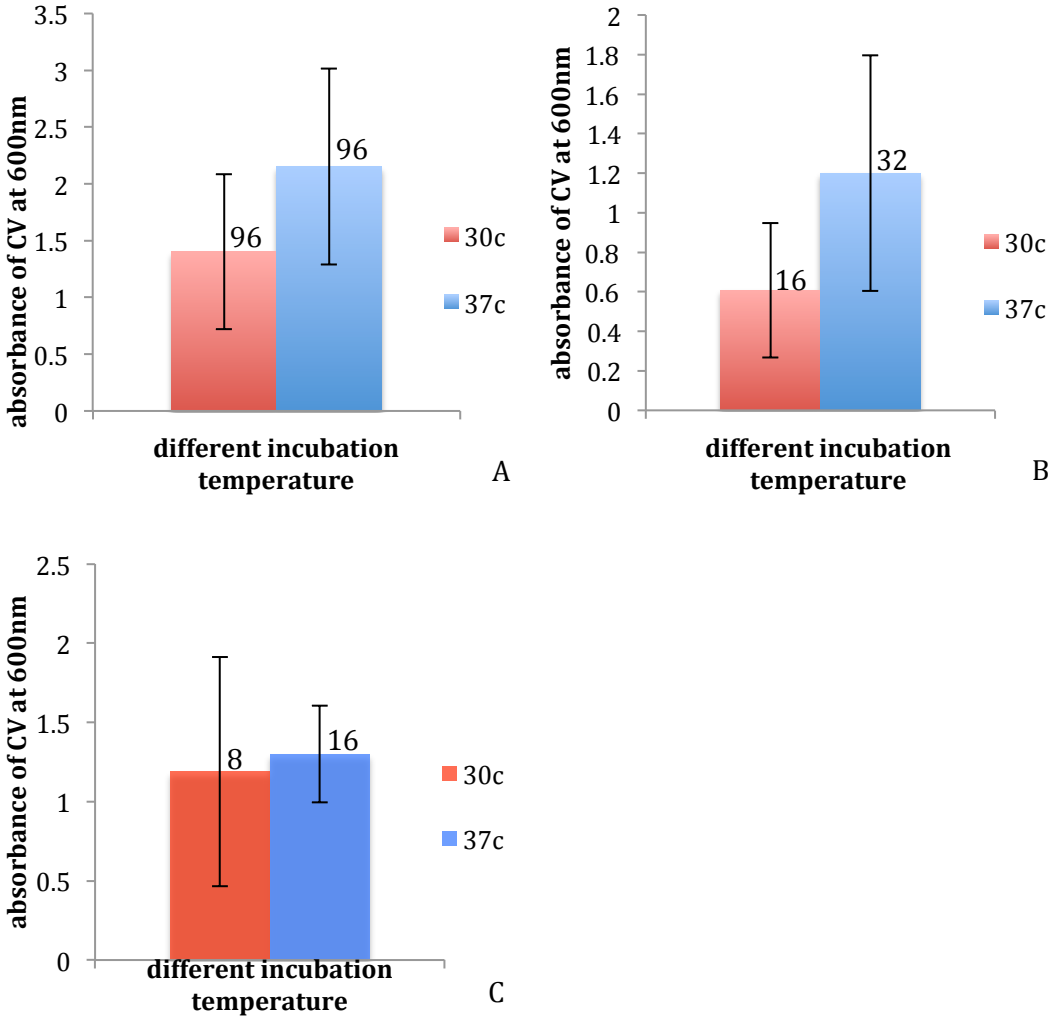

Figure 7. Effect of incubation temperature on *P. aeruginosa* growth. (A) Absorbance of CV at 600nm of *P. aeruginosa* after 12h incubation in 96-well-plate in LB medium at different incubation temperature. (B) Absorbance of CV at 600nm of *P. aeruginosa* after 12h incubation in 24-well-plate in R2A medium at different incubation temperature. (C) Absorbance of CV at 600nm of *P. aeruginosa* after 24h incubation in 24-well-plate in M63 medium at different incubation temperature.

The growth temperature of *P. aerugisnosa* was tested at 30°C and 37°C in 96-well-plate or 24-well-plate in LB, R2A or M63 media. Figure 7 showed that *P.*

aeruginosa grew better at 37°C than at 30°C, since *P. aeruginosa* obtained higher absorbance of CV at 600nm at 37°C than at 30°C. The incubation temperature was then set to be 37°C. Since it is the suitable temperature for *P. aerugisnosa* to proliferate. For *B. subtilis,* 37°C was also chosen as the incubation temperature, as *B. subtilis* proliferate faster in 37°C than in 30°C.

4.1.2 Effect of incubation time on biofilm growth

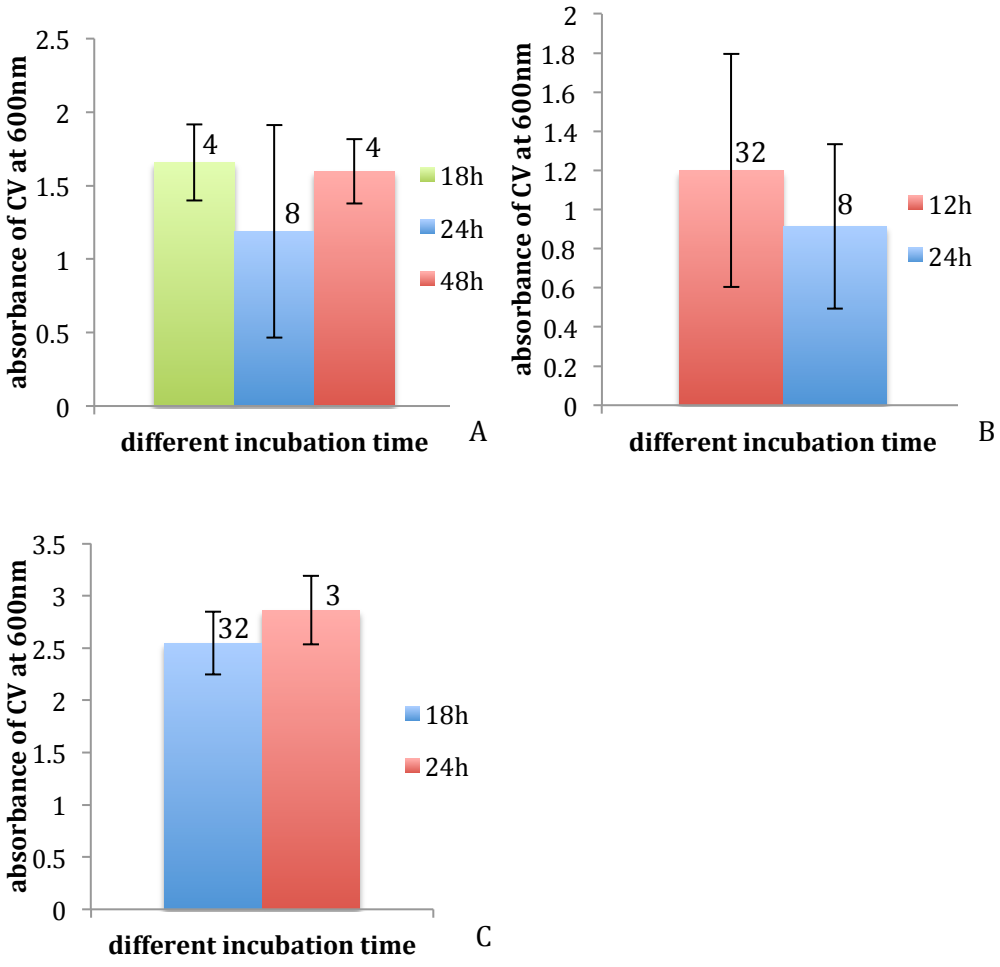

Figure 8. Effect of incubation time on *P. aeruginosa* growth. (A) Absorbance of CV at 600nm of *P. aeruginosa* incubated in 24-well-plate in M63 medium at 30°C after different incubation time. (B) Absorbance of CV at 600nm of *P. aeruginosa* incubated in 24-well-plate in R2A medium at 37°C after different incubation

time. (C) Absorbance of CV at 600nm of *P. aeruginosa* incubated in 12-well-plate in M63 medium at 37°C after different incubation time.

Incubation time is a key factor controlling the properties of the biofilm. If the incubation time were too long, this would cause the detachment of the biofilm due to the lack of nutrient; if the incubation time were too short, this would cause the immature of the biofilm formation.

From Figure 8, the incubation time of *P. aerugisnosa* was compared in 12h, 18h, 24h and 48h under different growth media. In all three figures, after incubated for 24h, *P. aerugisnosa* obtained even less biofilm (lower absorbance of CV at 600nm) in figure A and B, and the standard deviation was higher in all three figures, which meant that it was less reproducible. From figure A, after incubated for 48h, *P. aerugisnosa* formed less biofilm than incubated for 18h and 24h, and 48h was too long for achieving high throughput screening test results, so 48h was excluded. Figure A and C showed that *P. aerugisnosa* formed robust biofilm after incubated for 18 hours and the standard deviation was the smallest compared to other incubation time. So 18 hour is the best incubation time for *P. aerugisnosa.*

Also, *P. aerugisnosa* biofilm formed at 37°C in M63 medium after 8 hours, 12 hours, 18 hours, or 24 hours were visually examined. The biofilm was not visually observable by naked eyes after incubating for 8 hours (Figure 9) and 12 hours (Figure 10). After incubating for 24 hours (Figure 12), the biofilm detached after washing with PBS buffer. For *P. aerugisnosa*, 18 hours was the best incubation time for the bacteria to form robust and well-attached biofilm (Figure 11). This conclusion is consistent with the measurement of absorbance of CV shown in Figure 8.

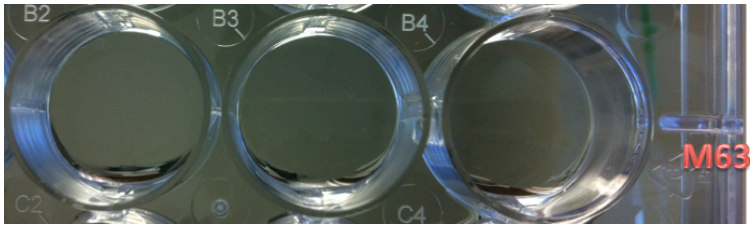

Figure 9. *P. aerugisnosa* incubated 8 hours at 37°C in M63 medium, shaking at rpm 95. The biofilm was not visually observable by naked eyes.

Figure 10. *P. aerugisnosa* incubated 12 hours at 37°C in M63 medium, shaking at rpm 95. The biofilm was not visually observable by naked eyes.

Figure 11. *P. aerugisnosa* incubated 18 hours at 37°C in M63 medium, shaking at rpm 95. Robust and well-attached biofilm formed.

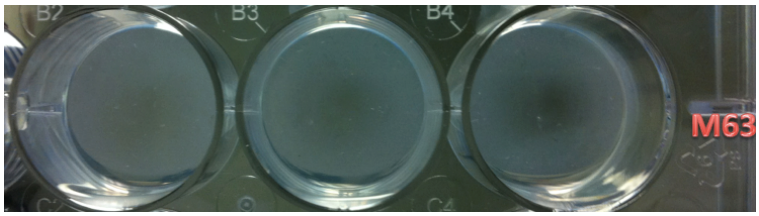

Figure 12. *P. aerugisnosa* incubated 24 hours at 37°C in M63 medium, shaking at rpm 95. After washing the biofilm started to peel off.

Similarly, the *B. subtilis* biofilm growth at 37°C in M63 medium was visually examined after 15 hours and 24 hours. After incubating for 15 hours (Figure 13), no

obvious biofilm was formed; after incubating for 24 hours (Figure 14), robust and well-attached biofilm was formed through observation of naked eyes, and more robust biofilm was formed without shaking (Figure 15). Thus for *B. subtilis*, 24 hours was the best incubation time to form robust biofilm.

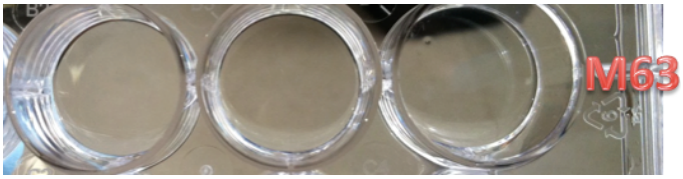

Figure 13. *B. subtilis* incubated 15 hours at 37°C in M63 medium, shaking at rpm 95. No obvious biofilm formed.

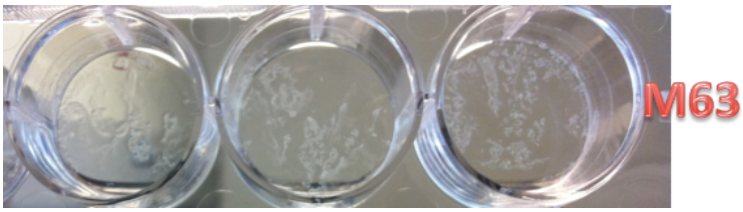

Figure 14. *B. subtilis* incubated 24 hours at 37°C in M63 medium, shaking at rpm 95. No robust biofilm was formed.

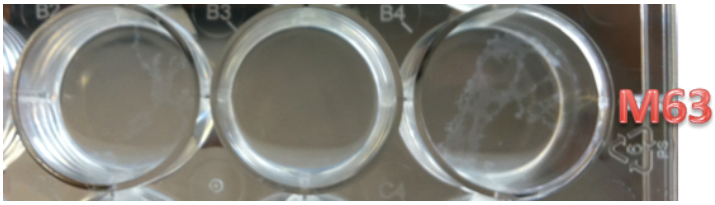

Figure 15. *B. subtilis* incubated 24 hours at 37°C in M63 medium, no shaking. Robust and well-attached biofilm formed.

4.1.3 Effect of nutrient medium on biofilm growth

The nutrient medium is the other key factor in biofilm formation. Several nutrient media including LB, R2A, M63 minimal medium as well as M63 with 2% glucose

were tested. LB medium is a rich medium that is commonly used to culture members of the Enterobacteriaceae. R2A medium is a low nutrient medium, bacteria grows slowly in this media. M63 medium is a minimum medium, on which bacteria grow easily yet slowly. M63 with 2% glucose would enhance the bacteria attachment onto the polystyrene surface of each well.

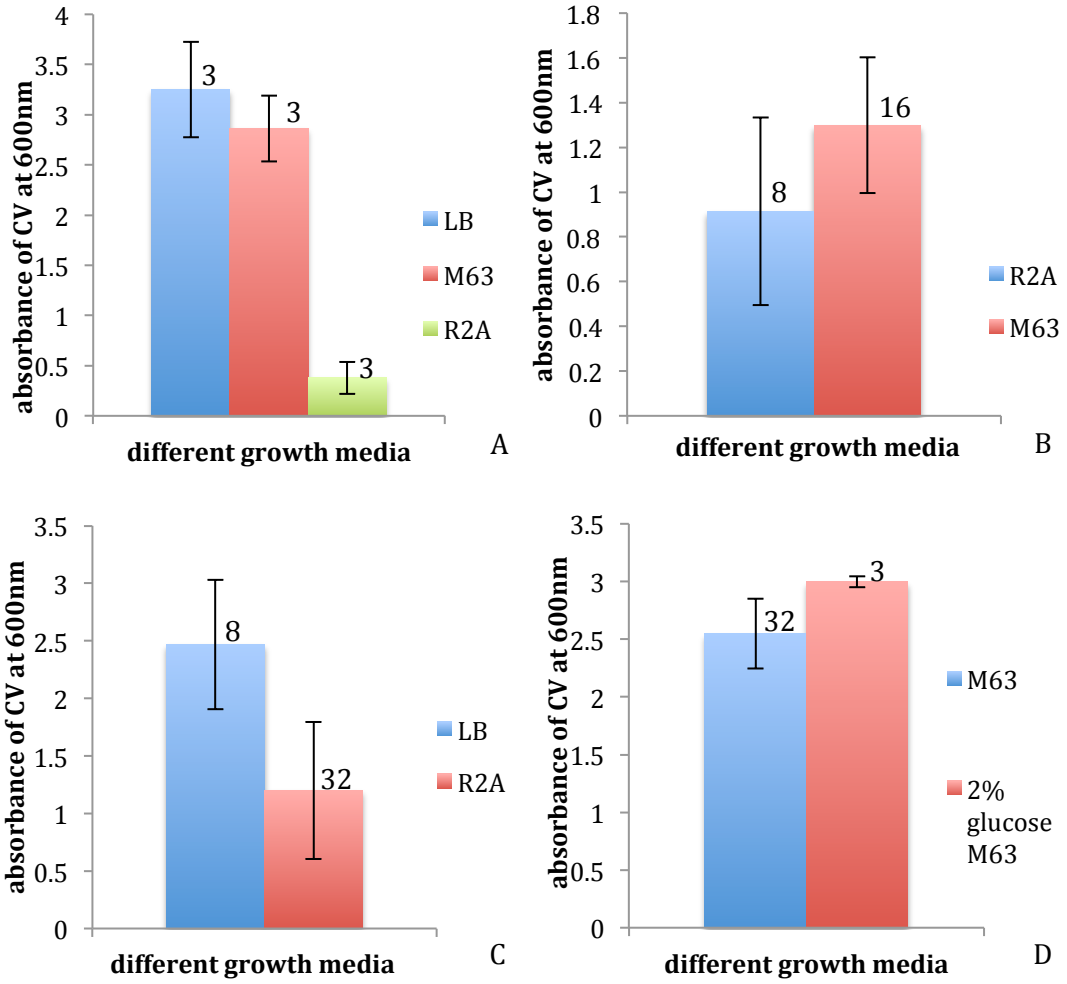

Figure 16. Effect of nutrient medium on *P. aeruginosa* growth. (A) Absorbance of CV at 600nm of *P. aeruginosa* after 24h incubation at 37°C in 12-well-plate, shaking at 95 rpm in different nutrient medium. (B) Absorbance of CV at 600nm of *P. aeruginosa* after 24h incubation at 37°C in 24-well-plate in different nutrient medium. (C) Absorbance of CV at 600nm of *P. aeruginosa* after 12h incubation at 37°C in 24-well-plate in different nutrient medium. (D)

Absorbance of CV at 600nm of *P. aeruginosa* after 18h incubation at 37°C in 12-well-plate, shaking at 95 rpm in different nutrient medium.

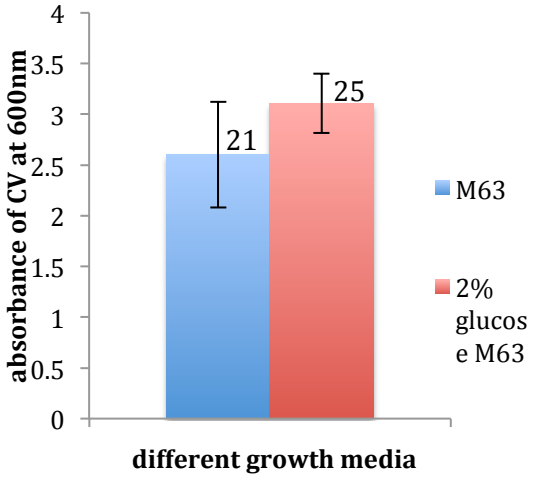

Figure 17. Effect of nutrient medium on *B. subtilis* growth. Absorbance of CV at 600nm of *B. subtilis* after 24h incubation at 37°C in 12-well-plate in different nutrient medium.

After incubated with LB, large amount of biofilm was formed by *P. aeruginosa*, which was very easy to detach from the bottom of the plate. This was reflected in the large standard deviation in the biomass measurement shown in Figure 16 (A and C) showed. After incubating with R2A, little biofilm was formed by *P. aeruginosa* as shown by the low absorbance values of the extracted CV solutions in Figure 16 (A, B and C). Also, biofilm formed in R2A had very big stand deviation, which meant that R2A had low reproducibility, so R2A was also excluded.

From Figure 16 (D) and 17, *P. aeroginosa* and *B. subtilis* formed robust biofilm in M63 with a relatively high absorbance of CV, so it was selected as the nutrient medium for both *P. aerugisnosa* and *B. subtilis* in this test. However, detachment of the grown biofilm still occurred during the washing protocol, leading to random loss of the biofilm and therefore relatively large variation of the measured absorbance of

CV data. Schleheck et al. [58] suggested that the switch of *P. aerugisnosa* from biofilm to planktonic cells was triggered by the lack of carbon source and oxygen, and starvation-induced biofilm dispersal usually happens in surface attached biofilms. Liquid medium supplemented with additional 0.25% to 4% of glucose was generally applied to address this issue [59]. As a result, the glucose concentration in the M63 nutrient medium was increased from 0.2% to 2% in the following experiments, and the seal was removed in order to avoid the low-oxygen condition.

From Figure 16 (D) and 17, both *P. aerugisnosa* and *B.subtilis* grown with 2% glucose M63 had higher absorbance and smaller standard deviation compared to M63 medium, which meant that bacteria formed more biofilm and was less likely to detach from the bottom of each well in the presence of 2% glucose M63. Supplementation of the nutrient media with glucose enhanced the bacteria to form vigorous biofilm and helped the bacteria to attach firmly on the bottom of each well.

4.1.4 Effect of microtiter plate size

Microtiter plates come with different bottom shapes including U-shaped, V-shaped and flat bottom. Flat-bottomed, tissue culture treated polystyrene microtiter plate with lid is frequently used for biofilm cultivation [60].

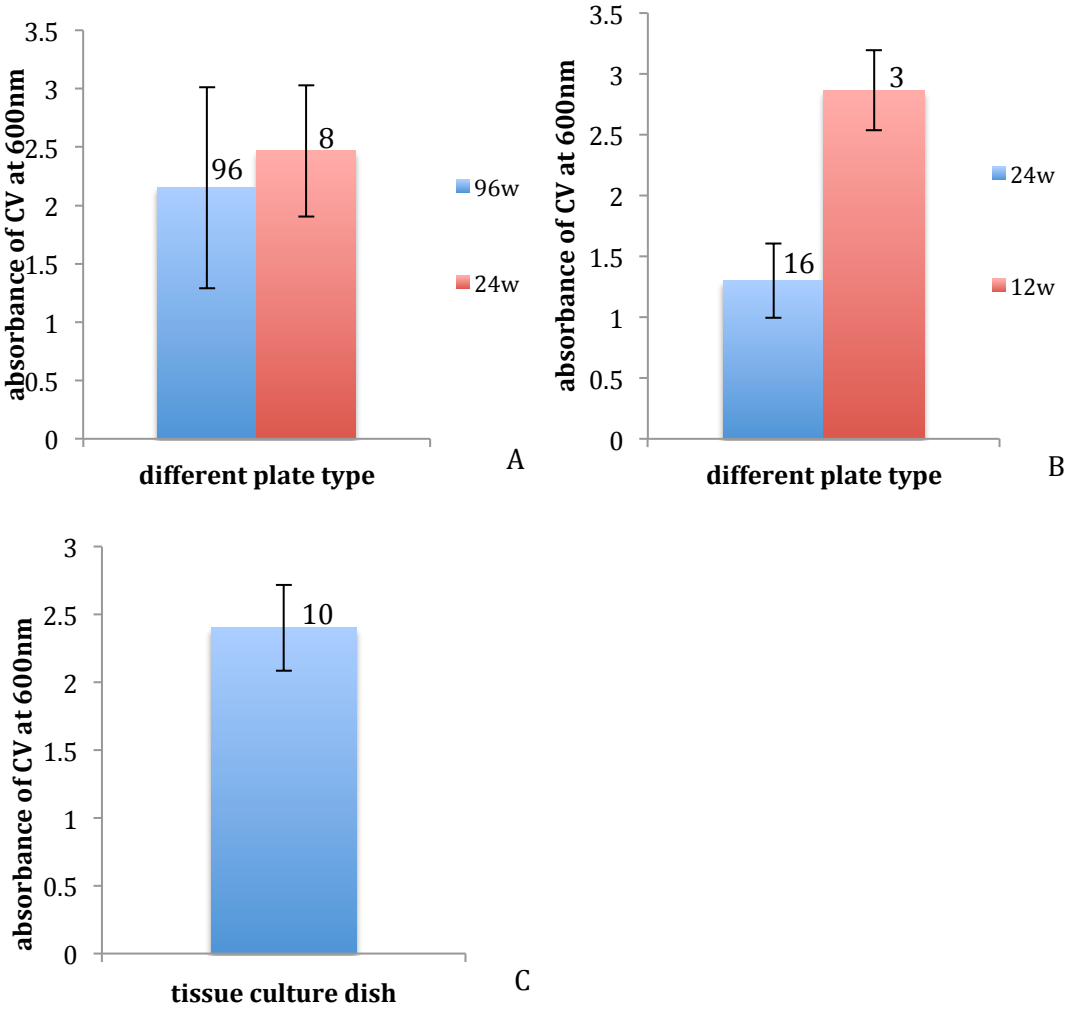

Figure 18. Effect of microtiter plate size. (A) Absorbance of CV at 600nm of *P. aeruginosa* after 12h incubation at 37°C in LB medium in different microtiter plate. (B) Absorbance of CV at 600nm of *P. aeruginosa* after 24h incubation at 37°C in M63 medium in different microtiter plate. (C) Absorbance of CV at 600nm of *P. aeruginosa* after 18h incubation at 37°C in M63 medium shaking at rpm 95 and stained with 0.2% CV, in different microtiter plate.

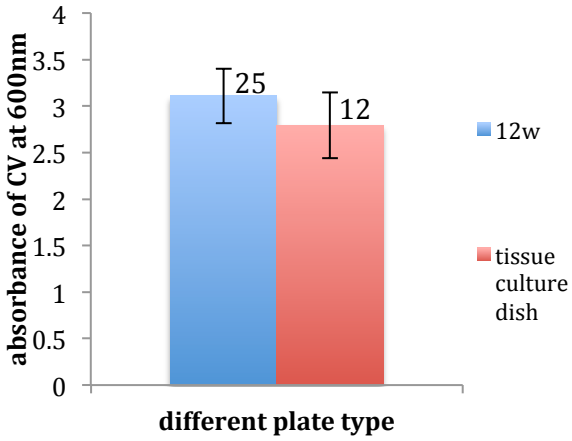

Figure 19. Effect of microtiter plate size. Absorbance of CV at 600nm of *B.subtilis* after 24h incubation at 37°C in M63 with 2% glucose medium in different microtiter plate.

Another factor that would affect the biofilm formation is the size of the microtiter plate. Plates with smaller size were found to perform severe biofilm lost during washing protocol. Figure 18 (A) showed that biofilm formed by *P. aerugisnosa* had big standard deviation in 96-well-plate, which was because the resulting biofilm detached easily from the bottom during washing with PBS buffer, leading to a reduced reproducibility. 24-well-plate, 12-well-plate and tissue culture dish (35x10 mm) were also tested in the screening experiments in order to tackle this problem. Tissue culture dish was tested due to its better control during the process of discarding the residual liquid and the washing protocol. From Figure 18 and 19, 24-well-plate had better result than 96-well-plate, 12-well-plate had better result than 24-well-plate, where better result meant that the biofilm formed by *P. aerugisnosa* and *B.subtilis* had lower standard deviation. 12-well-plate was found to perform well. A robust thin layer of biofilm was observed on the bottom of each well of the 12-well-plate and the biofilm attached firmly to the bottom of each well. 12-well plates were also used by Kolodkin-Gal *et al.* [5] to study the effect of D-amino acids on *B. subtilis* and *P.*

aeruginosa biofilms. Therefore, 12-well plates were used in most experiments discussed below.

4.1.5 Washing protocol

After incubation, the culture medium in each well was discarded and 2mL of PBS buffer was used to wash each well twice. Washing is a vital step in the protocol. The purpose of washing is to remove all the nonattached planktonic bacteria cells, and to wash off the residual nutrient medium to avoid its interference in biofilm measurement.

The number of washes and washing techniques used are also important based on my experience. Washing twice was suitable for this experiment, which was sufficient to remove all the nonattached bacteria and the residual nutrient medium. Washing for once was not enough to remove the residual nutrient medium, while washing more than twice would damage the integrity of the biofilm. Two washing techniques were tested: washing the plates by pipetting the sterilized PBS buffer into and out of each well, and by inverting the plates upside down to dump the liquid out. Washing by pipetting the wash solution in and out of the wells was found to cause notable damages to the integrity of the biofilm. Discarding the liquid by inverting the plates caused less biofilm loss. Therefore, this technique was used in all experiments.

4.1.6 Fixation

Biofilm needs to be fixed before staining with crystal violet to avoid loss of the biofilm in the following protocols. Three fixation methods were tested: air dry at room temperature, methanol fixation, and heat fixation at 60°C for 1 hour. Air dry at room temperature requires a long drying time, normally 2 hours, to achieve the

fixation. Fixation by methanol did not have very good effect, the biofilm was not fixed firmly, and removing the residual methanol also led to biofilm detachment. Heat fixation method was able to fix the biofilm firmly onto the bottom of each well and thus was applied in my experiments.

4.1.7 Staining

Crystal violet is commonly used to stain biofilm. Crystal violet stains the bacteria DNA, which shows the total cell number of the biofilm that contains a significant amount of EPS. After adding 1% crystal violet into each well, the plate was covered with lid and kept in room temperature for 20 minutes, allowing the crystal violet to diffuse through the biofilm and stain cells throughout the biofilm. After that, 95% ethanol was added into each well to extract the crystal violet. The plate was covered with lid and incubated at 37°C for 2 hours.

In earlier experiments, 1% crystal violet was added to stain the biofilm in 96-well-plate, 24-well-plate and 12-well-plate, which could be fully extracted by 95% ethanol. However, after incubating the bacteria in tissue culture dish, 1% crystal violet was added to stain the biofilm, but could not be fully extracted by 95% ethanol (Figure 20). As a result, the crystal violet concentration was changed to 0.2% in the experiments using tissue culture dish and the CV stain can be fully extracted by 95% ethanol (Figure 21).

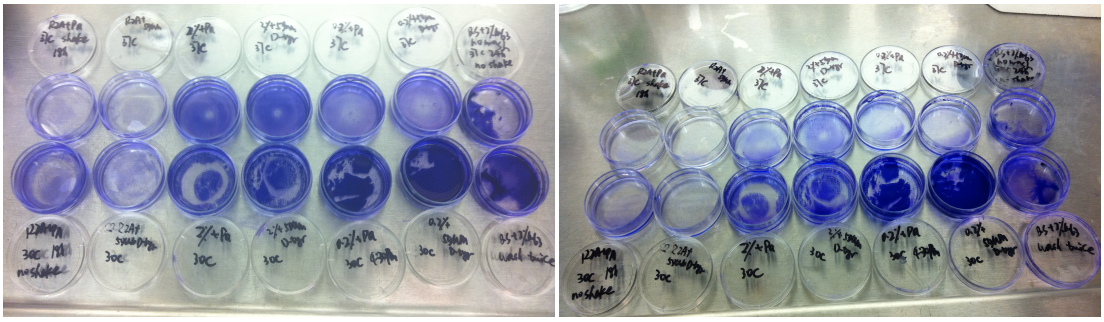

Figure 20. 1% crystal violet stained *P. aeruginosa,* after 18h incubation in M63 with 2% glucose, shaking at 95 rpm. Before extracted by 95% ethanol (left figure); after extracted by 95% ethanol (right figure), the crystal violet had not been fully extracted.

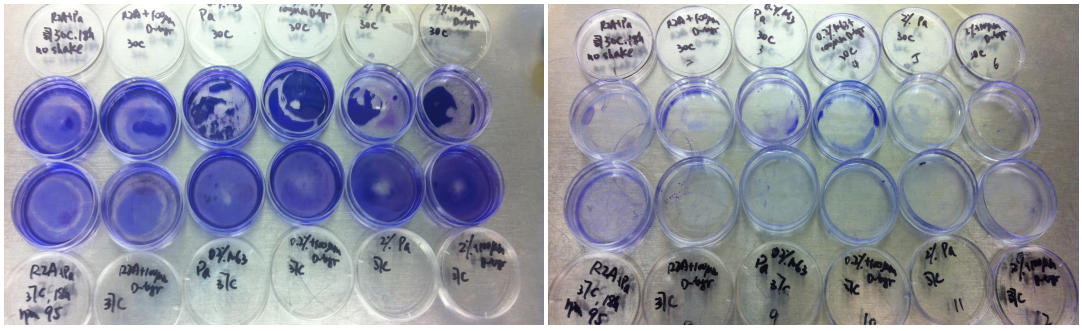

Figure 21. 1% crystal violet stained *P. aeruginosa,* after 18h incubation in M63 with 2% glucose, shaking at 95 rpm. Before extracted by 95% ethanol (left figure); after extracted by 95% ethanol (right figure), the crystal violet had been fully extracted

4.1.8 Measurement of the biofilm

After staining the biofilm with crystal violet (CV), CV was first extracted by 95% ethanol. The resulting extractions were subject to the measurement of absorbance of CV to determine the amount of biofilm that was formed. The absorbance of CV at 600 nm was measured by a microtiter plate reader (Molecular Devices, Sunnyvale,

CA) in all of my experiments.

The absorbance of CV at 600nm and the concentration of CV were related in Beer-Lambert Law:

$$A = -log_{10}\left(\frac{I}{I_0}\right) = \mathcal{E}\ell c \quad (2)$$

Where A is the absorbance, $\mathcal{E}$ is the molar absorptivity with units of L mol^{-1} cm^{-1}, ℓ is the path length of the sample, c is the concentration of the compound in solution with units of mol L^{-1}

There was a calibration curve between absorbance of CV at 600nm and the concentration of CV that was first stained within the biofilm and then extracted by 95% ethanol, which represented the amount of biofilm formed in each well. The calibration curve between absorbance of CV at 600nm and the concentration of CV was experimentally determined shown in Figure 22, which showed that it was a linear relationship between absorbance of CV at 600nm and the concentration of CV. Thus in my result and discussion part, the absorbance of CV at 600nm could be compared as the amount of biofilm formed in each well only if the absorbance of CV at 600nm was between 0.4 to 3.75.

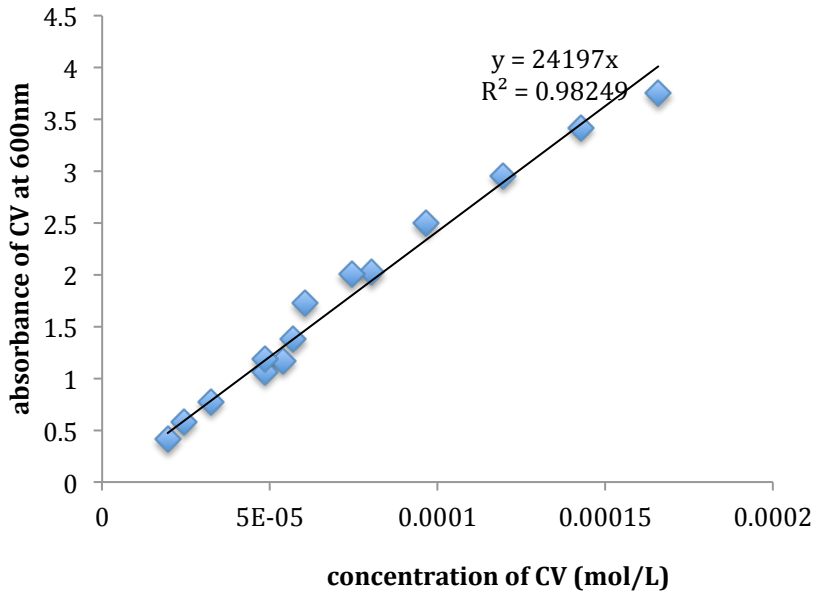

Figure 22. The calibration curve between absorbance of CV at 600nm and the concentration of CV

4.1.9 Interpretation of the results

Firstly, all the absorbance of CV at 600nm of each well under same condition (same incubation time, temperature, growth media, plate type, control or treatment, and with D-Amino acids added initially or with D-amino acids as clean protocol) was summarized as box plot shown in Appendix, which presented each experiment showing inhibition effect and cleaning effect of D-amino acids (D-tyrosine and the 4 mixture D-amino acids) on biofilm formed by *P. aeruginosa* and *B. subtilis.* The box data in each figure showed the range of all the data under each condition. For each of the box data, from top to bottom showed the 90th, 75th, 50th(median), 25th and 10th percentile of the data among all data sets. The * showed the outliers. However, there was a large range in each box data, showing big standard deviation in each experiment, which meant that there was a big variation of the absorbance of CV at 600nm for the same condition of wells between trial to trial (plate to plate), so this

method of analyzing the experimental data was excluded. The following statistical analysis method was chosen as the final interpretation of my data: the control and treatment well were only compared in each trial (plate). The Student T test with 90% confidential level was used to distinguish the differences between samples compared in each plate: control group compared to treatment group. If significant difference was found, the removal rate was calculated as Biofilm Removal Rate / Biofilm Reduction Rate = 1 – (treated OD) / (control OD); if no significant different was found, the Biofilm Removal Rate / Biofilm Reduction Rate = 0. The Biofilm Removal Rate / Biofilm Reduction Rate in the following figures are the average of the results from each plate.

4.2 Effect of D-amino acids on bacterial biofilm

In this study, the effect of D-amino acids on biofilms formed on a solid surface was examined. The effect of D-amino acids on biofilm formation was assessed by adding D-amino acids at the beginning of the biofilm formation process, and quantifying the attached biomass after a pre-defined incubation period. To determine the effect of D-amino acids on existing biofilms, biofilms grown under well defined conditions were exposed to D-amino acids, and the biomass remaining attached was quantified.

The number on top of each bar showed the number of experiments done under this condition; the ** on top of each bar showed that there was no experiments done under this condition; * with a number on top of each bar showed that the value of this bar is 0 and the number of experiments.

4.2.1 Effect of D-amino acids on *B. subtilis* biofilm formation

For *B. subtilis,* the effect of D-amino acids on biofilm formation was examined by adding different concentrations of D-amino acids (D-tyrosine and the mixture D-amino acids: D-tyrosine, D-leucine, D-tryptophan, and D-methionine) at the beginning of biofilm cultivation under different incubation conditions, including incubation time, temperature, growth media and plate type (24-well-plate, 12-well-plate and tissue culture dish) used.

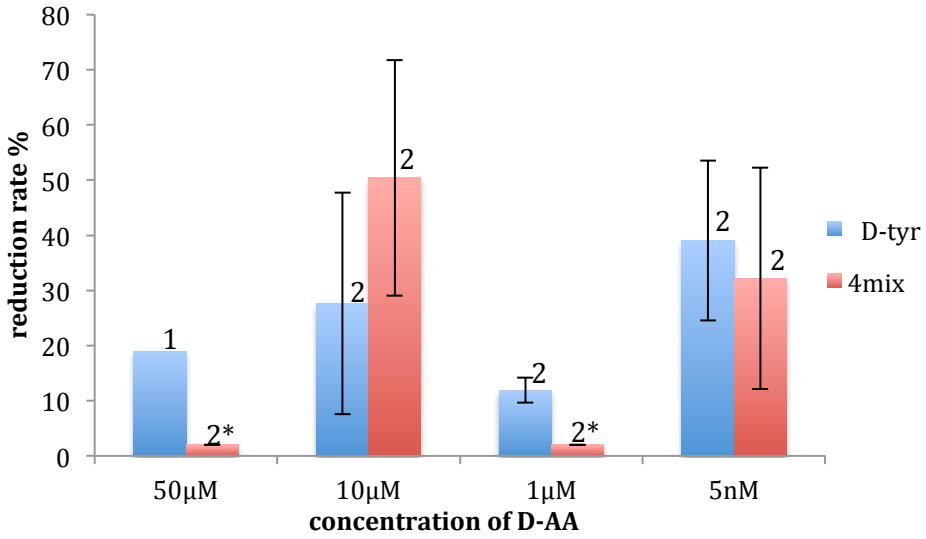

Figure 23. Effect of D-AA on biofilm reduction of *B. subtilis,* incubated in M63 with 2% glucose for 24h at 37°C without shaking, with addition of DAA initially (12-well-plate)

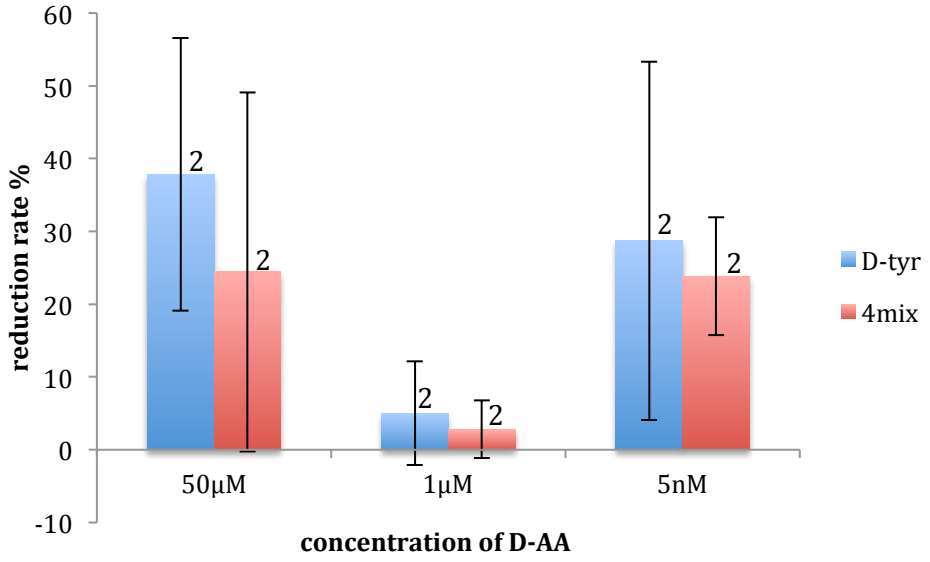

Figure 24. Effect of D-AA on biofilm reduction of *B. subtilis,* incubated in 2% glucose M63 for 24h at 37°C without shaking, with addition of DAA initially (tissue culture dish)

Figure 23 and 24 demonstrated that D-amino acids had strong inhibition effect on biofilm formation by *B. subtilis* (average reduction of 24.2% for D-tyrosine and 19.1% for mixture D-AA), which was consistent with the paper published by Kolodkin-Gal *et al.* [5]. Kolodkin-Gal *at el.* [5] discovered that in *B. subtilis*, D-tyrosine substituted the terminal D-alanine in the peptide side chains of peptidoglycan in bacteria cell wall. This led to the detachment of a fibrous protein, TasA that anchored on the D-alanine in the cell wall, and thus triggered the biofilm disassembly. This was found to strongly inhibit *B. subtilis* biofilm formation at the liquid-air interface. In my experiment the biofilm was formed on liquid-solid interface. These results suggest that D-amino acids are effective in inhibiting biofilm formation by *B. subtilis* at both liquid-air and liquid-solid interfaces.

The effect of D-amino acids strongly depended on their concentration. Figure 23 and 24 showed that both D-tyrosine and mix D-amino acids had little effect when

their concentration was 1μM (reduction rate of 11.9% for D-tyrosine, 0% for mixture D-AA in 12-well-plate and 5.05% for D-tyrosine, and 2.8% for mixture D-AA in tissue culture dish), but had good inhibition effect when their concentration increased to 50μM and 10μM (average reduction rate of 28.2% for D-tyrosine, and 37.4% for mixture D-AA) and decreased to 5nM (average reduction rate of 33.9% for D-tyrosine, and 28.1% for mixture D-AA). These suggested that there might be two different mechanisms through which D-amino acids affected biofilm formation. It is hypothesized that in one mechanism, D-tyrosine was incorporated into the peptidoglycan layer of the bacterial cell wall to replace D-alanine [5]. This mechanism is effective at the μM concentration level. This amount of D-tyrosine incorporated increases with increasing D-tyrosine concentration. Therefore, its effect also increases with increasing concentration. In the other mechanism, D-amino acids are hypothesized to act as signal molecules to trigger biofilm dispersal [5, 61] and work at low concentrations. It appears that the second mechanism is inactivated when the concentrations of D-amino acids are too high.

4.2.2 Effect of D-amino acids on existing *B. subtilis* biofilm

The effect of D-amino acids in disrupting existing biofilms formed by *B. subtilis* as cleaning protocol was tested under different conditions. The cleaning solutions were made by diluting D-amino acid with PBS buffer to predetermined concentrations.

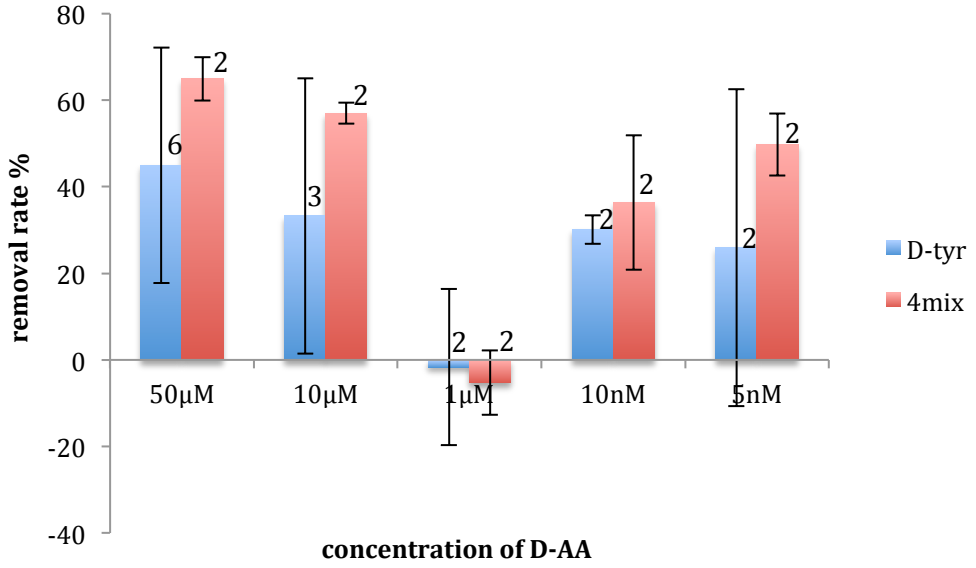

Figure 25. Effect of D-AA on biofilm removal of *B. subtilis,* incubated in 2% glucose M63 for 24h at 37°C without shaking, then clean with PBS diluted D-AA for 30min at room temperature (12-well-plate)

Figure 25 revealed that D-amino acids had good effect on cleaning existing biofilm formed by *B.sutilis,* since the average biofilm removal rate was 26.5% for D-tyrosine, and 40.6% for mixture D-amino acids. Xu *et al.* [62] illustrated that without exposure to D-amino acids, suspended microorganism carried negative surface charge. After exposed to D-tyrosine for 4 hours, microorganism carried 200% more negative surface charge compared to the control group that without exposure to D-amino acids. This illustrated that D-amino acids could enhance the negative surface charge of bacteria and substrate surface. Also, since D-amino acids were hydrophilic and negatively charged, D-amino acids could make the substrate surface more hydrophilic after adsorb on the surface, which was less likely for bacteria to attach. For cleaning protocol, after shaking the plate at rpm95 with D-amino acids addition, D-amino acids could diffuse into the biofilm and possibly contact the substrate surface. Contact with D-amino acids may change the physicochemical properties of

the biofilm and the substrate, rendering them more negatively charged and hydrophilic. This could potentially reduce the adhesion between the biofilm and the substrate surface, leading to detachment of the biofilm under the hydraulic shear force generated by shaking of the plate. Also, D-amino acids effective inhibited the cell-cell and cell-surface adhesion by diffusing into the biofilm contact with bacteria with the help of hydraulic shear force by shaking the plate, and caused biofilm removal.

The cleaning effect of D-amino acids was greatly influenced by their concentration shown in Figure 25. Both D-tyrosine and mix D-amino acids had little effect when their concentration was 1μM (removal rate of -1.65% for D-tyrosine and -5.25% for mixture D-AA) (Figure 25). Both lower (removal rate of 30.15% for 10nM D-tyrosine and 36.4% for 10nM mixture D-AA, removal rate of 25.9% for 5nM D-tyrosine and 49.75% for 5nM mixture D-AA) and higher concentration (removal rate of 44.95% for 50μM D-tyrosine and 64.95% for 50μM mixture D-AA, removal rate of 33.3% for 10μM D-tyrosine and 57% for 10μM mixture D-AA) of D-amino acids had better effect on cleaning existing biofilm. This was due to the two different mechanisms through which D-amino acids affected biofilm formation that was discussed earlier.

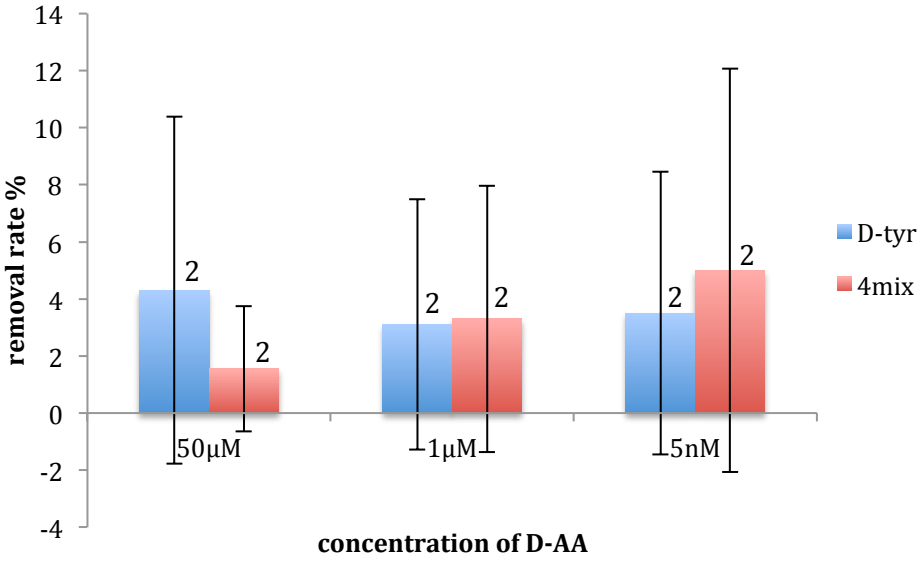

Figure 26. Effect of D-AA on biofilm removal of *B. subtilis,* incubated in 2% glucose M63 for 24h at 37°C without shaking, then clean with PBS diluted D-AA for 30min at room temperature (tissue culture dish)

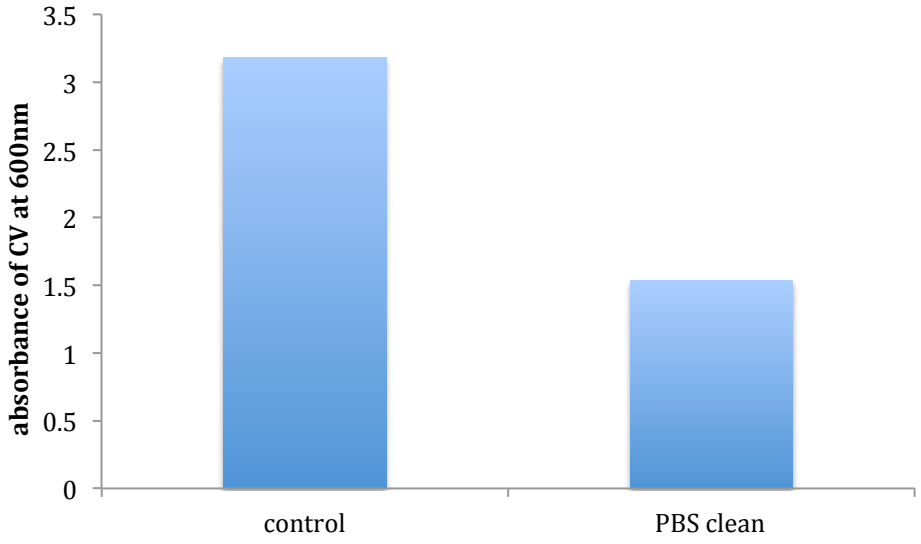

Figure 27. The absorbance of CV at 600nm of *B.sutilis* control group and PBS cleaned *B.sutilis* control group in tissue culture dish

The effect of D-amino acids on cleaning existing biofilm formed by *B.sutilis* incubated in tissue culture dish (average removal rate of 3.6% for D-tyrosine, and 3.3%

for mixture D-AA) was not as good as that in 12-well-plate (Figure 26). This was because while applying the shaking in cleaning protocol, tissue culture dish experienced higher hydraulic shear velocity:

$$V = \mu \cdot \frac{\partial u}{\partial y},\ \frac{\partial u}{\partial y} = -\frac{a\pi}{2} \cdot r^2, \quad (3)$$

Where V is hydraulic shear velocity and r is radium of each well. Since tissue culture dish had bigger radium than 12-well-plate, tissue culture dish experienced higher hydraulic shear velocity. 51.9% of the biofilm was removed by the hydraulic shear force (Figure 27). As a result, the additional removal of the biofilm by D-amino acids was smaller.

4.2.3 Effect of D-amino acids on *P. aeruginosa* biofilm formation

For *P. aeruginosa,* the effect of D-amino acids (D-tyrosine or the mixture of 4 D-amino acids: D-tyrosine, D-leucine, D-tryptophan, and D-methionine) on biofilm formation was tested under different growth conditions, including incubation time, temperature, growth media and plate type (24-well-plate, 12-well-plate and tissue culture dish). D-amino acids were also added at different times during the biofilm growth.

The concentration range of D-tyrosine (μM) and the mixture D-amino acids (nM) used was based on the paper published by Kolodkin-Gal *et al.* [5]. They demonstrated that D-tyrosine at concentration of 3μM and the mixture D-amino acids (D-tyrosine, D-tryptophan, D-leucine and D-methionine) at concentration of ~10nM were effective for inhibiting biofilm formation when *B.subtilis* biofilm was formed on liquid-air surface, and *P. aeruginosa* biofilm was formed on polystyrene surface.

D-amino acids have both positive and negative effect on inhibition of biofilm formation on *P. aeruginosa*, depending on the different incubation condition.

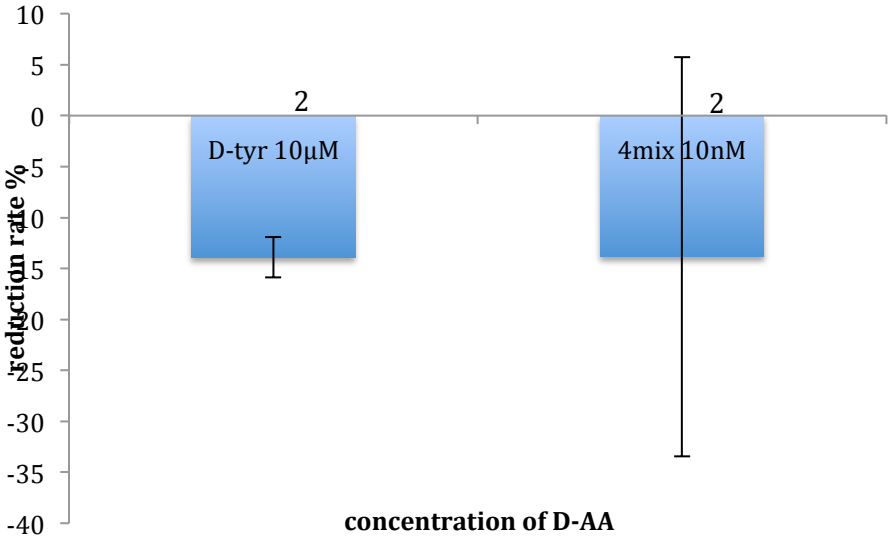

Figure 28. Effect of D-AA on biofilm formation by *P. aeruginosa*, after incubated in R2A for 14h at 30°C with addition of D-AA initially (24 well plate)

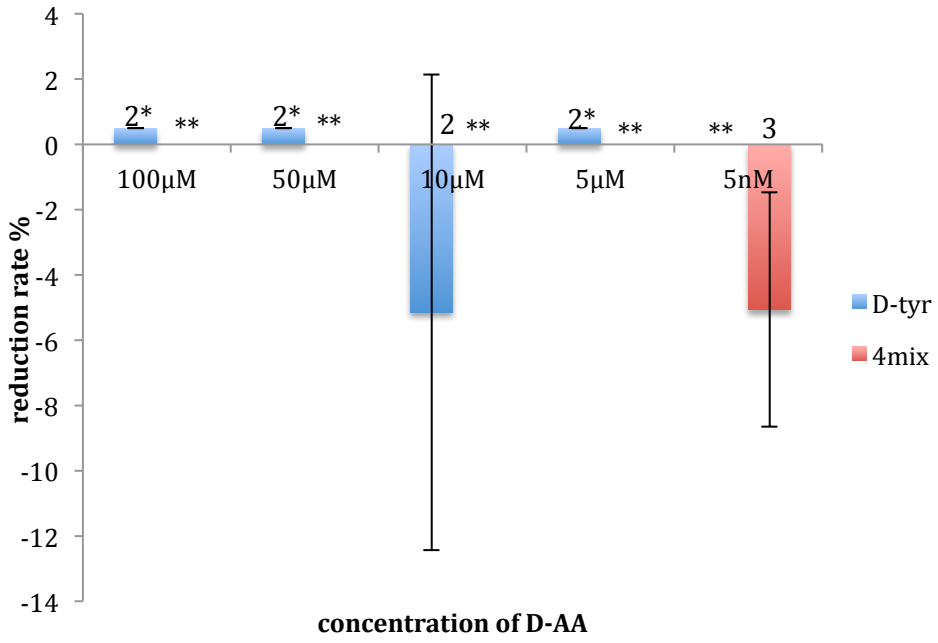

Figure 29. Effect of D-AA on biofilm formation by *P. aeruginosa*, after incubated in M63 at 37°C for 24h with addition of D-AA initially (24-well-plate)

As shown in Figure 28 and 29 D-amino acids had little effect on inhibition of *P. aeruginosa* biofilm formation under some incubation condition. The paper published

by Yu *et al.* [57] showed that D-tyrosine was effective in the inhibition of reversible and irreversible *P. aeruginosa* cell attachment onto NF270 membrane surface within one hour. This indicated that D-amino acids were effective to inhibit the initial adhesion between bacteria and bacteria, or between bacteria and the membrane surface. However, in my experiments, D-amino acids were not effective in inhibiting biofilm formation after long incubation time (12-24 hours). During long time incubation, bacteria produced extracellular polysaccharide (EPS) to form biofilm. The major components in EPS are proteins and polysaccharides. EPS is like a bio-glue that enhance the bacterial attachment to the solid surface [52]. A paper published by Fletcher *et al.* [63] also demonstrated that in unidentified gram-negative bacteria, primary acidic polysaccharide secreted by bacteria was responsible for both forced and natural bacteria adhesion to the filter surface. After attachment, secondary acidic polysaccharides, which were developed from primary acidic polysaccharides, would replace primary acidic polysaccharides and support the adhesion of bacteria to the filter surface by stretching and connecting the gap between bacteria and filter surface. In my experiments, secondary acidic polysaccharides supported the adhesion of bacteria to the surface of each well bottom.

It was assumed that after incubating for 12-24 hours, bacterial cells were being hold firmly by polysaccharide. Thus, even though D-amino acids were effective in inhibiting the reversible and irreversible attachment between *P. aeruginosa* bacteria cells, because they were not effective in disrupting polysaccharide matrix, in this condition bacteria cells still attached on the polystyrene surface and could not be removed because of the existence of polysaccharide, so D-amino acids have little effect in inhibiting biofilm formation. The minimal impact of D-amino acids on *P. aeruginosa* biofilm formation was due to the fact that D-amino acids could not inhibit

P. aeruginosa to secrete polysaccharide, nor disrupt polysaccharide after long incubation time. However, Xu *et al.* [52] illustrated that after exposed to D-tyrosine for 4 hours, a lower concentration of extracellular polysaccharides and protein was measured, which proved that D-tyrosine could effectively inhibit the production of extracellular polysaccharides and proteins by bacteria within 4 hours of incubation, whether this lower concentration measured was due to a smaller number of bacteria attached on the glass or polypropylene surface (therefore fewer bacteria contributing to EPS production) or the actual level of EPS production by each bacteria cell was reduced. However, in my experiments, after incubated for 12h to 24h, there were lots of polysaccharide existed and bacteria were hold firmly by EPS (Figure 30). Therefore, D-amino acids were effective to reduce extracellular polysaccharides and proteins production in early growth stage, since EPS production might not be as much as later stage. While after longer incubation time (12h to 24h), D-amino acids were less effective to inhibit EPS production.

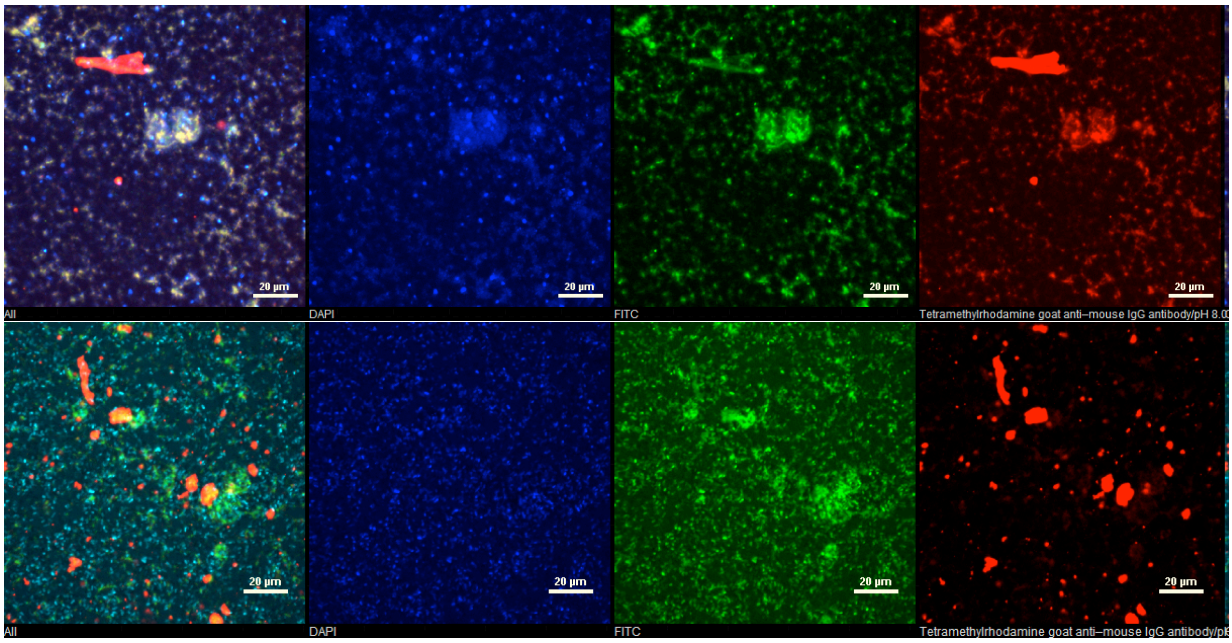

Figure 30. Confocal Laser Scanning Microscope images of single layer of biofilm formed by *P. aeruginosa,* after 24h incubation in glass slide in glass petri dish in

M63 with 2% glucose, with shaking at 95 rpm. Figures in the top showed the biofilm formed with addition of 100μM D-tyrosine initially, while figures in the bottom showed control group without D-tyrosine addition. The first figure in the left represented the amount of combination of DNA, protein and polysaccharides. Blue color represented the amount of DNA, green color represented the amount of protein, and red color represented the amount of polysaccharides, which showed that after addition of D-tyrosine, biofilm still formed lots of polysaccharides. Source: Cong Yu. Unpublished results

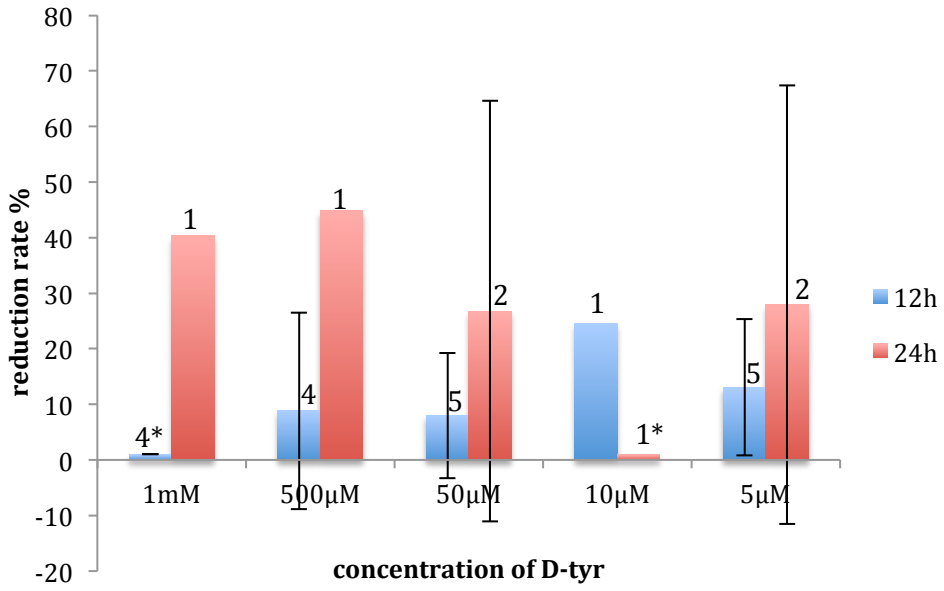

Figure 31. Effect of D-tyrosine on biofilm formation by *P. aeruginosa,* after incubated in R2A at 37°C for 12h/24h with addition of D-tyrosine initially (24-well-plate)

Figures 31 showed that D-tyrosine had better inhibition effect when the biofilm was incubated for longer time (average reduction rate of 34.9% for 24h-incubation) than was incubated for shorter time (average reduction rate of 13.6% for 12h-incubation), even though they were incubated in different growth medium. 12h-old microorganism was in stationary phase, while 24h-old microorganism was in

late-stationary phase. Microorganism at different growth state might have different attachment ability [62], whether was due to the bacteria itself or the change in EPS matrix. The effect of D-amino acids on inhibition of biofilm formation to *P. aeruginosa* was more effective when the biofilm was incubated for 24 hours than was incubated for 12 hours. This is assumed to be that since EPS production costs energy [64], after 24h incubation there was less nutrient in the environment, so *P. aeruginosa* excreted significantly less EPS to hold the bacteria cells, thus D-tyrosine was effective to inhibit biofilm formation by preventing the cell-cell and cell-polystyrene attachment. Another possible explanation of why D-tyrosine had better effect on inhibiting biofilm formation after longer incubation time than shorter incubation time was that D-tyrosine was effective on enhancing the cell dispersal after 24h incubation than 12h incubation.

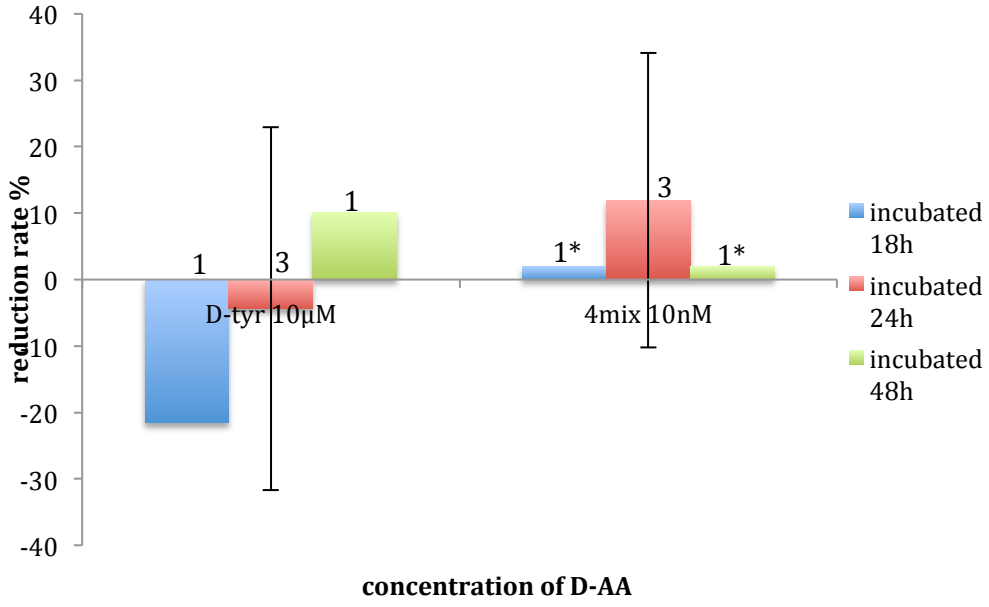

Figure 32. Effect of D-AA on biofilm formation by *P. aeruginosa*, after incubated in M63 at 30°C for different time with addition of D-AA initially (24-well-plate)

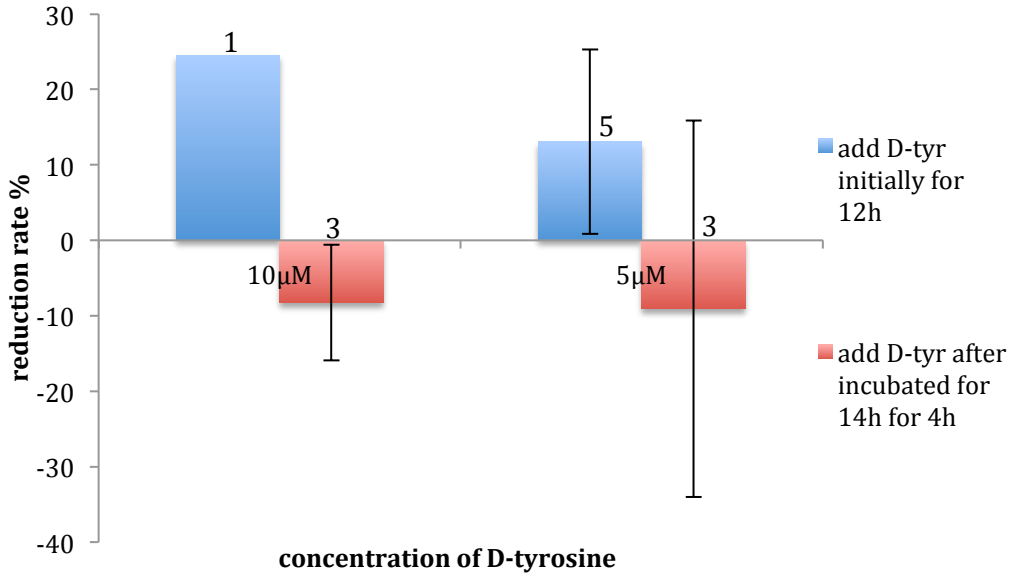

Figure 33. Effect of D-tyrosine on biofilm formation by *P. aeruginosa,* one condition is incubated in R2A at 37°C for 12h with addition of D-tyrosine initially, and the other condition is after incubated in R2A at 37°C for 14h then add D-tyrosine for 4h at 37°C (24 well plate)

Figure 33 showed that D-tyrosine had better inhibition effect of biofilm formation when it was added initially (reduction rate of 24.5% for 10μM, and 13.1% for 5μM) than it was added after the biofilm was already formed (reduction rate of -8.2% for 10μM and -9.1% for 5μM). This proved that D-tyrosine was not effective to disrupt the EPS matrix (organic substance) in the biofilm, so the bacteria were still attached firmly onto the polystyrene surface with EPS holding them together. This was consistent with the result discovered in the bench scale dead end filtration experiments (see section 4.3.1), where D-tyrosine was less effective to inhibit biofouling caused by *P. aeruginosa* after the membrane surface is fouled by organic matter. Thus D-amino acids are not effective in inhibiting biofilm formation after the biofilm has already formed, since D-tyrosine could not disrupt existing EPS.

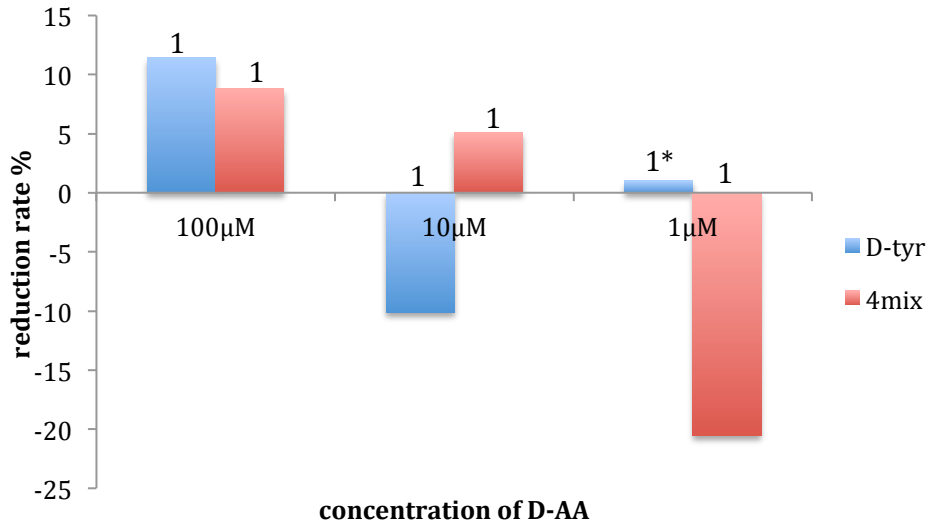

Figure 34. Effect of D-AA on biofilm formation by *P. aeruginosa,* after incubated in M63 at 37°C for 18h, shaking at rpm 95, with addition of D-AA initially (tissue culture dish)

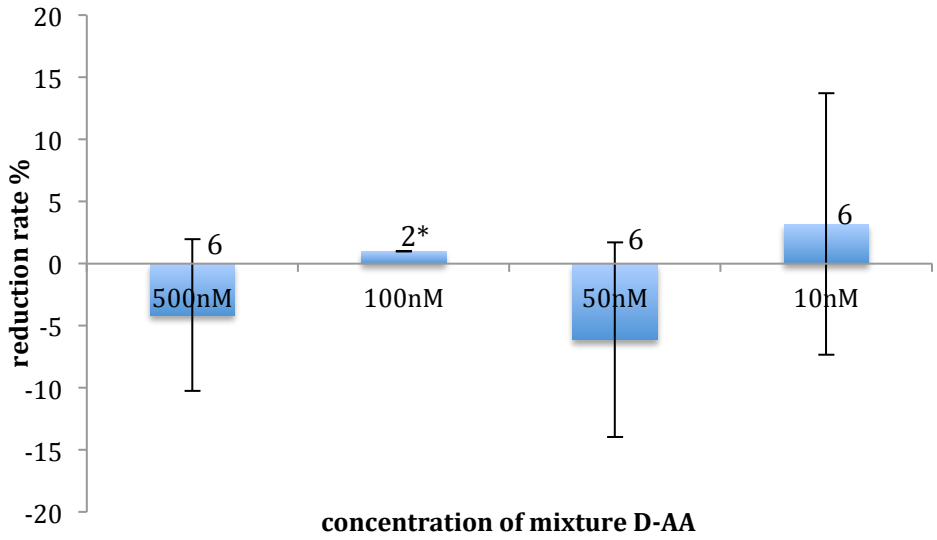

Figure 35. Effect of mixture D-AA on biofilm formation by *P. aeruginosa,* after incubated in R2A for 14h at 37°C with addition of mixture D-AA initially (24-well-plate)

Figure 34 revealed that for D-tyrosine and mixture D-amino acids, higher concentration (100μM of D-tyrosine and mixture D-AA) had better inhibition effect

(reduction rate of 11.4% for 100μM D-tyrosine and 8.8% for 100μM mixture D-AA) than lower concentration (reduction rate of -10.1% for 10μM D-tyrosine and 5.1% for 10μM mixture D-AA, reduction rate of 0% for 1μM D-tyrosine and -20.5% for 1μM mixture D-AA). However, for the mixture D-amino acids, lower concentration (10nM) had better inhibition effect (reduction rate of 3.2% for 10nM) than higher concentration (reduction rate of -4.2% for 500nM, 0% for 100nM and -6.1% for 50nM), as shown in Figure 35. This was due to the two different mechanisms through which D-amino acids affected biofilm formation that was discussed earlier.

4.2.4 Effect of D-amino acids on existing *P. aeruginosa* biofilm

The effect of D-amino acids on cleaning existing biofilms formed by *P. aeruginosa* was tested using a cleaning assay. Two cleaning protocols were employed, one was to dilute D-amino acids with nutrient medium to specific concentrations and added to each well for cleaning, and the other one was to dilute D-amino acids with PBS buffer.

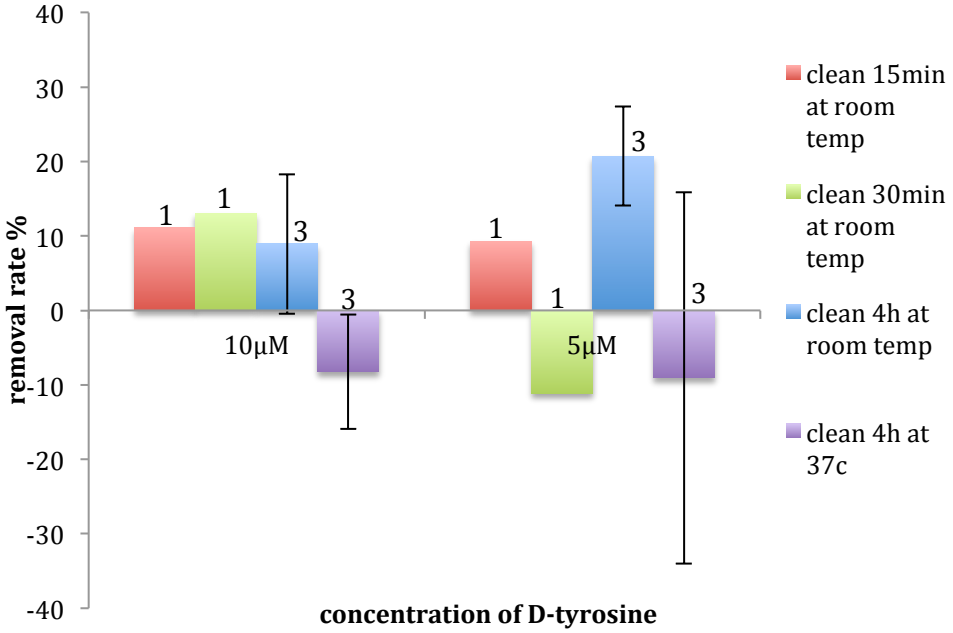

Figure 36. Effect of D-tyrosine on biofilm removal of *P. aeruginosa,* after incubated in R2A for 14h at 37°C, then clean with R2A diluted D-tyrosine for different time and temperature (24-well-plate)

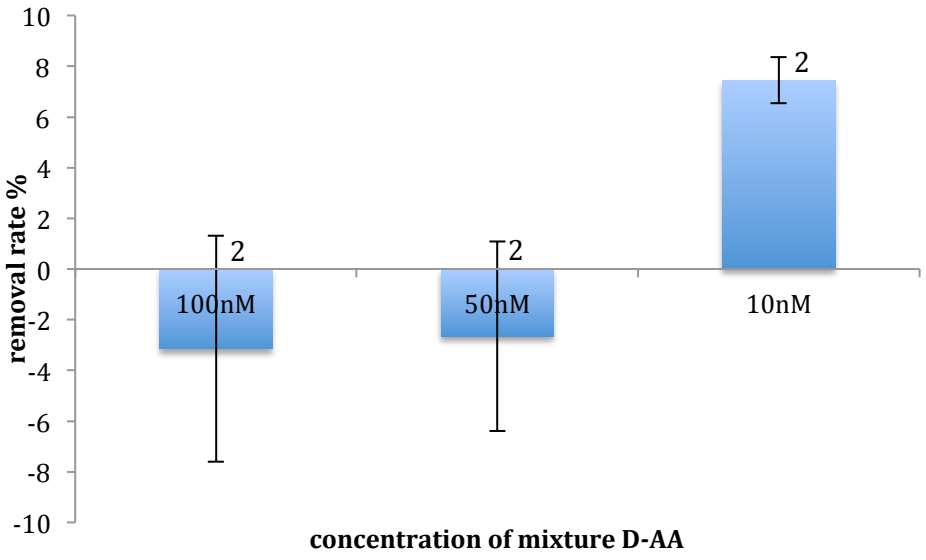

Figure 37. Effect of mixture D-AA on biofilm removal of *P. aeruginosa,* after incubated in R2A for 14h at 37°C, then clean with R2A diluted mixture D-AA for 4h at room temperature (24-well-plate)

As shown in Figure 36, cleaning at room temperature removed more biofilm biomass compared to cleaning at 37°C. Figure 37 showed that lower concentration of mixture D-amino acids (10 nM) was able to remove more biofilm (removal rate of 7.45%) than higher concentration of mixture D-amino acids (removal rate of -3.15% for 100 nM and removal rate of -2.65% for 50 nM). This suggested that the effect of D-amino acids was not simply physicochemical, and was consistent with the hypothesized signaling mechanism discussed earlier.

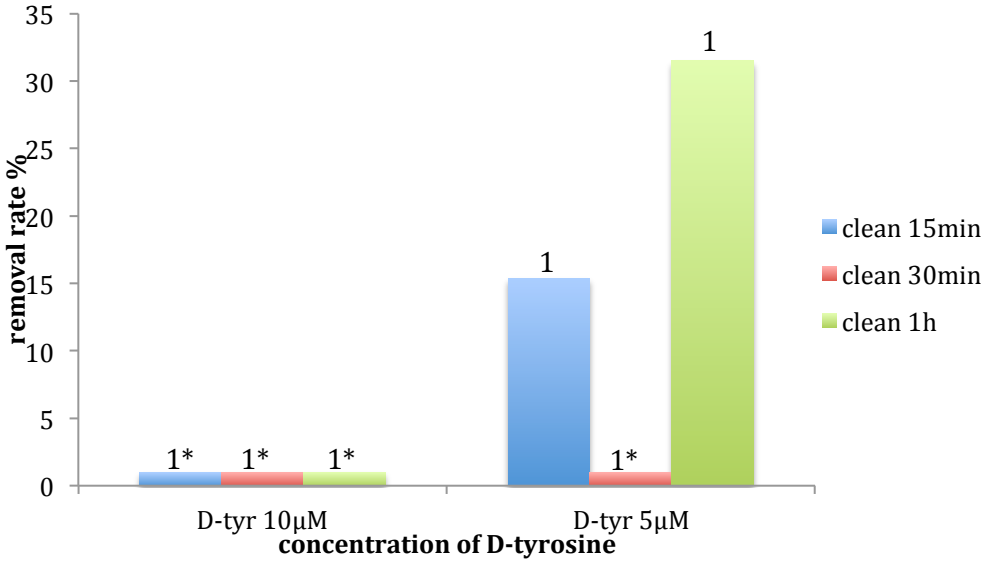

Figure 38. Effect of D-tyrosine on biofilm removal of *P. aeruginosa,* incubated in M63 for 24h at 30°C, then clean with M63 diluted D-tyrosine for different time at room temperature (24-well-plate)

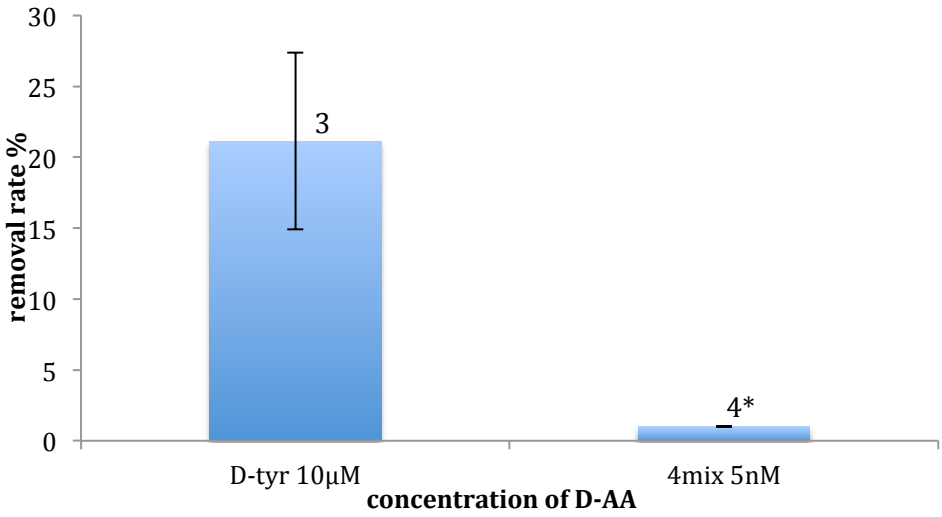

Figure 39. Effect of D-AA on biofilm removal of *P. aeruginosa,* after incubated in M63 with 2% glucose for 18h at 37°C, shaking at rpm 95, then clean with M63 with 2% glucose diluted D-AA for 1h at room temperature (12-well-plate)

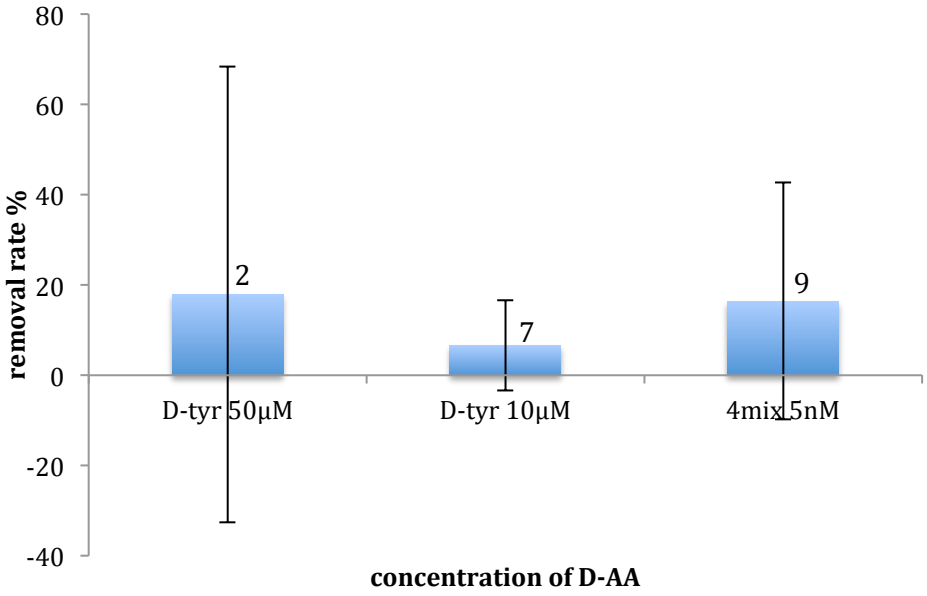

Figure 40. Effect of D-AA on biofilm removal of *P. aeruginosa,* incubated in M63 with 2% glucose for 18h at 37°C, shaking at rpm 95, then clean with PBS diluted D-AA for 0.5h at room temperature (12-well-plate)

Figure 37 and 40 indicated that cleaning with PBS diluted D-amino acids

(removal rate of 17.9% for 50μM D-tyrosine, removal rate of 6.6% for 10μM D-tyrosine, and removal rate of 16.4% for 5nM mixture D-AA) had better effect than cleaning with nutrient medium diluted D-amino acids (removal rate of -3.15% for 100nM mixture D-AA, removal rate of -2.65% for 50nM mixture D-AA, and 7.45% for 50nM mixture D-AA). This is assumed to be that without nutrient media, the growth of bacteria and excretion of EPS by bacteria all significantly decreased, without lots of polysaccharide holding bacteria together firmly, D-amino acids can be more effective to remove existing biofilm.

Figure 36, 38, 39 and 40 showed that D-amino acids had some effect on cleaning existing biofilm formed by *P.aeruginosa.* This was due to the physicochemical effect and biological effect of D-amino acids on removing existing bioiflm, which was discussed earlier.

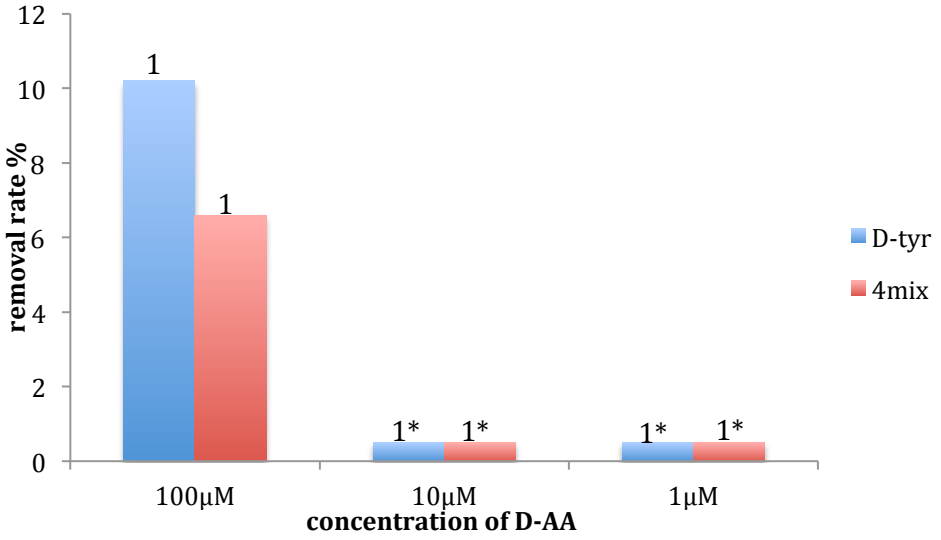

Figure 41. Effect of D-AA on biofilm removal of *P. aeruginosa,* after incubated in M63 for 18h at 37°C, shaking at rpm 95, then clean with PBS diluted D-AA for 0.5h at room temperature (tissue culture dish)

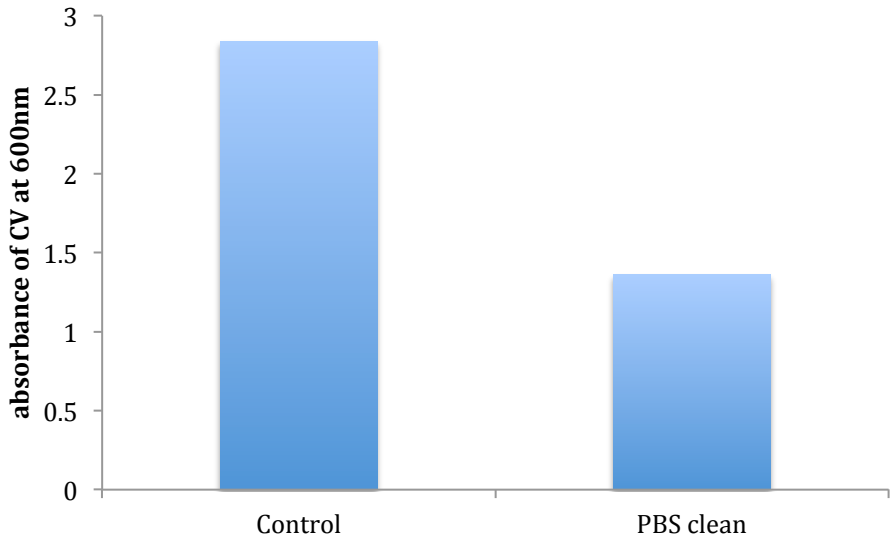

Figure 42. The absorbance of CV at 600nm of *P.aeruginosa* control group and PBS cleaned *P.aeruginosa* control group in tissue culture dish

The effect of cleaning existing biofilm with *P.aeruginosa* incubated in tissue culture dish was not as good as that in 12-well-plate (Figure 41). This was because while applying the shaking in cleaning protocol, tissue culture dish experienced higher hydraulic shear velocity.

From these experiments, the overall effect of D-amino acids on both inhibiting biofilm formation and cleaning existing biofilm were better for *B. subtilis* than *P.aeruginosa*. This is likely because of the different types of these two bacteria. *B. subtilis* is a gram-positive bacterium and *P.aeruginosa* is a gram-negative bacterium. The mechanisms of D-amino acids on biofilm inhibition and cleaning are different between *P.aeruginosa* and *B. subtilis.*

Kolodkin-Gal *at el.* [5] discovered that in Gram-positive bacteria, D-tyrosine substituted the terminal D-alanine in the peptide side chains of peptidoglycan in cell wall and caused the detachment of TasA fiber from their anchor in cell wall, which triggered the disassemble of biofilm. However, whether this mechanism is applied to

Gram-negative bacteria or not is still unknown. The bacterial cell wall structure is different between Gram-positive and Gram-negative bacteria. In Gram-positive bacteria, the cell wall consists of a thick peptidoglycan layer. While in Gram-negative bacteria, there are two membranes contained in the cell wall. The inner membrane is a thin peptidoglycan layer linked to the cytoplasmic membrane, and the outer membrane is consists of phospholipids and lipopolysaccharides. Since in Gram-negative bacteria there are no surface structures that are anchored in the peptidoglycan layer, the mechanism of how D-tyrosine inhibit biofilm formation cannot apply in Gram-negative bacteria. Thus, the mechanism of how D-amino acids inhibits bacterial attachment of Gram-negative bacteria still needs to be investigated.

4.3 Bench scale dead end filtration experiment

The effect of D-tyrosine on preventing bacteria biofouling and organic fouling on NF90 membrane surface during filtration process was tested. In the filtration experiment, feed solution was forced by pressure to go through the membrane, which was a good circumstance for bacteria to adhere onto the membrane surface. The solution was stirred in the filtration chamber to reduce concentration polarization.

Figure 43 showed the filtration data in a typical bench scale dead end NF90 filtration experiment during compaction, conditioning, inoculation and fouling stages without D-tyrosine addition. During compaction stage, the clean water flux stabilized at 2.9×10^{-5} m/s at 150 psi. In the conditioning stage, the flux decreased to 1.3×10^{-5} m/s after filtering the electrolyte feed solution. This flux decline was mainly due to the organic fouling and concentration polarization. Then during the inoculation of the bacteria solution (30 min), there was a sharp drop in flux. In the fouling stage, the flux decreased to 1.4×10^{-6} m/s. This flux decline was mainly caused by bacteria and

organic fouling on the membrane.

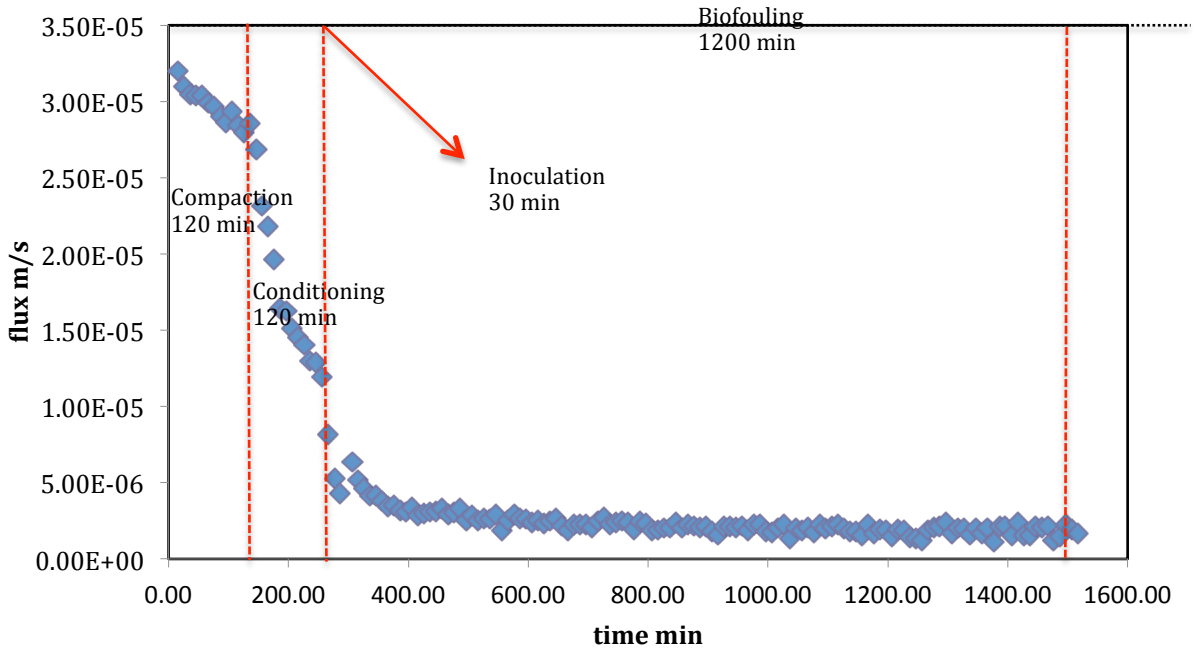

Figure 43. Bench scale dead end NF90 membrane filtration experiment without D-tyrosine addition

4.3.1 Effect of D-tyrosine in preventing organic fouling and biofouling in bench scale dead end NF90 filtration experiment

The objective of the NF90 filtration experiments was to find out the effect of D-tyrosine on preventing the flux decline caused by organic fouling (LB) and bacterial fouling (*P. aeruginosa*) on NF90 membrane surface.

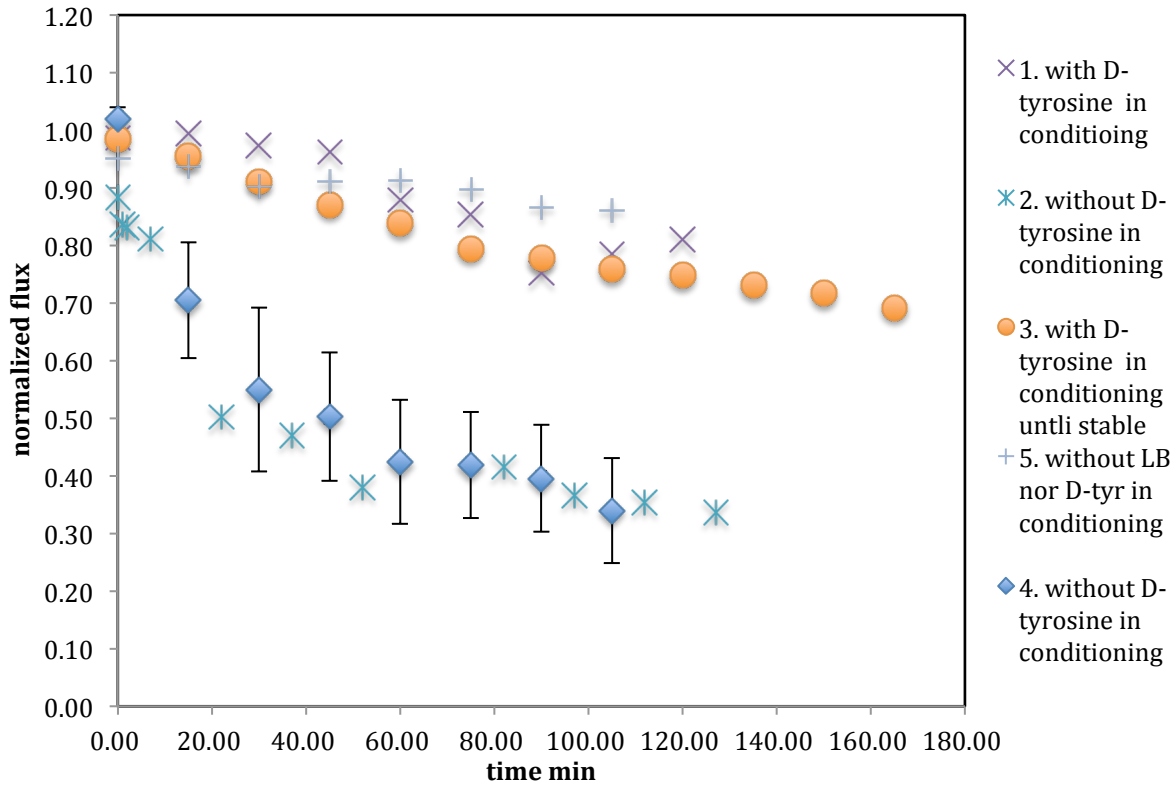

Figure 44. The effect of D-tyrosine on inhibiting flux decline caused by organic fouling (LB) in conditioning stage (normalized flux)

As shown in Figure 44, in the conditioning stage, the flux declined to ~0.87 when there was neither LB nor D-tyrosine in the electrolyte feed solution (data 5). Then the flux declined to ~0.34 after filtering the background solution that contains electrolytes and LB (data 2 and 4). Thus LB would cause flux decline due to organic fouling. When D-tyrosine was included in the background solution, the flux declined to ~0.80 (data 1 and 3), so D-tyrosine can greatly reduce the flux decline caused by LB and inhibit organic fouling. D-amino acids are negatively charged and hydrophilic, so after filtered onto the membrane surface, D-amino acids would change the surface property by making the surface negatively charged and hydrophilic, which decreased the possibility of LB to attach onto the membrane surface. From the result of data 3, LB and D-tyrosine were added into the electrolyte feed solution in conditioning stage, and the process of conditioning stage was not stopped until the flux was stable. This

indicated that LB fouling had been inhibited, and the flux decline observed in the subsequent biofouling stage could be solely attributed to bacterial biofouling.

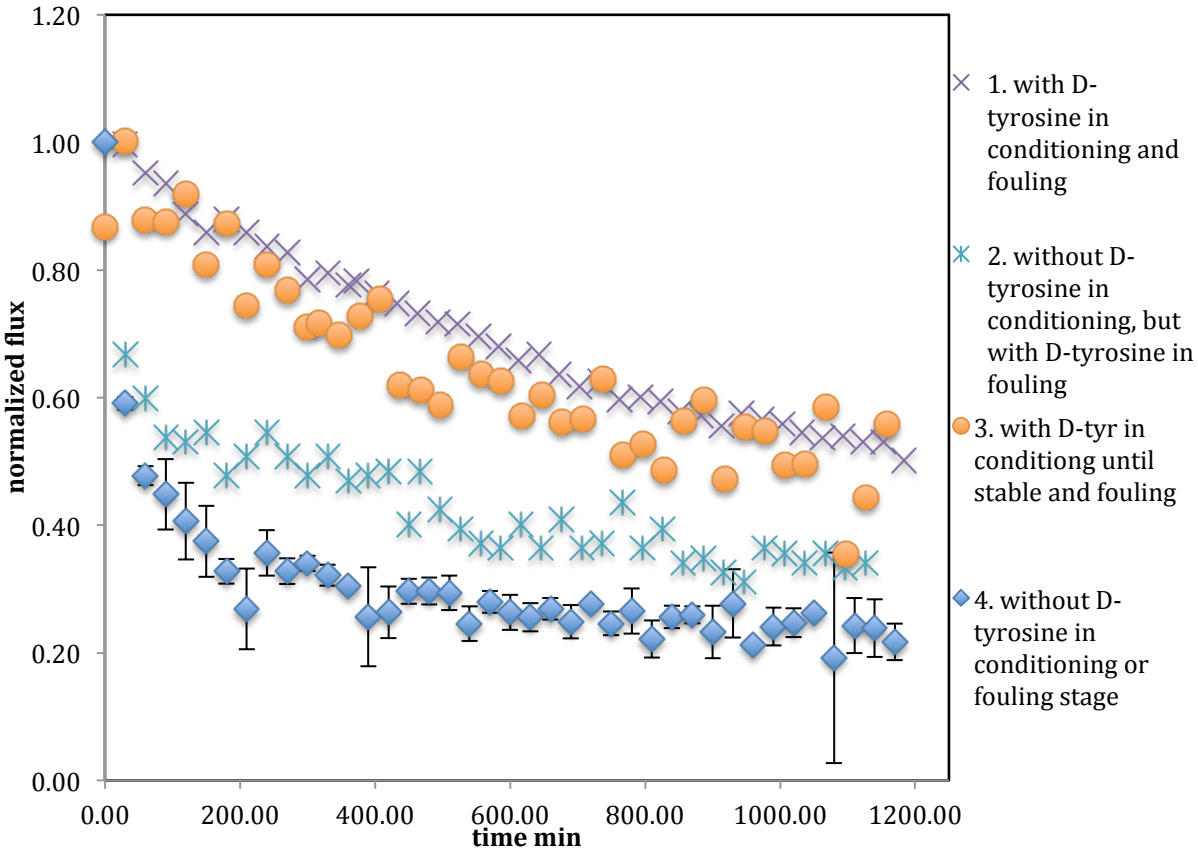

Figure 45. The effect of D-tyrosine on inhibiting flux decline caused by organic fouling (LB) and *P. aeruginosa* biofouling in fouling stage (normalized flux)

Figure 45 showed that in the biofouling stage, the flux declined to 24% of the initial flux (i.e., 76% flux decline) without D-tyrosine addition into the electrolyte feed solution in conditioning nor fouling stage (data 4). When D-tyrosine was added during both the conditioning and biofouling stages, the flux decline due to biofouling was significantly lower, ~53% (data 1 and 3). Because the flux decline due to LB fouling had stabilized before the biofouling stage started (data 3), the reduced flux decline in the biofouling stage was solely attributed to the effect of D-tyrosine on P. *aeruginosa* biofouling. This was consistent with the conclusion from the paper

published by Yu *et al.* [57], which showed that at low bacteria concentrations (low nutrient electrolyte solution was applied as the feed water), D-tyrosine greatly reduced the flux decline caused by *P. aeruginosa* biofouling in NF270 membrane. However, data 2 showed that when D-tyrosine was only added during the biofouling stage, but not in the conditioning stage, (i.e., the membrane was organically fouled before the biofouling stage), the inhibitive effect of D-tyrosine on biofouling is significantly lower. The flux declined to 32% of the initial flux, notably lower than the 53% observed in data 1, when D-tyrosine was added during both conditioning and biofouling stages; but the flux was still notably higher than that in the control (data 4). These results show that D-tyrosine can reduce both organic fouling by the organic compounds in the LB medium and *P. aeruginosa* biofouling. However, once organic fouling happens in the filtration system, the effect of D-tyrosine on inhibition of bacteria biofouling decreases, this suggests that D-tyrosine plays an important role in inhibiting cell-surface adhesion. When the surface is fouled and becomes highly adhesive, the effect of D-tyrosine on inhibition of biofilm formation decreases. These results are consistent with the screening test result on the effect of D-amino acids on inhibition of *P. aeruginosa* biofilm formation discussed earlier: after the EPS had been produced by bacteria, D-amino acids were less effective to inhibit biofilm formation.

To sum up, D-tyrosine inhibits the flux decline caused by organic (LB) fouling as well as *P. aeruginosa* biofouling in the bench scale dead end filtration experiment due to its ability to change the NF90 membrane surface property, which inhibited the organic fouling, and its ability to inhibit cell-surface adhesion, which inhibited the *P. aeruginosa* biofouling on the membrane surface.

5. Conclusions and future research

First of all, this study provides the optimized conditions for growing robust and well-attached biofilm on polystyrene surface, as well as the improved methods to measure biofilm. The robustness of the biofilm formed on a solid surface (polystyrene) strongly depends on the cultivation condition, including incubation temperature, incubation time, growth medium, and plate type. The optimized condition of growing robust and well attached biofilm for *P. aeruginosa* is incubated in 2% glucose M63 for 18h at 37°C, shaking at rpm 95; for *B. subtilis* is incubated in 2% glucose M63 for 24h at 37°C, without shaking. The microtitter plate assay generates data with large variations and requires rigorous experimental design and statistical analysis to draw sound conclusions.

Secondly, for *P. aeruginosa*, D-amino acids are effective in inhibiting the initial bacterial attachment and early stage biofilm formation. However, due to the existence of EPS production of a mature biofilm after long incubation time (12h-24h), bacteria cells are hold firmly by polysaccharide in the biofilm and D-amino acids are not effective to disrupt polysaccharide matrix, so D-amino acids are less effective on inhibiting biofilm formation of *P. aeruginosa* after long incubation time with the existence of EPS.

Thirdly, this study reveals that D-tyrosine and mixture D-amino acids (D-tyrosine, D-tryptophan, D-leucine and D-methionine) have smaller effect on inhibition of biofilm formation and disrupting existing biofilm for *P. aeruginosa* than for *B. subtilis*, when the biofilm is formed on polystyrene surface. This is because the different bacteria types of these two bacteria. *P. aeruginosa* is a Gram-negative

bacterium and *B. subtilis* is a Gram-positive bacterium, and cell wall structure of Gram-negative and Gram-positive bacteria is different. The mechanisms of D-amino acids work to inhibit biofilm formation are different between Gram-negative and Gram-positive bacteria. D-amino acids work as the mechanism revealed by Kolodkin-Gal *et al.* [5] to inhibit biofilm formation for Gram-positive bacteria, while the mechanism of how D-amino acids work to inhibit biofilm formation of Gram-negative bacteria still needs to be investigated.

Lastly, this study proves that D-tyrosine is effective on preventing organic fouling and *P. aeruginosa* biofouling on NF90 membrane in bench scale dead end filtration system, due to both physicochemical and biological mechanisms of D-tyrosine. However, D-tyrosine is less effective to inhibit *P. aeruginosa* biofouling on NF90 membrane surface with the existence of organic fouling.

Future research is needed to test the effect of D-amino acids on inhibition of biofilm formation and disrupting existing biofilm on biofilm formed on membrane surface by mixture bacteria species, which simulates the condition in real NF and RO treatment plant. Also, the applicability of applying D-amino acids in NF and RO treatment plant should be discussed. Another approach is to incorporate D-amino acids into the membrane surface, so that the membrane can release D-amino acids continuously. The D-amino acids in the membrane surface would be replenished by re-incorporated them into the membrane surface. There will be a relatively high concentration of D-amino acids on the membrane surface, which can effectively inhibit bacterial attachment onto the membrane and inhibit membrane biofouling.

REFERENCES

1. Matin, A.; Khan, Z.; Zaidi, S. M. J.; Boyce, M. C., Biofouling in reverse osmosis membranes for seawater desalination: Phenomena and prevention. *Desalination* **2011,** *281*, 1-16.

2. Ivnitsky, H.; Katz, I.; Minz, D.; Shimoni, E.; Chen, Y.; Tarchitzky, J.; Semiat, R.; Dosoretz, C. G., Characterization of membrane biofouling in nanofiltration processes of wastewater treatment. *Desalination* **2005,** *185*, (1-3), 255-268.

3. Xiong, Y.; Liu, Y., Biological control of microbial attachment: a promising alternative for mitigating membrane biofouling. *Applied microbiology and biotechnology* **2010,** *86*, (3), 825-37.

4. Hubert Lam, D.-C. O., Felipe Cava, Constantin N. Takacs, Jon Clardy, Miguel A. de Pedro, Matthew K. Waldor, D- Amino acids govern stationary phase cell wall remodeling in bacteria. **2009,** *325*, 1552-1555.

5. Kolodkin-Gal, I.; Romero, D.; Cao, S.; Clardy, J.; Kolter, R.; Losick, R., D-amino acids trigger biofilm disassembly. *Science* **2010,** *328*, (5978), 627-9.

6. Guo, W.; Ngo, H. H.; Li, J., A mini-review on membrane fouling. *Bioresource technology* **2012,** *122*, 27-34.

7. Xu, P.; Drewes, J. E.; Kim, T.-U.; Bellona, C.; Amy, G., Effect of membrane fouling on transport of organic contaminants in NF/RO membrane applications. *Journal of Membrane Science* **2006,** *279*, (1-2), 165-175.

8. Leppard, J. B. a. G. G., Characterization of Aquatic Colloids and Macromolecules. *Environ. Sci. Technol.* **1995,** *29*, (9).

9. Le-Clech, P.; Chen, V.; Fane, T. A. G., Fouling in membrane bioreactors used in wastewater treatment. *Journal of Membrane Science* **2006,** *284*, (1-2), 17-53.

10. A.L. Lim, R. B., Membrane fouling and cleaning in microfiltration of activated sludge wastewater. *Journal of Membrane Science* **2003,** *216*, (1-2), 279-290.

11. J.S. Baker, L. Y. D., <Biofouling in membrane systems - A review.pdf>. *Desalination* **1998,** *118 (1998) 81-90*.

12. Schneider, R.; Ferreira, L.; Binder, P.; Bejarano, E.; Goes, K.; Slongo, E.; Machado, C.; Rosa, G., Dynamics of organic carbon and of bacterial populations in a

conventional pretreatment train of a reverse osmosis unit experiencing severe biofouling. *Journal of Membrane Science* **2005,** *266*, (1-2), 18-29.

13. KOLTER, P. W. A. R., Minireview Biofilm, City of Microbes. *Journal of bacteriology* **2000,** *May 2000*, 2675–2679.

14. Vigeant, M. A. S.; Ford, R. M.; Wagner, M.; Tamm, L. K., Reversible and Irreversible Adhesion of Motile Escherichia coli Cells Analyzed by Total Internal Reflection Aqueous Fluorescence Microscopy. *Applied and Environmental Microbiology* **2002,** *68*, (6), 2794-2801.

15. Donlan, R. M., <R.M. Donlan Biofilms microbial life on surfaces Emerging Infect.pdf>. **2002**.

16. Matsukawa, M.; Greenberg, E. P., Putative exopolysaccharide synthesis genes influence Pseudomonas aeruginosa biofilm development. *Journal of bacteriology* **2004,** *186*, (14), 4449-56.

17. Mansouri, J.; Harrisson, S.; Chen, V., Strategies for controlling biofouling in membrane filtration systems: challenges and opportunities. *Journal of Materials Chemistry* **2010,** *20*, (22), 4567.

18. Fritzmann, C.; Löwenberg, J.; Wintgens, T.; Melin, T., State-of-the-art of reverse osmosis desalination. *Desalination* **2007,** *216*, (1-3), 1-76.

19. Flemming, H.-C., Reverse osmosis membrane biofouling. *Exp. Therm. Fluid Sci.* **1997,** *14 (1997) 382–391*.

20. Flemming, H. C., Biofouling in water systems--cases, causes and countermeasures. *Applied microbiology and biotechnology* **2002,** *59*, (6), 629-40.

21. Huertas, E.; Herzberg, M.; Oron, G.; Elimelech, M., Influence of biofouling on boron removal by nanofiltration and reverse osmosis membranes. *Journal of Membrane Science* **2008,** *318*, (1-2), 264-270.

22. Herzberg, M.; Elimelech, M., Biofouling of reverse osmosis membranes: Role of biofilm-enhanced osmotic pressure. *Journal of Membrane Science* **2007,** *295*, (1-2), 11-20.

23. Herzberg, M.; Kang, S.; Elimelech, M., Role of Extracellular Polymeric Substances (EPS) in Biofouling of Reverse Osmosis Membranes. *Environmental Science & Technology* **2009,** *43*, (12), 4393-4398.

24. Andrew P. Murphy, C. D. M., Robert L. Riley, Shui Wai Lin, Balasingam Murugaverl, Patricia Rusin Microbiological damage of cellulose acetate RO

membranes. *Journal of Membrane Science* **2001,** *193*, 111-121.

25. H.-C. Flemminga, G. S., T. Griebea,J. Schmitta,A. Tamachkiarowaa, Biofouling - the Achilles heel of membrane processes. *DESALINATION* **1997,** *113 (1997)*, 215-225.

26. MARSHA, K., Bacterial Adhesion in Oligotrophic Habitats. *Microb. Sci.* **1985,** *2*, 321-326.

27. M. Kumar, S. S. A., W.R. Pearce, Investigation of seawater reverse osmosis fouling and its relationship to pretreatment type. *Environ. Sci. Technol.* **2006,** *40* 2037–2044.

28. Prihasto, N.; Liu, Q.-F.; Kim, S.-H., Pre-treatment strategies for seawater desalination by reverse osmosis system. *Desalination* **2009,** *249*, (1), 308-316.

29. Wolf, P. H.; Siverns, S.; Monti, S., UF membranes for RO desalination pretreatment. *Desalination* **2005,** *182*, (1-3), 293-300.

30. Vedavyasan, C. V., Pretreatment trends — an overview. *Desalination* **2007,** *203*, (1-3), 296-299.

31. S.B. Sadr Ghayeni, P. J. B., R.P. Schneider, A.G. Fane Adhesion of waste water bacteria to reverse osmosis membranes. *Journal of Membrane Science* **1998,** *138*, 29-42.

32. ORMEROD, V. L. a. K., The influence of disinfection processes on biofilm formation in water distribution systems. *Water research* **1995,** *29*, 1013-1021.

33. G. Petrucci, M. R., G. Petrucci, M. Rosellini, Chlorine dioxide in seawater for fouling control and post-disinfection in potable networks. *Desalination* **2005,** *182*, 283-291.

34. Dooil Kima, S. J., Jinsik Sohn, Hyungsoo Kim, Seockheon Lee, Biocide application for controlling biofouling of SWRO membranes — an overview. *Desalination* **2009,** *238*, 43–52.

35. Kang, G.-D.; Gao, C.-J.; Chen, W.-D.; Jie, X.-M.; Cao, Y.-M.; Yuan, Q., Study on hypochlorite degradation of aromatic polyamide reverse osmosis membrane. *Journal of Membrane Science* **2007,** *300*, (1-2), 165-171.

36. Perrins, J. C.; Cooper, W. J.; van Leeuwen, J.; Herwig, R. P., Ozonation of seawater from different locations: formation and decay of total residual oxidant--implications for ballast water treatment. *Marine pollution bulletin* **2006,** *52*, (9), 1023-33.

37. Liu, C. X.; Zhang, D. R.; He, Y.; Zhao, X. S.; Bai, R., Modification of membrane surface for anti-biofouling performance: Effect of anti-adhesion and anti-bacteria approaches. *Journal of Membrane Science* **2010,** *346*, (1), 121-130.

38. Li, Q.; Mahendra, S.; Lyon, D. Y.; Brunet, L.; Liga, M. V.; Li, D.; Alvarez, P. J., Antimicrobial nanomaterials for water disinfection and microbial control: potential applications and implications. *Water research* **2008,** *42*, (18), 4591-602.

39. FUHRMANN, T. S. A. F., Photocatalytic surface reactions on indoor wall paint. *Environ. Sci. Technol.* **2007,** *41*, 6573-6578.

40. Yoshihiko Kikuchi, K. S., Tomokazu Iyoda , Kazuhito Hashimoto,; Fujishima, A., Photocatalytic bactericidal effect of TiO2 thin films dynamic view of the active oxygen species responsible for the effect. *Journal of Photochemistry and Photobiology A: Chemistry* **1997,** *106*, 51-56.

41. Kim, J. Y.; Lee, C.; Cho, M.; Yoon, J., Enhanced inactivation of E. coli and MS-2 phage by silver ions combined with UV-A and visible light irradiation. *Water research* **2008,** *42*, (1-2), 356-62.

42. Cho, K.-H.; Park, J.-E.; Osaka, T.; Park, S.-G., The study of antimicrobial activity and preservative effects of nanosilver ingredient. *Electrochimica Acta* **2005,** *51*, (5), 956-960.

43. Q.L. Feng, J. W., G.Q. Chen, F.Z. Cui, T.N. Kim, J.O. Kim, A mechanistic study of the antibacterial effect of silver ions on Escherichia coli and Staphylococcus aureus. *J. Biomed. Mat. Res.* **2000,** *52*, 662-668.

44. Morones, J. R.; Elechiguerra, J. L.; Camacho, A.; Holt, K.; Kouri, J. B.; Ramirez, J. T.; Yacaman, M. J., The bactericidal effect of silver nanoparticles. *Nanotechnology* **2005,** *16*, (10), 2346-53.

45. Al-Amoudi, A. S.; Farooque, A. M., Performance restoration and autopsy of NF membranes used in seawater pretreatment. *Desalination* **2005,** *178*, (1-3), 261-271.

46. T. Mohammadi, S. S. M., M.K. Moghadam, Investigation of membrane fouling. *Desalination* **2002,** *153*, 155-160.

47. Bereschenko, L. A.; Prummel, H.; Euverink, G. J.; Stams, A. J.; van Loosdrecht, M. C., Effect of conventional chemical treatment on the microbial population in a biofouling layer of reverse osmosis systems. *Water research* **2011,** *45*, (2), 405-16.

48. Bassler, C. M. W. a. B. L., Quorum Sensing Cell-to-Cell Communication in Bacteria. *The Annual Review of Cell and Developmental Biology* **2005,** *21*, 319-346.

49. Williams, P.; Winzer, K.; Chan, W. C.; Camara, M., Look who's talking: communication and quorum sensing in the bacterial world. *Philosophical transactions of the Royal Society of London. Series B, Biological sciences* **2007,** *362*, (1483), 1119-34.

50. Xavier, K. B.; Bassler, B. L., LuxS quorum sensing: more than just a numbers game. *Current Opinion in Microbiology* **2003,** *6*, (2), 191-197.

51. Gonzalez, J. E.; Keshavan, N. D., Messing with bacterial quorum sensing. *Microbiology and molecular biology reviews : MMBR* **2006,** *70*, (4), 859-75.

52. Xu, H.; Liu, Y., d-Amino acid mitigated membrane biofouling and promoted biofilm detachment. *Journal of Membrane Science* **2011,** *376*, (1-2), 266-274.

53. KYUNG-MIN YEON; WON-SEOK CHEONG, H.-S. O., WOO-NYOUNG LEE,; BYUNG-KOOK HWANG; CHUNG-HAK LEE, H. B., AND ZBIGNIEW LEWANDOWSKI, Quorum Sensing: A New Biofouling Control Paradigm in a Membrane Bioreactor for Advanced Wastewater Treatment.pdf. *Environ. Sci. Technol.* **2009,** *43*, 380-385.

54. Roy, V.; Adams, B. L.; Bentley, W. E., Developing next generation antimicrobials by intercepting AI-2 mediated quorum sensing. *Enzyme and microbial technology* **2011,** *49*, (2), 113-23.

55. Zhang, L.-H., Quorum quenching and proactive host defense. *Trends in Plant Science* **2003,** *8*, (5), 238-244.

56. ESAKI, T. Y. A. N., Amino acid racemases: Functions and mechanisms. *JOURNAL OF BIOSCIENCE AND BIOENGINEERING* **2003,** *96*, 103-109.

57. Yu, C.; Wu, J.; Contreras, A. E.; Li, Q., Control of nanofiltration membrane biofouling by Pseudomonas aeruginosa using d-tyrosine. *Journal of Membrane Science* **2012,** *423-424*, 487-494.

58. Schleheck, D.; Barraud, N.; Klebensberger, J.; Webb, J. S.; McDougald, D.; Rice, S. A.; Kjelleberg, S., Pseudomonas aeruginosa PAO1 preferentially grows as aggregates in liquid batch cultures and disperses upon starvation. *PloS one* **2009,** *4*, (5), e5513.

59. Srdjan Stepanovic, D. V., Veronika Hola, Giovanni Di Bonaventura, Slobodanka Djukic, Ivana C´ Irkovi and Filip Ruzicka, Quantification of biofilm in microtiter plates: overview of testing conditions and practical recommendations for assessment of biofilm production by staphylococci.pdf. *Journal Compilation* **2007,**

APMIS 115: 891–9, 2007.

60. G D Christensen, W. A. S., J J Younger, L M Baddour, F F Barrett, D M Melton and E H Beachey, Adherence of coagulase-negative staphylococci to plastic tissue culture plates: a quantitative model for the adherence of staphylococci to medical devices. *journal of clinical microbiology* **1985,** *22*, 996-1006.

61. Lam, H.; Oh, D. C.; Cava, F.; Takacs, C. N.; Clardy, J.; de Pedro, M. A.; Waldor, M. K., D-amino acids govern stationary phase cell wall remodeling in bacteria. *Science* **2009,** *325*, (5947), 1552-5.

62. Xu, H.; Liu, Y., Reduced microbial attachment by D-amino acid-inhibited AI-2 and EPS production. *Water research* **2011,** *45*, (17), 5796-804.

63. FLOODGATE, M. F. A. G. D., An Electron-microscopic Demonstration of an Acidic Polysaccharide Involved in the Adhesion of a Marine Bacterium to Solid Surfaces. *journal of General Microbiology* **1972,** *74* 325-334.

64. Wimpenny, J.-U. K. a. J. W. T., Effect of EPS on biofilm structure and function as revealed by an individual-based model of biofilm growth. *Water Science and Technology* **2001**.

APPENDIX

Box plot of each experiment showing inhibition effect and cleaning effect of D-amino acids (D-tyrosine and the 4 mixture D-amino acids) on biofilm formed by *P. aeruginosa* and *B. subtilis.* The box data in each figure showed the range of all the data under each condition. For each of the box data, from top to bottom showed the 90^{th}, 75^{th}, 50^{th}(median), 25^{th} and 10^{th} percentile of the data among all data sets. The * showed the outliers. The number labeled on top of each box plot showed the number of wells done under this condition.

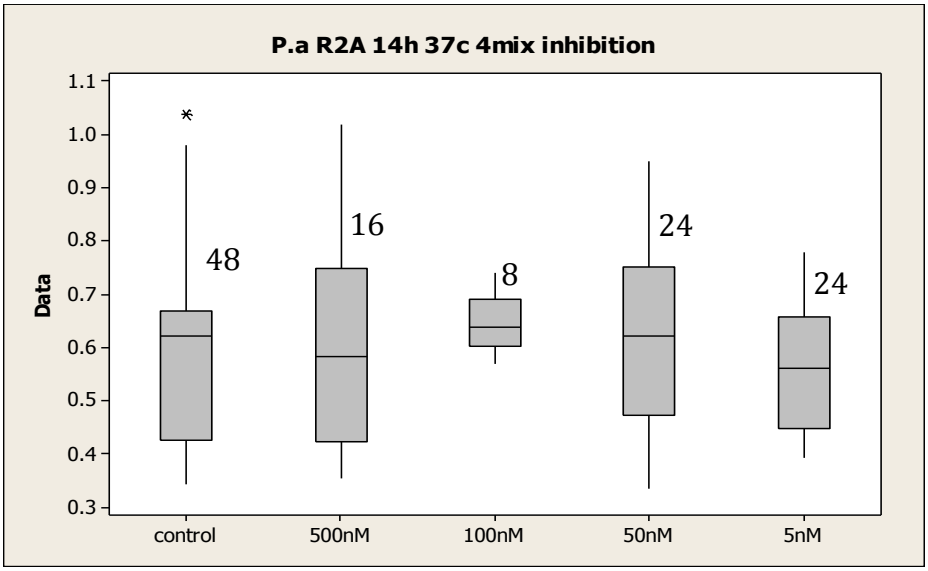

Figure 46. Effect of 4-mixture D-AA on *P. aeruginosa* biofilm formation, after 14h incubation at 37°C in R2A medium, with addition of 4-mixture D-AA initially.

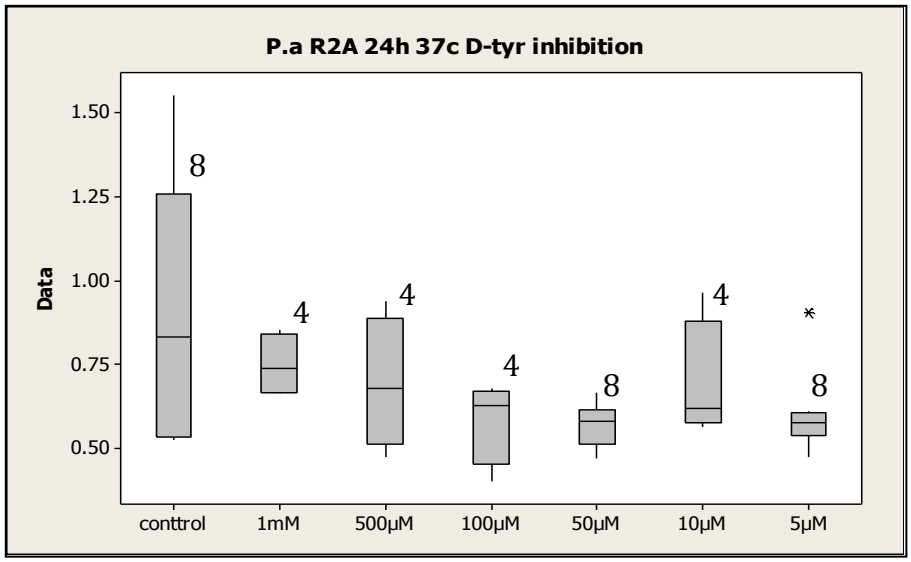

Figure 47. Effect of D-tyrosine on *P. aeruginosa* biofilm formation, after 24h incubation at 37°C in R2A medium, with addition of D-tyrosine initially.

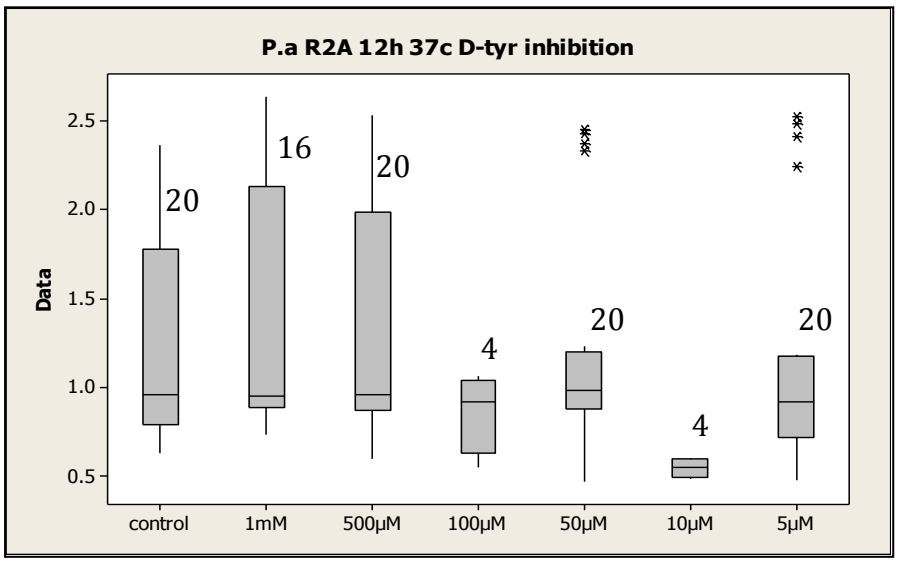

Figure 48. Effect of D-tyrosine on *P. aeruginosa* biofilm formation, after 12h incubation at 37°C in R2A medium, with addition of D-tyrosine initially.

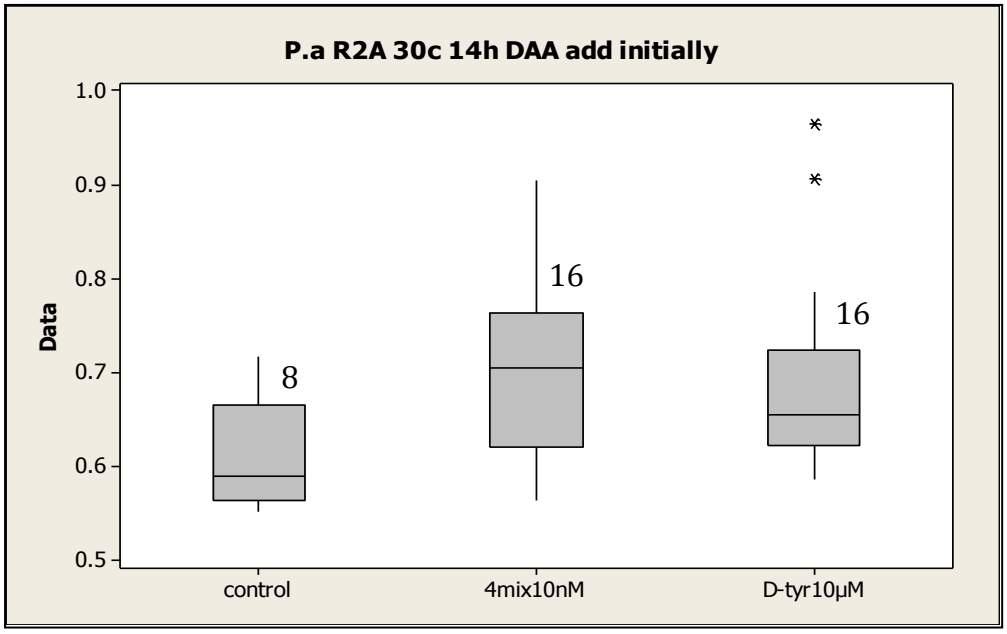

Figure 49. Effect of D-AA on *P. aeruginosa* biofilm formation, after 14h incubation at 30°C in R2A medium, with addition of D-AA initially.

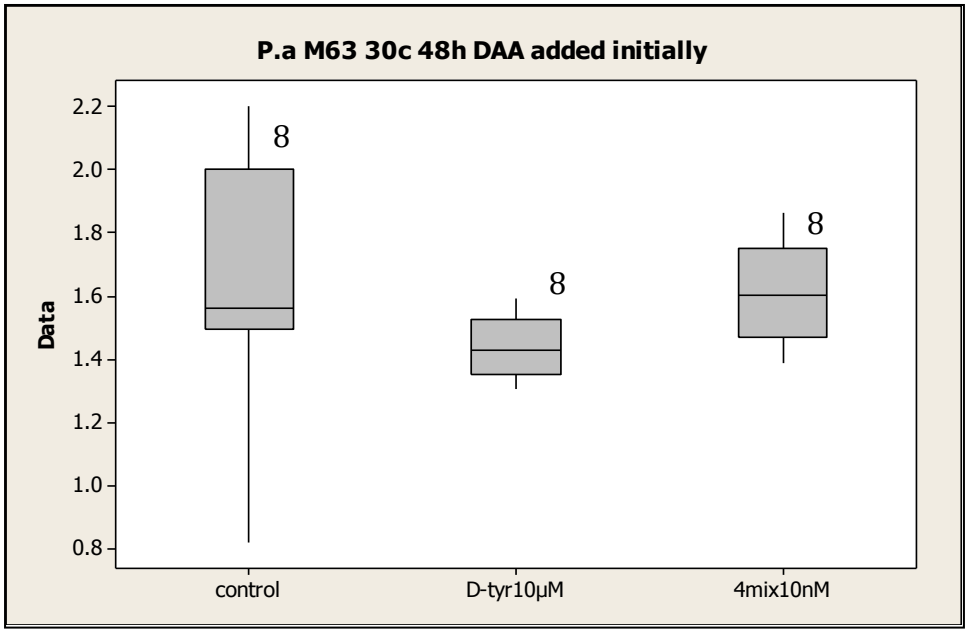

Figure 50. Effect of D-AA on *P. aeruginosa* biofilm formation, after 48h incubation at 30°C in M63 medium, with addition of D-AA initially.

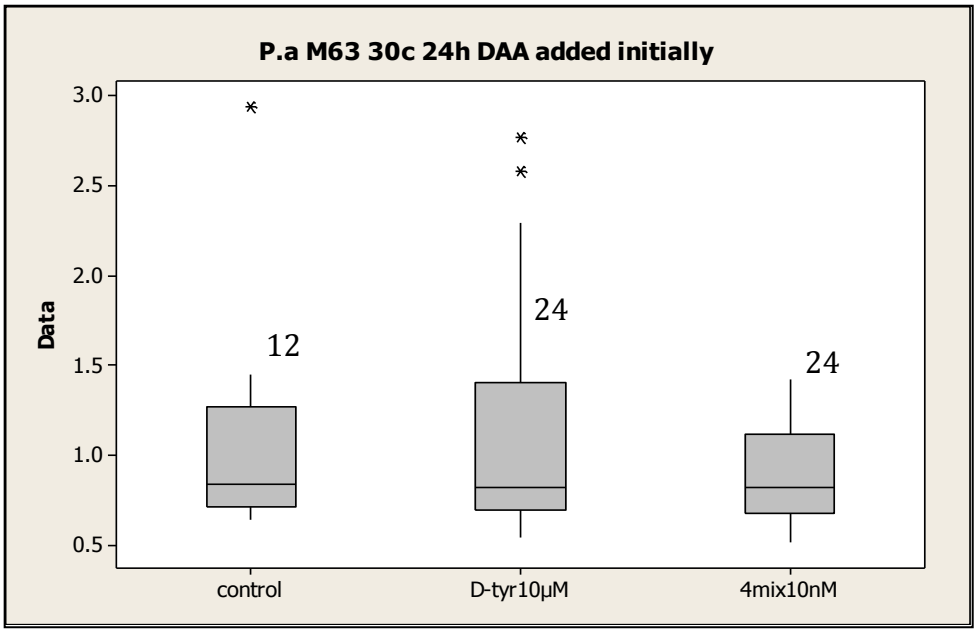

Figure 51. Effect of D-AA on *P. aeruginosa* biofilm formation, after 24h incubation at 30°C in M63 medium, with addition of D-AA initially.

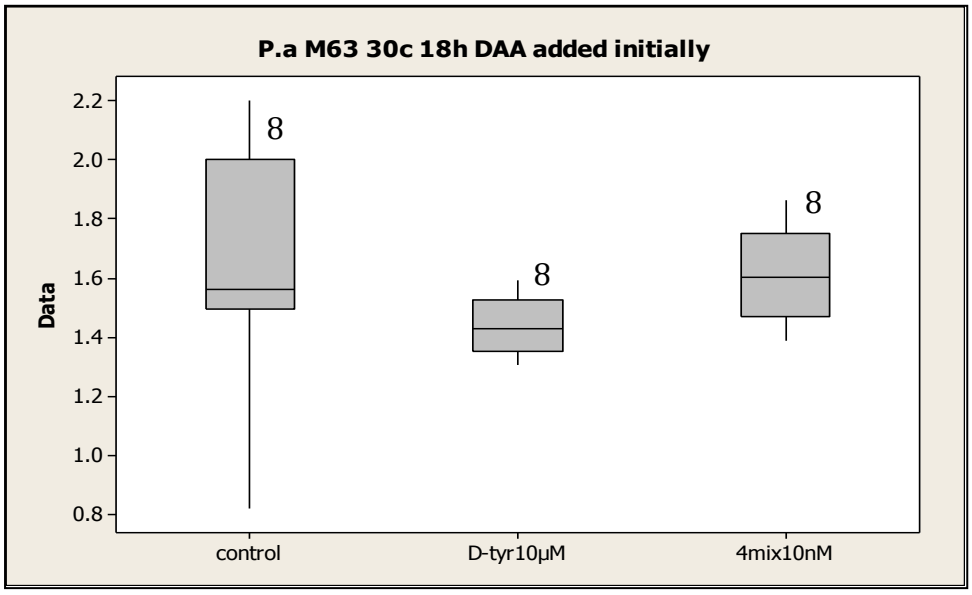

Figure 52. Effect of D-AA on *P. aeruginosa* biofilm formation, after 18h incubation at 30°C in M63 medium, with addition of D-AA initially.

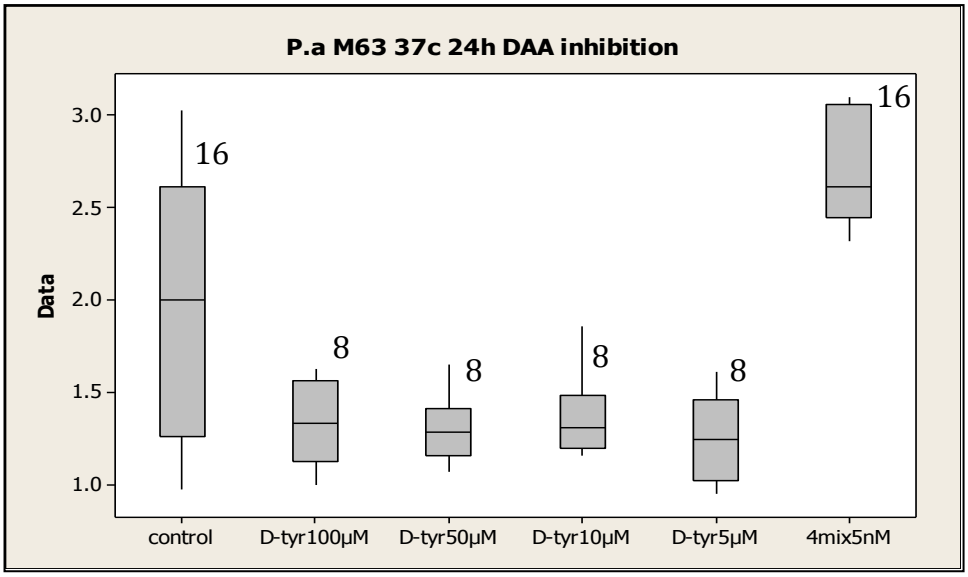

Figure 53. Effect of D-AA on *P. aeruginosa* biofilm formation, after 24h incubation at 37°C in M63 medium, with addition of D-AA initially.

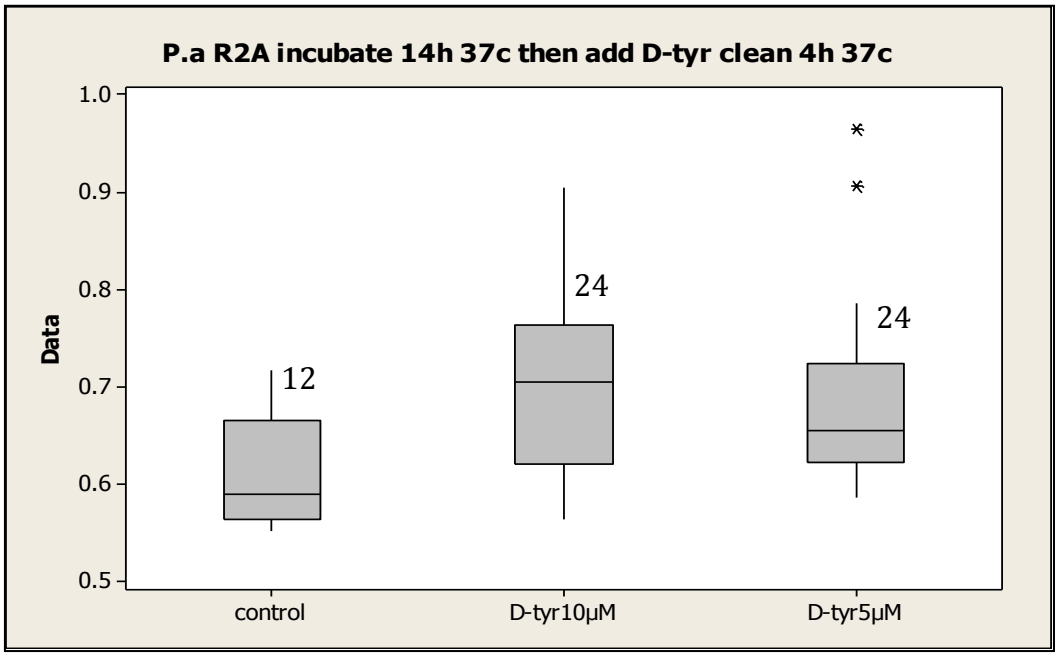

Figure 54. Effect of D-tyrosine on existing *P. aeruginosa* biofilm, after 14h incubation at 37°C in R2A medium, then clean with R2A diluted D-tyrosine for 4h at 37°C.

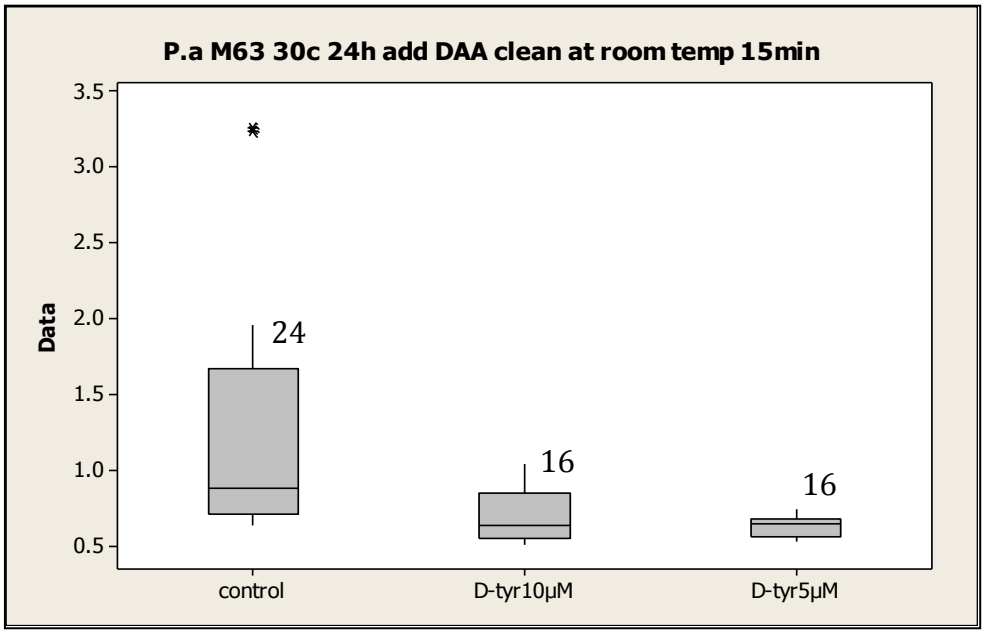

Figure 55. Effect of D-tyrosine on existing *P. aeruginosa* biofilm, after 24h incubation at 30°C in M63 medium, then clean with M63 diluted D-tyrosine for 15min at room temperature.

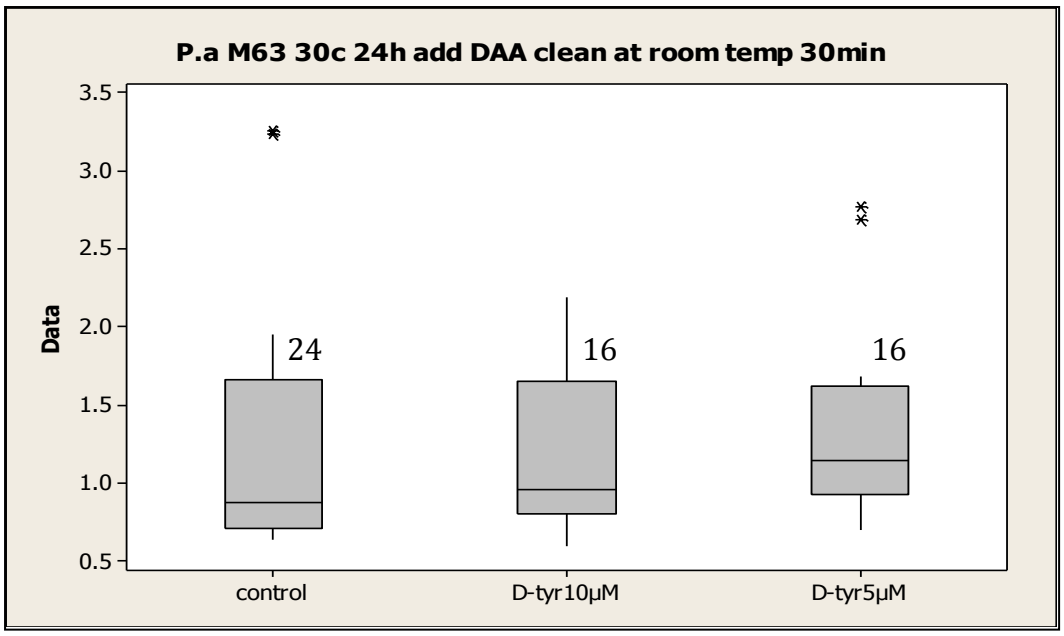

Figure 56. Effect of D-tyrosine on existing *P. aeruginosa* biofilm, after 24h incubation at 30°C in M63 medium, then clean with M63 diluted D-tyrosine for

30min at room temperature.

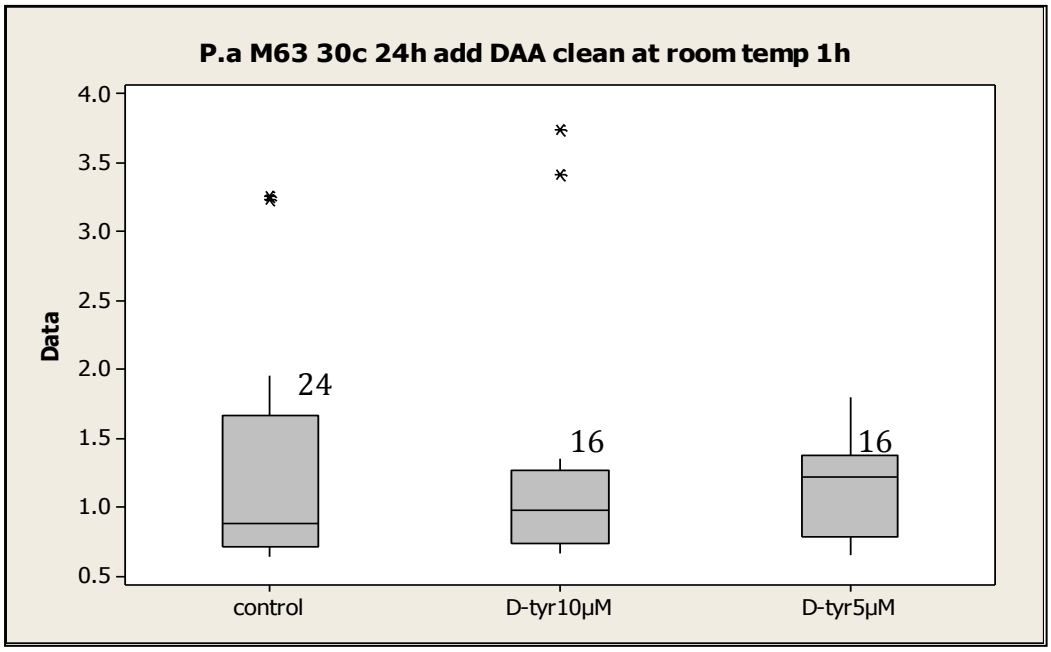

Figure 57. Effect of D-tyrosine on existing *P. aeruginosa* biofilm, after 24h incubation at 30°C in M63 medium, then clean with M63 diluted D-tyrosine for 1h at room temperature.

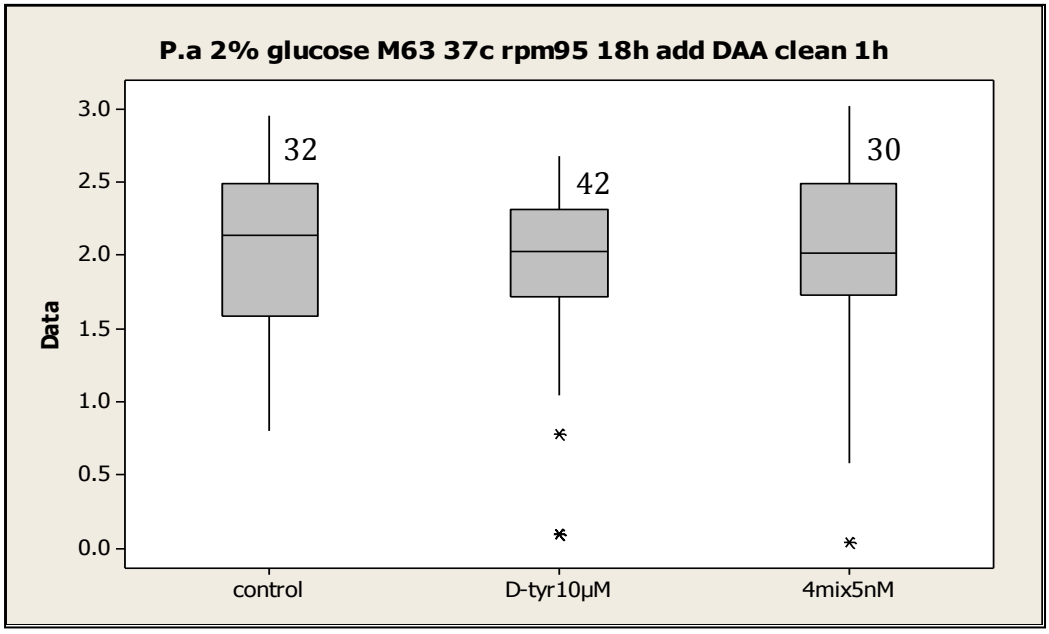

Figure 58. Effect of D-AA on existing *P. aeruginosa* biofilm, after 18h incubation

at 37°C in M63 with 2% glucose with shaking at 95 rpm, then clean with M63 with 2% glucose diluted D-AA for 1h at room temperature.

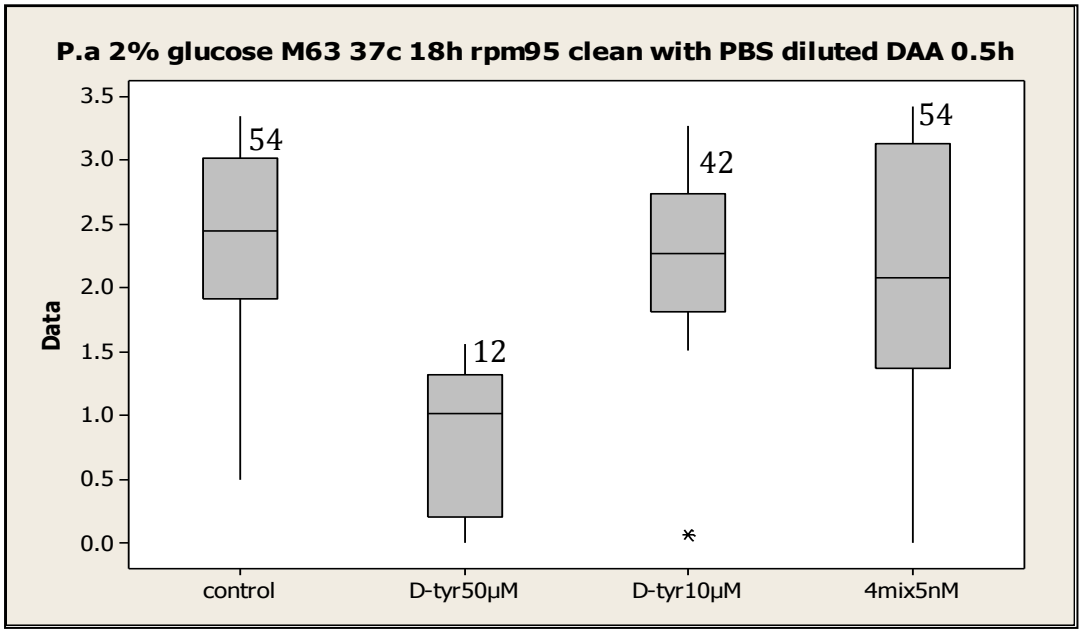

Figure 59. Effect of D-AA on existing *P. aeruginosa* biofilm, after 18h incubation at 37°C in M63 with 2% glucose with shaking at 95 rpm, then clean with PBS diluted D-AA for 0.5h at room temperature.

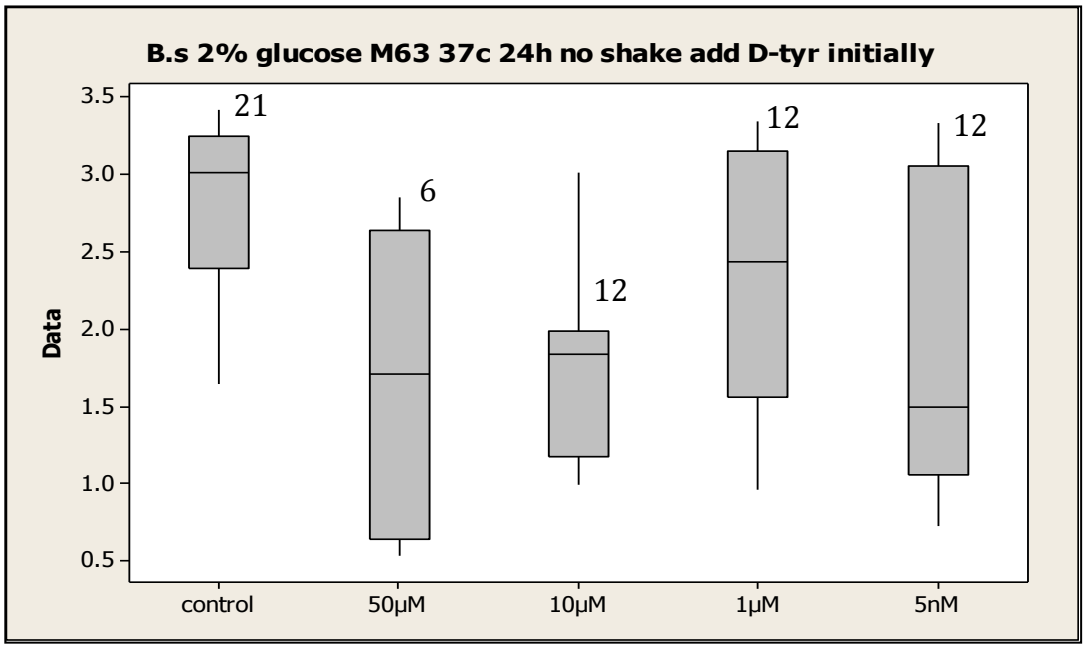

Figure 60. Effect of D-tyrosine on *B. subtilis* biofilm formation, after 24h incubation at 37°C in M63 with 2% glucose, with addition of D-tyrosine initially.

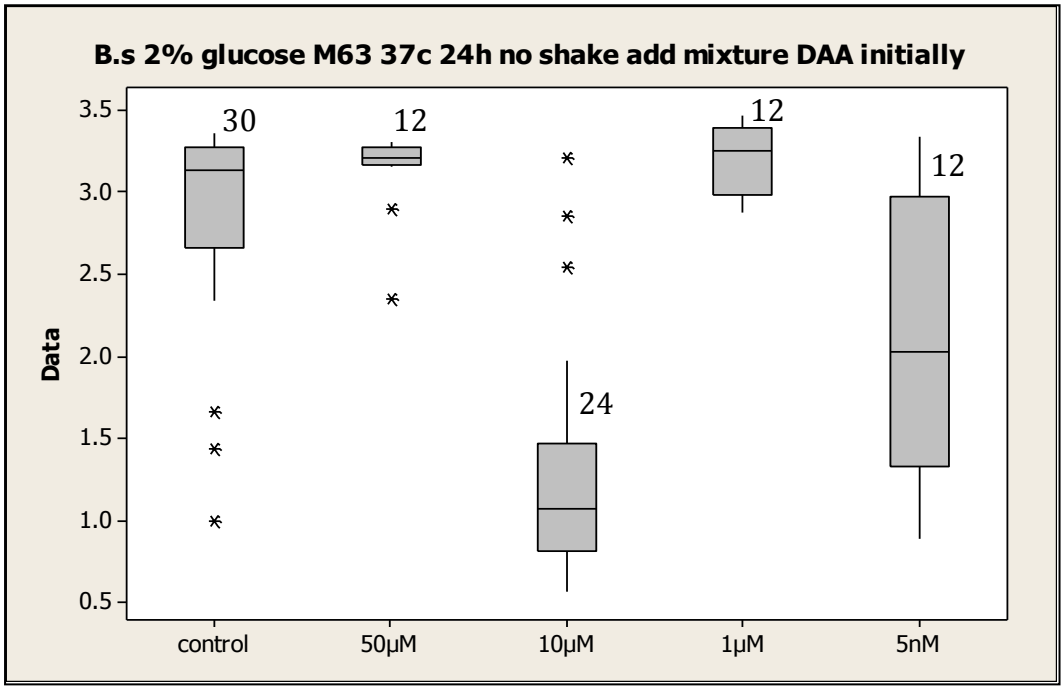

Figure 61. Effect of 4-mixture D-AA on *B. subtilis* biofilm formation, after 24h incubation at 37°C in M63 with 2% glucose, with addition of 4-mixture D-AA initially.

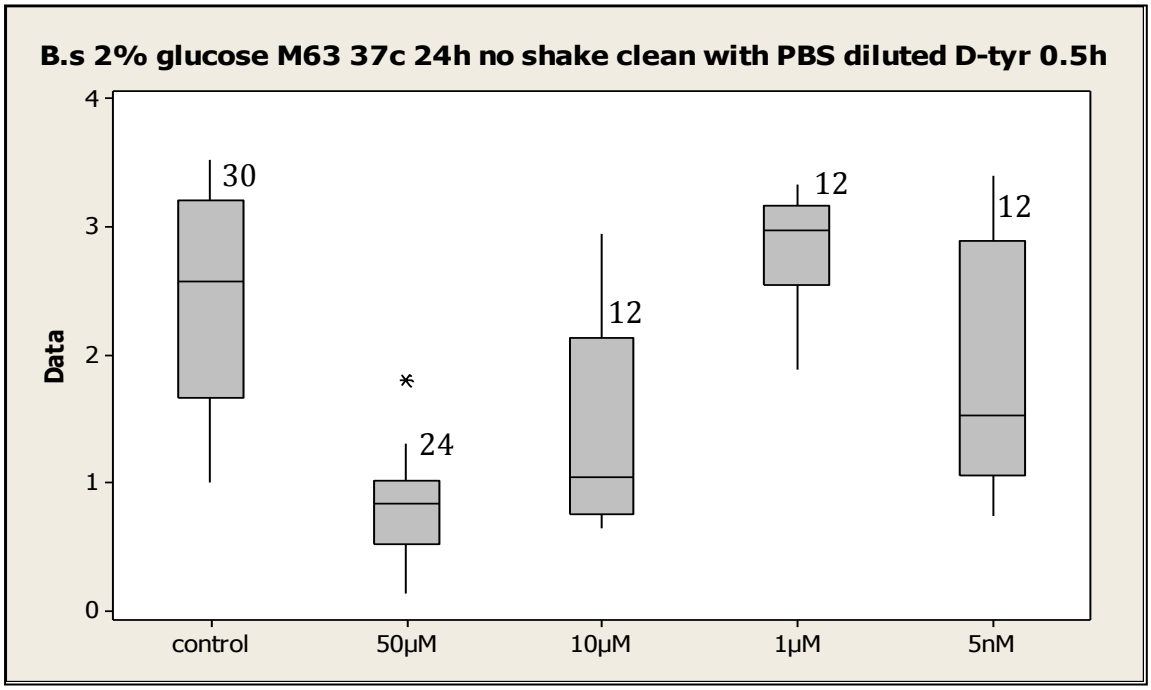

Figure 62. Effect of D-tyrosine on existing *B. subtilis* biofilm, after 24h incubation at 37°C in M63 with 2% glucose, then clean with PBS diluted D-tyrosine for 0.5h at room temperature.

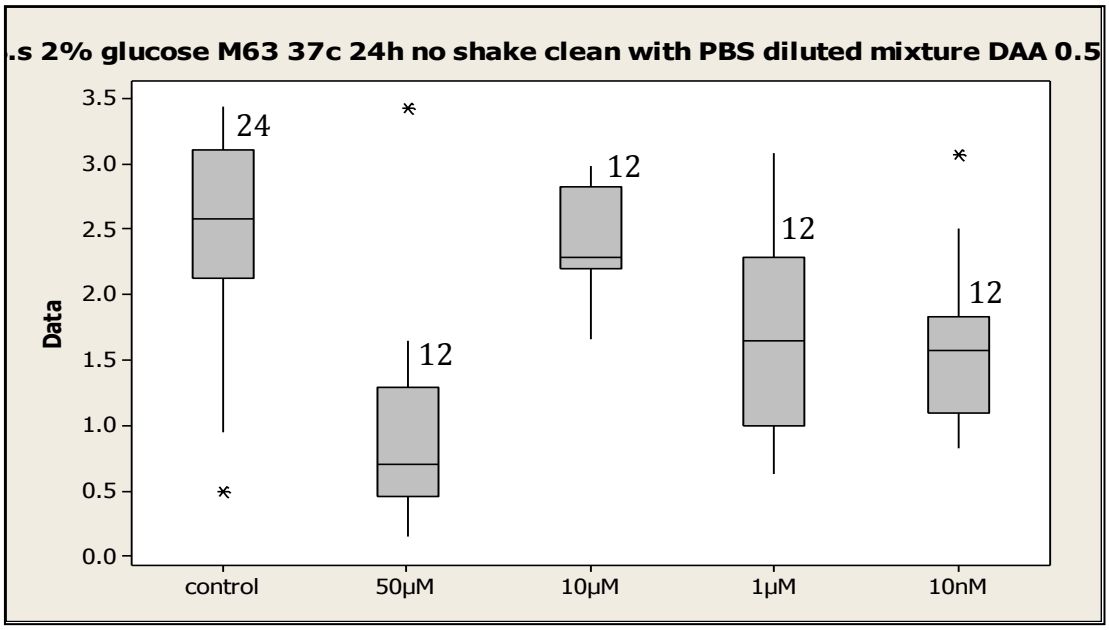

Figure 63. Effect 4-mixture D-AA on existing *B. subtilis* biofilm, after 24h incubation at 37°C in M63 with 2% glucose, then clean with PBS diluted 4-mixture D-AA for 0.5h at room temperature.